An efficient modelling technique for analysis of thin-walled laminated composite beams having open and closed cross sections

Arash Asadi Khansari

B.Sc. (Civil & Structural), M.Sc. (Earthquake)
MIEAust, CPEng NER RPEQ IntPE

Thesis submitted for the degree of

Doctor of Philosophy

School of Civil, Environmental and Mining Engineering

Faculty of Engineering, Computer & Mathematical Sciences

The University of Adelaide, Australia

February 2019

An efficient modelling technique for analysis of thin-walled laminated composite beams having open and closed cross sections

By:

Arash Asadi Khansari

B.Sc. (Civil & Structural), M.Sc. (Earthquake)
MIEAust CPEng NER RPEQ IntPE

Supervised by:

Associate Professor Abdul Hamid Sheikh, Ph.D.,
School of Civil, Environmental & Mining Engineering,
The University of Adelaide

Professor Deric Oehlers, Ph.D.,
School of Civil, Environmental & Mining Engineering,
The University of Adelaide

Thesis submitted in fulfilment of the requirements for the degree of
Doctor of Philosophy

School of Civil, Environmental & Mining Engineering,
Faculty of engineering, Computer and Mathematical Sciences
The University of Adelaide
North Terrace, Adelaide, SA 5005, Australia
Tel: +61(8) 8303 4323
Fax: +61(8) 8303 4359
Email: arash.asadikhansari@adelaide.edu.au, arash.asadi.k@gmail.com

Abstract

This thesis contains a series of journal and conference papers focused on the development of an efficient technique based on a one-dimensional beam finite element model for analysis of thin-walled composite beams having both open and closed cross sections.

The formulation derived in this study has sufficient generality for accommodating any stacking sequence of individual beam walls and it has considered all possible couplings between axial, shear, bending and torsional deformation modes of the beam. The effect of transverse shear deformation of walls and out of plane warping of the beam section is considered where provision exists to restrain or allow the cross-sectional warping.

Composite laminates are generally weak in transverse shear due to their low shear stiffness relative to the extensional rigidity. Thus, it is important to incorporate the effect of shear deformation to ensure reliable predictive capability for all relevant loading scenarios. However, the implementation of shear deformation in a finite element framework has been found to be challenging. The different techniques proposed so far by other researchers to address these difficulties are unfortunately having some issues such as instability/spurious deformation modes in the results or presence of non-physical displacement components in these formulations.

In this thesis, the incorporation of shear deformation within a finite element formulation for thin-walled composite beams is successfully achieved in a novel way. The proposed model is further developed for Vibration, Vibration with preloading, Buckling, Preloaded Buckling and Dynamic Stability of thin-walled laminated composite beams. Numerical examples of open sections I beams and closed section box beams are solved by the proposed approach. A large number of results obtained in this study are compared with those available in literature for the validation of the proposed model, which show a very good performance of the model. The effect of preloading in the form of axial load, end moments and their combined actions on the behaviour of these composite beams are studied.

Statement of Originality

I, Arash Asadi Khansari, certify that this work contains no material which has been accepted for the award of any other degree or diploma in my name in any university or other tertiary institution and, to the best of my knowledge and belief, contains no material previously published or written by another person, except where due reference has been made in the text. In addition, I certify that no part of this work will, in the future, be used in a submission in my name for any other degree or diploma in any university or other tertiary institution without the prior approval of the University of Adelaide and where applicable, any partner institution responsible for the joint award of this degree.

I give consent to this copy of my thesis when deposited in the University Library, being made available for loan and photocopying, subject to the provisions of the Copyright Act 1968.

The author acknowledges that copyright of published works contained within this thesis resides with the copyright holder(s) of those works.

I give permission for the digital version of my thesis to be made available on the web, via the University's digital research repository, the Library Search and also through web search engines, unless permission has been granted by the University to restrict access for a period of time.

Signed: Arash Asadi Khansari Date: 19 February 2019

Acknowledgement

I would like to express my deep and sincere gratitude to my supervisors Associate Professor Abdul Hamid Sheikh and Professor Derek Oehlers for their valuable guidance, consistent encouragement, understanding, patience, and most importantly, their friendship throughout my research work.

I am extremely grateful to my main supervisor Associate Professor Abdul Hamid Sheikh, for his guidance, all the technical discussions and his patience during my candidature. His vast knowledge and his exemplary flexibility and understanding made my long journey through various stages of my research, life and career possible and I would always be grateful.

My endless gratitude is extended to my family, specially my mother for her continuous support and encouragement. My special gratitude to my brother Arman Asadi, for his support and friendship throughout my life. I would like to dedicate this thesis to my precious daughter, Aida and my loving, supportive, encouraging, and patient wife Mina Pazandeh; whose faithful support made this journey possible.

1. Chapter 1 –Thesis General Overview

1.1. Introduction

During the last decades, the use of composite materials in various engineering applications has been popular steadily. New production methods and quality assurance procedure developed by this time have made composite materials cheaper, reliable and more competitive than ever before. Moreover, the multilayer composite materials can be customized by changing the number of layers, fibre orientations and other parameters to provide a desired characteristic at different locations. This customized design across different structural components can lead to further reduction of structure mass which is very important in weight sensitive structures. In addition to the orthotropic material response of fibre reinforced composites, the multi-layered construction significantly increases the complexity of the behaviour due to strong coupling effects between different modes of deformation.

In reality, many applications of such multi-layered composite materials are found in the form of beam like structures such as wind turbine blades, helicopter blades, handrails, vehicle chassis framing and many others. Also, the thin-walled nature of these structures increases modelling complexity due to distortions such as cross-sectional warping. This wide range of application of these composite beams requires powerful and efficient tools for their analysis and design proposes. This has drawn a considerable interest of many researchers who have contributed significantly in this area. This is good start but there are many other issues which need to be addressed to exploit the full capability of these material and structural system with improved confidence.

In principle, the structural response of thin-walled structural members having open or closed cross section made of laminated composite materials may be simulated by adopting a full 3D finite element (FE) modelling strategy based on solid or shell elements. However, such a modelling strategy can be infeasible in many cases due to high computational demand. This type of modelling leads to a gigantic finite element mesh with a very large number of nodes/nodal unknowns. It's known that number of arithmetic operations required for solving a set of simultaneous equations needs at least square of the number of unknown. Thus, as the problem size increases, computational demand/cost to solve the problem increases exponentially. It should be noted that while the computational power of computers are increasing with time, the demand for analysing these structures is also increasing due to a steady increase of their size and complexity. Also, the demand for an optimum design needs an iterative technique where the computation efficiency of a structural analysis play a big role.

In order to address the above problem, a group of researchers have attempted to develop alternative modelling techniques where the approach based on 1D beam elements appeared to be most attractive due to their efficiency and affordability in real life applications. However, a major challenge in developing such reduced order FE models is the inclusion of all relevant physical effects and their coupling in the condensed (1D) formulation for thin-walled composite beams.

The developments of an efficient technique based on a one-dimensional beam finite element model for the analysis of thin-walled laminated composite beams having

open/closed sections under different scenarios are presented in this thesis in the form of a number of papers as outlined in following section.

1.2. Scope of the present work

The primary objective of this research is to develop a new formulation for efficient yet accurate analysis of thin-walled laminated composite beams having open and closed cross section with minimal level of computational cost. In order to achieve this aim, the following objectives are fulfilled.

Objective 1- Develop a generalized model for the prediction of free vibration characteristics of thin-walled laminated composite beams having open and closed cross sections. The beam cross-sectional matrices necessary for stiffness and mass matrices are derived analytically for box and I sections which are utilised in developing the 1D beam finite element required for vibration analysis. For the implementation of this model, a computer program is developed using FORTRAN which is used to study the free vibrational response of various composite beams.

Objective 2- Develop a model based on similar considerations for buckling analysis of thin-walled laminated composite beams having open and closed cross sections. The beam cross-sectional matrices necessary for geometric stiffness matrices are derived analytically for box and I sections and these are used along with the stiffness matrices (Objective 1) to develop the 1D beam finite element for buckling analysis of these beams. A computer program developed using MATLAB for its implementation which is used to predict the buckling characteristics of various beams with or without preloads in the form of axial force and end moments.

Objective 3- Develop a model for preloaded vibration of thin-walled laminated composite beams having open and closed cross section. The effects of preloads were explored taking a wide number of cases where the preload can be axial force, end moments and their combinations. It is two stage analysis where a buckling problem is solves to get the critical buckling load. The vibration analysis is conducted in the second phase taking a fraction of the critical load as preload. A computer program is developed using MATLAB for the implementation of this model utilising stiffness matrices (Objective 1), mass matrices (objective 1) and geometric stiffness matrices (objective 2) and the program is used to study the behaviour of these thin-walled laminated composite beams.

Objective 4- Develop an all-inclusive model for dynamic stability of these composite beams under axial load and end moments preload for both open and closed cross sections. It is a three stage analysis where an addition vibration analysis is needed to get boundaries of the instability region. For the implementation of the model, a computer program is developed using MATLAB which is applied to study the dynamic stability behaviour of various beam problems under different levels of axial and end moments preload.

1.3. Thesis Outline

This thesis is written in a publication-based format. The main body of this thesis consists of three journal papers and two conference papers which are presented in Chapters 2 to 4. In Chapter 5, the conclusions are drawn and recommendations for future work are discussed.

Chapter 2 (Journal Paper 1) [Sheikh AH, Asadi A, Thomsen, OT (2015) [2]] were initially presented in the 18th International Conference of Composite Structures [1]. The conference technical committee assessed all the submissions and suggested a selection of papers to be expanded as a full length journal paper and submitted to Composite Structures for publication. This is one of these selected papers which has finally been published in Composite Structures [2]. This paper presents analytical formulations and derives principal cross-sectional matrices corresponding to stiffness and mass matrices which are incorporated within a 1D beam finite element model for vibrational analysis of thin-walled laminated composite beams having open and closed section. Different examples were presented for I and box sections and different lamination scheme were taken to study the vibrational response of thin-walled composite beams (**Objective 1**).

Chapter 3 (Journal Paper 2) [Asadi A., Sheikh AH, Thomsen, OT (2018) [3]] This paper presents analytical formulations and derives principal cross-sectional matrices corresponding to geometric stiffness matrices which are incorporated along with the stiffness matrices within a 1D beam finite element model for buckling analysis thin-walled laminated composite beams having open and closed section under axial and end moments. Different numerical examples for both I and box sections are solved by this model taking different lamination scheme, boundary condition, axial load, end moments and simultaneous axial load and end moments as preloads to study the vibrational characteristics of thin-walled composite beams (**Objective 2**).

Sub-Chapter 3A (Conference Paper 1) [Asadi A., Sheikh AH, Thomsen, OT (2015) [4]] were presented in the 20th International Conference on Composite Materials [4]. This may be considered as a sub-set of journal paper 2. However, most of the numerical examples presented in this conference paper are different from those presented in the journal paper.

Chapter 4 (Journal Paper 3) [Asadi A., Sheikh AH, Thomsen, OT (2018) [5]] This paper presents a 1D beam finite element model utilising the relevant matrices derived in previous sections for static and dynamic instability analysis of preloaded thin-walled laminated composite beams having open and closed section. A number of examples were solved for both I and box sections taking different lamination scheme, boundary condition, axial load, end moments and simultaneous axial load and end moments as preloads to study the static and dynamic stability of thin-walled composite beams (**Objective 3 and 4**).

Sub-Chapter 4A (Conference Paper 2) [Asadi A., Sheikh AH (2017) [6]] were presented in the 9th Australasian Congress on Applied Mechanics [6]. This may be considered as a sub-set of paper 3. However, the numerical examples presented in this conference paper are different from those presented in the journal paper.

1.4. **Publications**

[1] A.H. Sheikh, A. Asadi, O.T. Thomsen, Vibration of Thin-Walled Laminated Composite Beams having Open and Closed Sections, 18th International Conference on Composite Structures (ICCS18) , Lisbon, Portugal, 2015

[2] A.H. Sheikh, A. Asadi, O.T. Thomsen, Vibration of Thin-Walled Laminated Composite Beams having Open and Closed Sections, Composite Structures 134(2015) 209–215.

[3] A. Asadi, A.H. Sheikh, O.T. Thomsen, Buckling Behaviour of Thin-Walled Laminated Composite Beams Having Open and Closed Sections Subjected to Axial Load and End Moment, Thin-walled Structures, Submitted, September 2018

[4] A. Asadi, A.H. Sheikh, O.T. Thomsen, Bucking and Vibration Characteristics of Thin-Walled Laminated Composite Beams Having Open and Closed Sections, 20th International Conference on Composite Materials (ICCM20), Copenhagen, Denmark, 2015

[5] A. Asadi, A.H. Sheikh, O.T. Thomsen, Vibrational and Dynamic Stability of Thin-Walled Laminated Composite Beams under Axial Load and End Moments, Journal of Sound and Vibration, Submitted, November 2018

[6] A. Asadi, A.H. Sheikh, Buckling of Thin-Walled Laminated Composite Beams Having Open and Closed Sections Subjected to Axial Load and End Moment,9th Australian Congress on Applied Mechanics (ACAM9), Sydney, Australia,2017

2. Chapter 2 – Vibration of Thin-Walled Laminated Composite Beams having Open and Closed Sections

Journal Paper 1, Published

A.H. Sheikh, A. Asadi, O.T. Thomsen, Vibration of Thin-Walled Laminated Composite Beams having Open and Closed Sections, Composite Structures 134(2015) 209–215.

Seminar Paper 1 –Presented

ICCS18 - 18th International Conference on Composite Structures
Event: Conference
Duration: 15 - 18 Jun 2015
City: Lisbon
Country: Portugal
Degree of recognition: International event

Statement of Authorship

Title of Paper	VIBRATION OF THIN-WALLED LAMINATED COMPOSITE BEAMS HAVING OPEN AND CLOSED SECTIONS
Publication Status	☑ Published ☐ Accepted for Publication ☐ Submitted for Publication ☐ Unpublished and Unsubmitted w ork w ritten in manuscript style
Publication Details	A.H. Sheikh, A. Asadi, O.T. Thomsen, Vibration of thin-walled laminated composite beams having open and closed sections, Composite Structures 134(2015) 209–215.

Principal Author

Name of Principal Author (Candidate)	Arash Asadi Khansari		
Contribution to the Paper	Developed model, programming, performed all the analyses, prepared Manuscript		
Overall percentage (%)	80%		
Certification:	This paper reports on original research I conducted during the period of my Higher Degree by Research candidature and is not subject to any obligations or contractual agreements with a third party that would constrain its inclusion in this thesis. I am the primary author of this paper.		
Signature		Date	9-NOV-2018

Co-Author Contributions

By signing the Statement of Authorship, each author certifies that:

i. the candidate's stated contribution to the publication is accurate (as detailed above);

ii. permission is granted for the candidate in include the publication in the thesis; and

iii. the sum of all co-author contributions is equal to 100% less the candidate's stated contribution.

Name of Co-Author	Abdul Hamid Sheikh		
Contribution to the Paper	Supervised research, Provided critical manuscript evaluation, acted as corresponding author		
Signature		Date	09/11/2018

Name of Co-Author	Ole Thybo Thomsen		
Contribution to the Paper	Provided critical manuscript evaluation		
Signature		Date	13 September 2018

Please cut and paste additional co-author panels here as required.

Composite Structures 134 (2015) 209–215

Contents lists available at ScienceDirect

Composite Structures

journal homepage: www.elsevier.com/locate/compstruct

Vibration of thin-walled laminated composite beams having open and closed sections

Abdul Hamid Sheikh [a,*], Arash Asadi [a], Ole Thybo Thomsen [b,c]

[a] School of Civil, Environmental and Mining Engineering, The University of Adelaide, Adelaide, Australia
[b] Engineering and the Environment, University of Southampton, Highfield, Southampton, United Kingdom
[c] Department of Mechanical and Manufacturing, Aalborg University, Aalborg, Denmark

ARTICLE INFO

Article history:
Available online 8 August 2015

Keywords:
Finite element model
Thin-walled composite beams
Warping
Shear deformation
Vibration frequency

ABSTRACT

An efficient technique based on one dimensional beam finite element analysis for vibration of thin-walled laminated composite beams having open and closed sections is proposed in this paper. The developed technique is quite generic which can accommodate any stacking sequence of individual walls and considers all possible couplings between different modes of deformation. The formulation has accommodated the effect of transverse shear deformation of walls as well as out of plane warping of the beam section where the warping can be restrained or released. The inclusion of shear deformation has imposed a problem in the finite element formulation of the beam which is solved successfully utilising a concept developed by one of the authors. A number of numerical examples of open section (I and C sections) beams and closed section box beams are solved by the proposed technique and the results predicted by the proposed model are compared with those obtained from literature as well as detailed finite element analysis using a commercial code. The results show a very good performance of the proposed modelling technique.

1. Introduction

The use of thin-walled beam like slender structures made of laminated composite materials is found in many engineering applications such as helicopter rotor blades, construction industry, long wind turbine blades and few other situations. The behavior of these structures can be accurately predicted by a detailed finite element model using three-dimensional (3D) or shell elements but the computational demand of such model is extremely high. In order to avoid this problem, a group of researchers tried to model these structures as a condensed one-dimensional (1D) beam elements which will drastically improve the computational efficiency but the major challenge in that approach is the formulation of a suitable beam element that will be able to capture all effects and their couplings found in these complex thin-walled composite structural system. This has drawn attention of a number of researchers which made this topic an active area of research in recent years. Some representative samples of these models are provided in references [1–8]. The studies carried out so far can be divided into two broad groups based on the technique used to determine the cross-sectional matrixes which can be used to formulate the one dimensional beam element. The first approach is based on 'analytical techniques' while the second approach uses a two-dimensional (2D) cross-sectional analysis based on a 2D finite element model for the determination of the cross-sectional matrixes which can be utilised to carry out the 1D beam analysis.

Hodges and his co-workers [3] have significantly contributed toward the development of the second approach where the three dimensional (3D) elasticity problem defining the deformation of these beam like structures is systematically divided into a one-dimensional (1D) beam problem and a 2D cross-sectional problem. This method is generally referred to as variational asymptotic beam section analysis (VABS) which is based on variational asymptotic method (VAM) [9]. This approach is also suitable for modelling solid and the thick walled cross-sections. The same group of researchers ([10–14]) has also attempted to solve the 2D cross-sectional problem defined within the framework of VAM analytically but this approach involves rigorous mathematical treatments to evaluate the cross-sectional stiffness coefficients.

Since the present paper is primarily focusing on the analysis of thin-walled composite beams, the analytical approach (first approach) is used for determination of cross-sectional matrixes. Moreover, the 2D finite element analysis or a complex mathematical treatment involved with the other approach is avoided in the present investigation. Specifically, the current study has adopted

* Corresponding author.
E-mail address: abdul.sheikh@adelaide.edu.au (A.H. Sheikh).

http://dx.doi.org/10.1016/j.compstruct.2015.08.025
0263-8223/

the analytical approach proposed by Sheikh and Thomsen [8] and extended to vibration. The different modes of deformation considered in the development of present closed-form analytical solution are axial, torsion, bi-axial bending, bi-axial shear as well as out of plane warping for the torsional deformation. The cross-sectional matrices are explicitly derived for the open I section, C section and closed box section. The present formulation considered both plane stress and plain strain conditions of a lamina. The 1D beam problem is solved by the finite element approximations. The incorporation of the out of plane warping displacement demands a C^1 continuous finite element formulation for the twisting rotation, which is accommodated using Hermetian interpolation functions. On the other hand, the usual treatment of the transverse shear deformation requires a C^0 formulation. This needs the use of reduced integration technique for avoiding any shear locking problem. The different degrees of continuity for the different modes of deformation and their coupling impose a problem for their numerical implementation. This problem is addressed satisfactorily utilising the concept proposed by Sheikh [15] which permits a full integration and avoid the problem of using any reduced integration. For the 1D beam finite element analysis, a three node beam element as shown in Fig. 1 has been developed.

A computer code is written in FORTRAN to implement the present formulation. Numerical examples of thin-walled composite beams having different cross sections and other conditions are analysed by the proposed model and the results obtained in the form of vibration frequencies are validated with the available results in literature. These results demonstrate a very good performance of proposed model.

2. Formulation

Fig. 2 shows a segment of the composite beam shell wall where x–y–z is taken as the global Cartesian coordinate system with x being directed along the beam axis which is passing through the centroid of the beam section. A local orthogonal coordinate system x–s–n is also defined where x–s plane passes through the tangential plane of beam wall mid-plane (local x-axis is parallel to the global x-axis) and n is directed along the wall thickness. The displacement components at the mid-plane of the shell wall in the local coordinate system (x–s–n) can be expressed in term of the global displacement components of the beam [1] as

$$\begin{aligned}\bar{u} &= U + y\theta_y + z\theta_z + \varphi\theta_x',\\ \bar{v} &= V\cos\alpha + W\sin\alpha - r\theta_x,\\ \bar{w} &= -V\sin\alpha + W\cos\alpha + q\theta_x,\end{aligned} \tag{1}$$

where φ is the warping function, θ_x is the torsional rotation and θ_y, θ_z are bending rotations of the cross-section of the beam along (not about) y and z, respectively. These bending rotations can be expressed as $\theta_y = -V' + \Psi_y$ and $\theta_z = -W' + \Psi_z$, where Ψ_y, Ψ_z are shear rotations of the beam section about z and y, respectively, and V', W' and θ_x' are respectively the derivatives of V, W and θ_x with respect to x.

It has been observed that the warping displacement of a closed section beam is relatively less than that of an open section beam [14] but the present formulation has considered the effect of warping in all cases. Considering the effects of bending and transverse shear deformation of the beam shell wall, the displacements at any point of the shell wall away from its mid-plane may be expressed as

$$\begin{aligned}u &= \bar{u} + n\left(-\tfrac{\partial\bar{w}}{\partial x} + \psi_{xn}\right),\\ v &= \bar{v} + n\left(-\tfrac{\partial\bar{w}}{\partial s} + \psi_{sn}\right),\\ w &= \bar{w},\end{aligned} \tag{2}$$

where ψ_{xn} and ψ_{sn} are shear rotations of the shell wall section about s and x, respectively. It is assumed that $\psi_{sn} = 0$ whereas ψ_{xn} can be expresses in terms of the corresponding global components (Ψ_y and Ψ_z) as $\psi_{xn} = -\Psi_y\sin\alpha + \Psi_z\cos\alpha$. Substituting this as well as Eq. (1) in the above Eq. (2), the displacements at any point within the shell wall along its local coordinate system (x–s–n) can be expressed in terms of the global displacement components of the 1D beam as

$$\begin{aligned}u &= U + (y - n\sin\alpha)\theta_y + (z + n\cos\alpha)\theta_z + (\varphi - nq)\theta_x',\\ v &= V\cos\alpha + W\sin\alpha - (r + n)\theta_x,\\ w &= -V\sin\alpha + W\cos\alpha + q\theta_x.\end{aligned} \tag{3}$$

With the above beam kinematics (3), the free vibration governing equation for the beam can be derived from its total energy. The total energy of a structure consists of strain energy (U) and kinetic energy (T) which can be used to derive the stiffness matrix [K] and mass matrix[M], respectively used in finite element analysis of the structure. As the derivation of the stiffness matrix [K] has already been shown elsewhere [8], it is not repeated here. Taking ρ as density of the material, the kinetic energy for free vibration of a beam may be written as

$$T = \frac{1}{2}\int_V \{\dot{U}\}^T\rho\{\dot{U}\}dv = -\frac{\omega^2}{2}\int_V \{U\}^T\rho\{U\}dv. \tag{4}$$

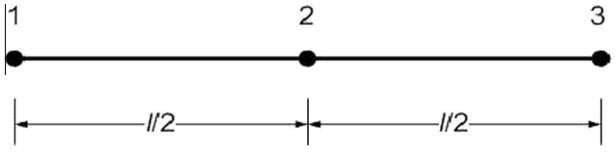

Fig. 1. A typical beam element.

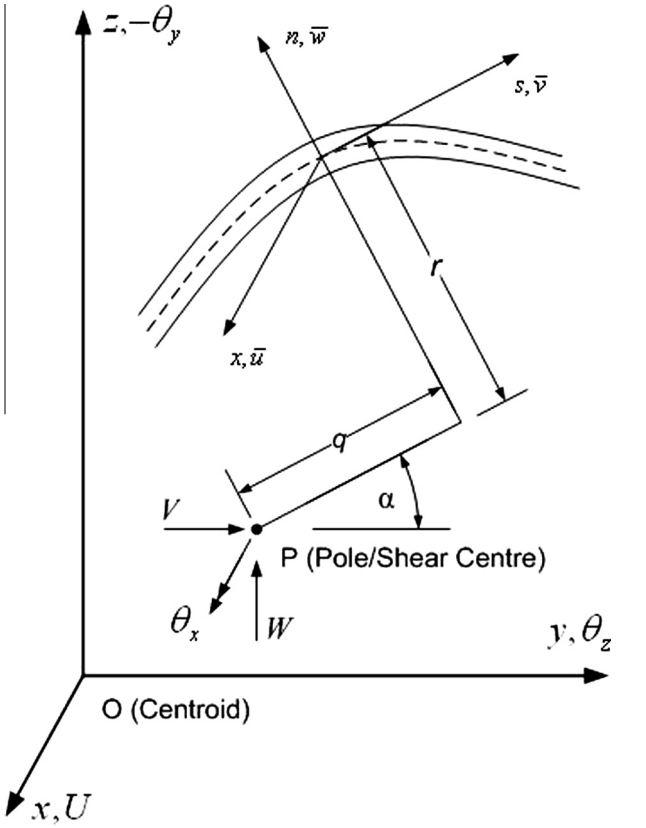

Fig. 2. Cross-section of a portion of beam shell wall with local and global coordinate system and displacement components.

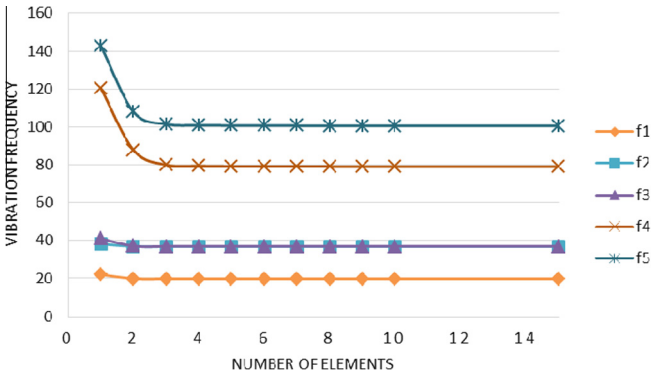

Fig. 3. Variation of natural frequencies with respect to the number of element.

Table 1
Natural frequencies of a 2 m long simply supported I-beam (Hz).

Lay-ups	References	Mode number					
		1	2	3	4	5	6
$[0]_{16}$	Present	24.16	35.21	45.04	96.29	109.39	177.75
	Vo and Lee [17]	24.19	35.23	45.24	96.73	109.44	180.62
	Kim et al. [16]	24.15	35.17	45.06	96.39	109.01	178.13
$[15/-15]_{4s}$	Present	22.97	36.11	42.84	91.60	107.44	169.31
	Vo and Lee [17]	23.00	36.25	43.00	91.94	107.66	171.68
	Kim et al. [16]	22.96	36.07	42.85	91.70	107.16	169.62
$[30/-30]_{4s}$	Present	19.80	36.83	36.95	79.03	100.62	146.46
	Vo and Lee [17]	19.82	37.05	37.86	79.23	102.16	147.94
	Kim et al. [16]	19.78	36.80	36.95	79.13	100.47	146.66
$[45/-45]_{4s}$	Present	16.48	30.76	35.16	65.80	90.52	122.14
	Vo and Lee [17]	16.49	30.83	37.92	65.92	94.88	123.09
	Kim et al. [16]	16.45	30.76	35.13	65.90	90.45	122.29
$[60/-60]_{4s}$	Present	14.66	27.36	32.24	58.53	82.03	108.68
	Vo and Lee [17]	14.67	27.42	35.37	58.63	87.05	109.48
	Kim et al. [16]	14.63	27.36	32.21	58.62	81.97	108.80
$[75/-75]_{4s}$	Present	14.07	26.26	29.97	56.17	77.22	104.22
	Vo and Lee [17]	14.08	26.32	31.31	56.28	79.33	105.09
	Kim et al. [16]	14.04	26.26	29.95	56.26	77.15	104.34
$[0/90]_{4s}$	Present	13.96	26.05	29.16	55.74	75.73	103.37
	Vo and Lee [17]	13.97	26.12	29.18	55.85	75.77	104.29
	Kim et al. [16]	13.94	26.06	29.13	55.82	75.65	103.49

where ρ is the mass density of the material, ω is the vibration frequency, $\{U\}^T = [u\ v\ w]$ (Eq. (3)) is the displacement vector and $\{\dot{U}\} = d\{U\}/dt$ is the velocity vector. The displacement vector (Eq. (3)) can be conveniently written as

$$\{U\} = [H_m]\{\bar{u}\}. \tag{5}$$

where $[H_m]$ contains sectional parameters (y, z, n, r, φ, q, α dependent on y and z whereas $\{\bar{u}\}$ contains global parameters (U, V, W, θ_z, θ_y and θ_z) of the 1D beam (depended on x). After substitution of the above Eq. (5) in Eq. (4), it can be written as

$$T = -\frac{\omega^2}{2}\int_V \{U\}^T\rho\{U\}dv = -\frac{\omega^2}{2}\int_L \{\bar{u}\}^T[F_m]\{\bar{u}\}dx \tag{6}$$

where $[F_m] = \int_A [H_m]^T\rho[H_m]dsdn = \int(\int [H_m]^T\rho[H_m]dn)\,ds = \int([C_m])\,ds$

For I, C and box section beams, all elements of the above matrices $[F_m]$ and $[C_m]$ are explicitly derived which are given in Appendix A and B.

For finite element implementation of the beam, quadratic Lagrangian interpolation functions are used for the axial deformation while cubic Hermetian interpolation functions are used for torsional deformation which will ensure the desired C^1 continuity of torsional rotation (θ) as the displacement field (Eq. (3)) contains derivative of θ. As mentioned earlier, the bending deformations are treated in a different manner along with shear deformations

Table 2
Natural frequency (Hz) of a cantilever composite box-beam (fundamental mode).

Model	I	II	III	IV	V
Top Flange	$[30]_6$	$[45]_6$	$[15]_6$	$[0/30]_3$	$[0/45]_3$
Bottom Flange	$[-30]_6$	$[-45]_6$	$[15]_6$	$[0/30]_3$	$[0/45]_3$
Left Web	$[30/-30]_3$	$[45/-45]_3$	$[15]_6$	$[0/30]_3$	$[0/45]_3$
Right Web	$[30/-30]_3$	$[45/-45]_3$	$[15]_6$	$[0/30]_3$	$[0/45]_3$
Mode	TV	TV	VB	VB	VB
ANSYS			28.42	33.665	32.061
Vo et al. [18]+	21.80	14.86	32.02	34.47	32.41
Vo & Lee [19]*	22.07	15.13	38.65	35.53	32.52
Qin and Librescu [20]*	21.80	15.04	30.06	34.58	32.64
Chandra & Chopra [21]x	20.96	16.67	28.66	30.66	30.00
Present+	22.24	14.89	31.88	34.29	32.24

+ Includes shear effects.
* Shear effects not included.
x Experimental TV: twist-vertical bending coupling VB: vertical bending.

Table 3
Natural frequencies of a cantilever composite box-beam having an asymmetric lamination scheme.

Mode	Mitra et al. [22]			Vo and Lee [19]+	Vo et al. [18]+	Present+
	No shear	With Shear	ANSYS			
1	31.06	31.02	30.99	31.30	31.04	31.54
2	49.34	49.17	49.19	49.86	49.54	50.02
3	194.57	192.55	187.22	196.16	194.06	195.82
4	308.75	301.63	298.13	312.48	304.79	306.82
5	862.40	817.54	794.24	874.97	826.46	831.46
6	1757.35	1642.38	1680.80	1779.29	1659.92	1670.83
7	2107.33	2107.28	2111.70	2145.28	2145.09	2144.65
8	2619.31	2381.89	2349.40	2657.98	2437.71	2423.24
9	2771.02	2409.78	2418.00	2834.36	2440.04	2448.82
10	3321.34	3220.05	3198.00	3419.13	3262.88	3275.80

+ Includes shear effects.

following the concept of Sheikh [15] where the shear rotations Ψ_y and Ψ_z are adopted as field variables instead of θ_y and θ_z in addition to the bending displacements V and W. Taking a linear approximation of Ψ_y, Ψ_z and a cubic approximation of V and W, the field variables can be written as

$$\begin{aligned} U &= a_1 + a_2x + a_3x^2 \\ V &= a_4 + a_5x + a_6x^2 + a_7x^3 \\ W &= a_8 + a_9x + a_{10}x^2 + a_{11}x^3, \\ \Psi_y &= a_{12} + a_{13}x, \quad \Psi_z = a_{14} + a_{15}x \\ \theta_x &= a_{16} + a_{17}x + a_{18}x^2 + a_{19}x^3 \end{aligned} \tag{7}$$

Though Ψ_y and Ψ_z are taken as field variables, they are not used as nodal degrees of freedom. Interestingly, the corresponding nodal degrees of freedom are θ_y and θ_z which are introduced with the help of bending deformations and may be expressed using the above equations as

$$\begin{aligned} \theta_y &= \Psi_y - V' = a_{12} + a_{13}x - a_5 - 2a_6x - 3a_7x^2, \\ \theta_z &= \Psi_z - W' = a_{14} + a_{15}x - a_9 - 2a_{10}x - 3a_{11}x^2. \end{aligned} \tag{8}$$

The unknown constants ($a_1, a_2, a_3 \ldots a_{19}$) found in Eq. (7) can be replaced in terms of nodal displacement parameters by substitution of U, V, W, θ_y and θ_z (Eqs. (7) and (8)) at all three nodes of the beam element (Fig. 1), and θ_x (Eq. (7)) and its derivative θ'_x at the two end nodes as

$$\{\delta\} = [R]\{a\} \text{ or } \{a\} = [R]^{-1}\{\delta\} \tag{9}$$

where $\{a\}^T = [a_1\ a_2\ a_3 \cdots a_{19}]$, $[R]$ consists of coordinates (x values) of the 3 nodes and $\{\delta\}^T = [U_1\ V_1\ W_1\ \theta_{x1}\ \theta_{y1}\ \theta_{z1}\ \theta'_{x1}\ U_2\ V_2\ W_2\ \theta_{y2}\ \theta_{z2}\ U_3\ V_3\ W_3\ \theta_{x3}\ \theta_{y3}\ \theta_{z3}\ \theta'_{x3}]$ is the nodal displacement vector.

With the help of Eqs. (7–9), the vector $\{\bar{u}\}$ as defined in Eq. (5) may be expressed in terms of nodal displacement vector $\{\delta\}$ as

$$\{\bar{u}\} = [S_m]\{a\} = [S_m][R]^{-1}\{\delta\} = [B_m]\{\delta\}. \tag{10}$$

Again this equation is substituted in Eq. (6) and it is rewritten as

$$T = -\frac{\omega^2}{2}\int_L \{\bar{u}\}^T[F_m]\{\bar{u}\}dx = -\frac{\omega^2}{2}\int_L \{\delta\}^T[B_m]^T[F_m][B_m]\{\delta\}dx = -\frac{\omega^2}{2}\{\delta\}^T[M]\{\delta\} \tag{11}$$

where $[M] = \int_L [B_m]^T[F_m][B_m]dx$ is the mass matrix of an element.

The stiffness and mass matrices of all elements are assembled together to form the corresponding matrices of the whole structure. Taking the same notations of these assembled matrices, the governing equation of free vibrating beams may be expressed as

$$[K]\{\delta\} = \omega^2[M]\{\delta\} \tag{12}$$

This is an Eigen-value problem which is solved to get the vibration frequencies as Eigen values and modes of vibration as Eigen vectors.

3. Results and discussions

In the section, numerical examples of thin-walled composite beams having I, C and Box sections are solved using the proposed model and the results obtained are validated with the analytical and numerical results available in literature and/or produced with a detailed finite element analysis of these structures using a commercial code (ANSYS).

Example 1: The problem of a simply supported thin-walled composite I-beam having a span of 2 m is studied using plane stress condition ($\sigma_s = 0$) of the plies. The flanges are 50 mm wide and the web is 50 mm deep whereas all these walls are made with symmetrical laminates consist of 16 glass–epoxy layers each 0.13 mm thick. Material properties used for the glass–epoxy layers are: E_1 = 53.78 GPa, E_2 = 17.93 GPa, $G_{12} = G_{13}$ = 8.96 GPa, G_{23} = 3.45 GPa, ν_{12} = 0.25 and ρ = 1970 kg/m^3. Taking 30° fibre orientation for all layers, the beam is analysed using different number of elements and the variations of first five natural frequencies predicted by the proposed technique are plotted in Fig. 3. The results show a rapid and monotonic convergence of all these natural frequencies as the number of elements increased.

Example 2: The same beam used in the previous example is analysed with 10 elements taking different fiber orientations of the web and flanges. The first six vibration frequencies obtained in the present analysis are presented in Table 1 along with those produced by Kim et al. [16], and Vo and Lee [17] who studied this problem earlier with their approach. The table shows that the present results have good agreement with the existing results [16,17].

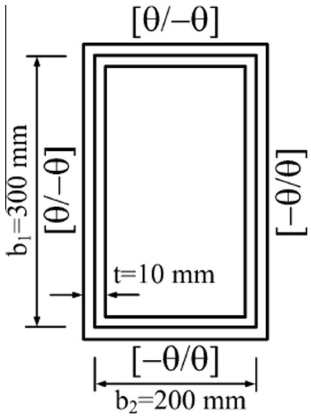

Fig. 4. Cross section and laminate configuration of a thin-walled composite box-beam.

Table 4
Non-dimensional natural frequencies for different fiber angle and $l/b_1 = 20$, all results includes shear effect.

Fiber Angle (θ)	Mode	1	2	3	4
0	Present	26.327	31.944	41.900	61.632
	Orthotropic Solution [18]	26.759	32.442	41.594	63.252
	FEM [18]	26.759	32.442	41.594	
15	Present	25.830	33.794	65.054	72.192
	Orthotropic Solution [18]	25.959	33.911	65.630	71.530
	FEM [18]	25.941	33.903	65.581	
30	Present	16.184	21.690	43.093	56.955
	Orthotropic Solution [18]	16.215	21.716	43.242	57.085
	FEM [18]	16.202	21.709	43.209	
45	Present	9.344	12.583	25.297	33.741
	Orthotropic Solution [18]	9.354	12.593	25.358	33.801
	FEM [18]	9.350	12.591	25.348	
60	Present	7.036	9.479	19.121	25.525
	Orthotropic Solution [18]	7.041	9.486	19.163	25.574
	FEM [18]	7.041	9.486	19.161	
75	Present	6.434	8.661	17.490	23.314
	Orthotropic Solution [18]	6.349	8.669	17.531	23.367
	FEM [18]	6.439	8.669	17.530	
90	Present	6.322	8.508	17.184	22.887
	Orthotropic Solution [18]	6.327	8.516	17.226	22.944
	FEM [18]	6.327	8.516	17.226	

Example 3: The behavior of an 844.5 mm long cantilever thin-walled composite beam having a box section (flange width: 24.21 mm, web depth: 13.46 mm) made of 6-ply laminates (thickness of each ply: 0.127 mm) for all walls is investigated for different ply orientations of the flanges and webs. The material properties used for these layers are: E_1 = 141.9 GPa, E_2 = 9.78 GPa, $G_{12} = G_{13}$ = 6.13 GPa, G_{23} = 4.8 GPa, ν_{12} = 0.42, ρ = 1445 kg/m^3. Taking plane stress condition ($\sigma_s = 0$) of the plies, the analysis is carried out with 13 elements in all cases and the results obtained are presented in Table 2 along with those of Vo et al. [18], Vo and Lee [19], Qin and Librescu [20] and experimental results of Chandra and Chopra [21]. The table shows close agreements between the results for different model configurations.

The same beam is analysed again taking an asymmetric lamination scheme [0/90] and [90/0] for the top and bottom flanges respectively and similar configuration for the webs. A number of vibration frequencies obtain by the proposed technique are presented in Table 3 and compared with the results reported by Mitra et al. [22], Vo and Lee [19], and Vo et al. [18]. The table also includes results produced from a full-blown finite element model of the beam with eight-node brick elements which was undertaken by Mitra et al. [22] using the finite element code ANSYS. Table 3 shows an acceptable correlation between the results obtained from different approaches developed by different researchers.

Example 4: In order to study the effect of shear deformation on the natural frequencies and mode shapes as well as coupling between different modes of deformation, a 6 m long thin-walled composite box-beam having a cross-section as shown in Fig. 4 is analysed for different ply orientations taking different values of θ (Fig. 4). Taking clamped boundaries at the two ends of the beam, the analysis is carried out using plane stress condition of the plies which are having the following properties: E_1/E_2 = 25, G_{12}/E_2 = 0.6, $G_{12} = G_{13} = G_{23}$, ν_{12} = 0.25. The natural frequencies predicted by the proposed model are presented in non-dimensional forms ($\bar{\omega} = \omega l^2\sqrt{\rho/E_2}/b_1$) along with those obtained by Vo et al. [18] using two approaches in Table 4 which shows a good agreement between them.

Table 5
Natural frequencies for different ply orientations of the asymmetric laminated walls $[\pm\theta]_3$ of a clamped beam having a channel section.

Mode	Fibre Angle (θ)	0	15	30	45	60	75	90
1	Present[+]	15.931	14.345	9.781	6.174	4.708	4.281	4.121
	Ansys[*]	15.902	14.247	9.749	6.221	4.752	4.286	4.187
2	Present[+]	32.692	39.532	26.959	17.018	12.977	11.802	11.359
	Ansys[*]	34.549	39.187	26.874	17.153	13.099	11.813	11.540
3	Present[+]	43.890	40.662	37.271	25.031	19.262	17.485	16.798
	Ansys[*]	43.705	43.059	39.260	25.921	19.873	17.828	17.115
4	Present[+]	71.641	68.182	52.854	33.367	25.444	23.140	22.272
	Ansys[*]	72.895	68.591	52.687	33.632	25.678	23.155	22.615
5	Present[+]	73.098	77.480	55.454	44.278	36.631	32.689	30.903
	Ansys[*]	75.059	76.756	66.488	55.605	4 2.446	38.267	32.479

[+] Includes shear effect.
[*] Detailed finite element model (ANSYS).

Table 6
Natural frequencies for different ply orientations of the symmetric laminated walls $[\theta]_6$ of a clamped beam having a channel section.

Mode	Fiber Angle (θ)	0	15	30	45	60	75	90
1	Present[+]	15.931	12.751	8.393	5.744	4.648	4.271	4.184
	Ansys[*]	15.904	10.498	6.754	5.210	4.536	4.260	4.187
2	Present[+]	32.692	35.105	23.127	15.833	12.812	11.774	11.534
	Ansys[*]	34.797	28.887	18.606	14.357	12.502	11.739	11.540
3	Present[+]	43.890	41.106	37.271	25.059	19.367	17.486	17.057
	Ansys[*]	43.712	37.865	27.752	21.599	18.771	17.502	17.115
4	Present[+]	71.641	68.156	45.318	31.042	25.120	23.086	22.616
	Ansys[*]	72.929	54.821	36.472	28.142	24.505	23.007	22.615
5	Present[+]	73.098	68.840	55.808	44.702	36.928	32.702	31.381
	Ansys[*]	75.534	56.590	56.314	46.488	40.482	35.150	32.479

[+] Includes shear effect.
[*] Detailed finite element model (ANSYS).

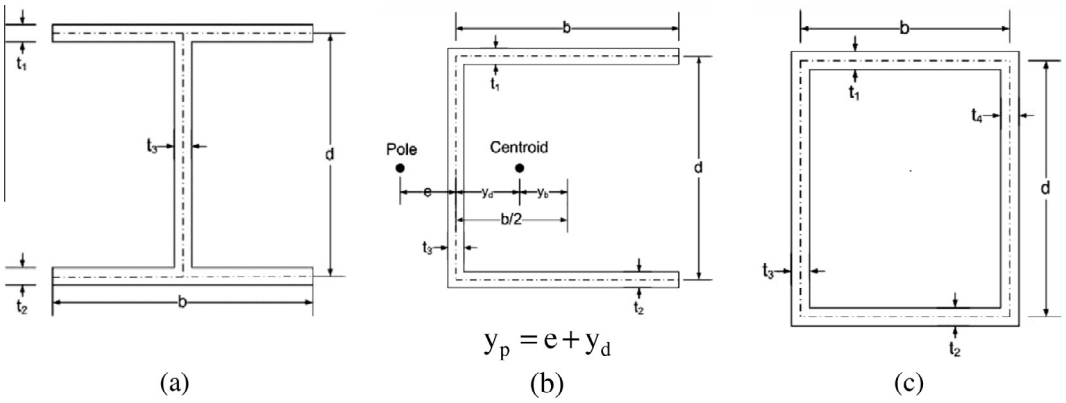

Fig. 5. Thin-walled beam having open and closed section.

Example 5: A 2 m long thin-walled composite beam having a channel section with 6 mm wide flanges 20 mm deep web is analysed with the proposed technique. The beam is clamped at its ends and all the walls are made of 6-ply asymmetrical laminate $[\pm\theta]_3$ where each ply has a thickness of 0.127 mm and the following material properties: E_1 = 141.9 GPa, E_2 = 9.78 GPa, G_{12} = G_{13} = 6.13 - GPa, G_{23} = 4.8 GPa, ν_{12} = 0.42, ρ = 1445 kg/m^3. For the validation of the present results, a detailed finite element analysis of the beam using 8 node shell elements is carried out using ANSYS. The results produced by the two approaches are presented in Table 5 which shows a very good performance of the proposed beam element. In this example, the pole/shear centre (Fig. 2) of the beam section and its centroid are located in different places where the distance between them (y_p) is calculated based on method proposed by Shan and Qiao [23].

In order to study the effect of ply orientations of the laminated walls further, the beam is analysed again in a similar manner taking symmetric layup $[\theta]_6$ of the walls and the results obtained for different values of θ are presented in Table 6. A closed examination of the results shows a conformity between the results produced by the proposed beam model and the detailed finite element model (ANSYS) in most of the cases. However, some visible differences are found when the fiber angle varied from 15° to 45°. A review of the mode shapes found from the detailed finite element model of the beam shows a pronounced sectional distortion which is not considered in the beam model.

4. Conclusions

An efficient one dimensional beam element is developed for vibration analysis of thin-walled composite beams of open and closed cross sections considering axial displacement, torsion, bi-axial bending and transverse shear deformations as well as out of plane sectional warping. The cross-sectional matrices required for the formulation of mass matrices of the beam are derived analytically where all possible couplings between the abovementioned modes of deformation are considered. The effect of shear deformation of the beam walls is included which requires a C^0 continuous finite element formulation of the bending deformation coupled with the shear deformation. On the other hand, the torsional deformation requires a C^1 continuous FE formulation due to the incorporation of warping deformation. The difficulty associated with the implementation of both these formulations in the present coupled problem is successfully overcome by using a novel concept of one of the authors. The proposed analysis technique is used to solve numerical examples of thin-walled laminated composite beams having open I, C and closed box sections taking different boundary conditions and stacking sequences of the beam walls. In many cases, the results predicted by the proposed technique are validated with the analytical and/or numerical results available in literature. The agreement between the results is found to be very good in most of the cases which ensures the reliability and range of applicability of the proposed element. New results are also presented in this paper which should be useful to future researchers.

Appendix A.

The non-zero elements appeared in the upper triangle of the symmetric matrix $[C_m]$ (Eq. (6)) are presented in their explicit form as follows (applicable for I, C and box sections).

$$C^m_{11} = C^m_{22} = C^m_{33} = A, \quad C^m_{15} = Ay, \quad C^m_{16} = Az, \quad C^m_{17} = A\phi,$$
$$C^m_{24} = -A(q\sin\alpha + r\cos\alpha),$$

$$C^m_{34} = A(q\cos\alpha - r\sin\alpha), \quad C^m_{44} = A(q^2 + r^{\wedge 2}) + C/12,$$
$$C^m_{55} = Ay^2 + C\sin^2\alpha/12,$$

$$C^m_{56} = Ayz - C\sin(2\alpha)/24, \quad C^m_{57} = Ay\phi + Cq\sin\alpha/12,$$
$$C^m_{66} = Az^2 + C\cos^2\alpha/12,$$

$$C^m_{67} = Az\phi - Cq\cos\alpha/12, \quad C^m_{77} = A\phi^2 + Cq^2/12$$

where $A = \sum t_i\rho_i$, $B = \sum t_i^2\rho_i$ and $C = \sum t_i^3\rho_i$

Appendix B.

The non-zero elements appeared in the upper triangle of the symmetric matrix $[F_m]$ (Eq. (9)) are presented in their explicit form as follows (applicable for I section, Fig. 5a).

$$F^m_{11} = F^g_{22} = F^g_{33} = b_1A_1 + b_2A_2 + dA_3,$$
$$F^m_{16} = -F^m_{24} = d(b_1A_1 - b_2A_2)/2,$$

$$F^m_{44} = (b_1^3A_1 + b_2^3A_2 + d^3A_3)/12 + d^2(b_1A_1 + b_2A_2)/4 + (b_1C_1 + b_2C_2 + dC_3)/12,$$

$$F^m_{55} = (b_1^3A_1 + b_2^3A_2)/12 + dC_3/3, \quad F^m_{57} = d(b_1^3A_1 - b_2^3A_2)/24,$$
$$F^m_{66} = d^3A_3/12 + d^2(b_1A_1 + b_2A_2)/4 + (b_1C_1 + b_2C_2)/3,$$
$$F^m_{77} = d^2(b_1^3A_1 + b_2^3A_2)/48 + d^3C_3/36$$

The non-zero elements appeared in the upper triangle of the symmetric matrix $[F_m]$ (Eq. (9)) are presented in their explicit form as follows (applicable for channel section, Fig. 5b).

$$F^m_{11} = F^g_{22} = F^g_{33} = b(A_1 + A_2) + dA_3, \quad F^m_{15} = by_b(A_1 + A_2) - dy_dA_3,$$

$$F^m_{16} = -F^m_{24} = bd(A_1 - A_2)/2, \quad F^m_{17} = bd(A_1 - A_2)(y_b + 2y_d - y_p)/2$$

$$F^m_{34} = b(A_1 + A_2)(y_b + y_p) - d(y_d - y_p)A_3,$$

$$F^m_{44} = b(A_1 + A_2)(b^2/12 + d^2/4 + (y_b + y_p)^2] + dA_3[d^2/12 + (y_d - y_p)^2] + [b(C_1 + C_2) + dC_3]/12,$$

$$F^m_{55} = b(A_1 + A_2)(b^2/12 + y_b^2) + dA_3y_d^2 + dC_3/12,$$
$$F^m_{56} = bdy_b(A_1 - A_2)/2$$

$$F^m_{57} = bd(A_1 - A_2)[b^2/12 + y_b(y_b + 2y_d - y_p)]/2,$$

$$F^m_{66} = d^3A_3/12 + bd^2(A_1 + A_2)/4 + b(C_1 + C_2)/12,$$

$$F^m_{67} = bd^2(A_1 + A_2)(y_b + 2y_d - y_p)/4 + d^3A_3(y_d - y_p)/12 - b(y_p + y_b)(C_1 + C_2)/12,$$

$$F^m_{77} = bd^2(A_1 + A_2)[b^2/48 + (y_b - y_p)^2/4 + y_d(y_d + y_b - y_p)] + d^3A_3(y_d - y_p)^2/12 + b(C_1 + C_2)[b^2/12 + (y_b) + (y_p)^2]/12 + d^3C_3/144$$

The non-zero elements appeared in the upper triangle of the symmetric matrix $[F_m]$ (Eq. (9)) are presented in their explicit form as follows (applicable for box section, Fig. 5c).

$$F^m_{11} = F^g_{22} = F^g_{33} = b(A_1 + A_2) + d(A_3 + A_4),$$
$$F^m_{15} = F^m_{34} = bd(A_4 - A_3)/2,$$

$$F^m_{16} = -F^m_{24} = bd(A_1 - A_2)/2,$$

$$F^m_{44} = [b^3(A_1 + A_2) + d^3(A_3 + A_4)]/12 + bd[d(A_1 + A_2) + b(A_3 + A_4)]/4 + [b(C_1 + C_2) + d(C_3 + C_4)]/12,$$

$$F^m_{55} = b^3(A_1 + A_2)/12 + b^2d(A_3 + A_4)/4 + d(C_3 + C_4)/3,$$
$$F^m_{57} = b^3d(A_1 - A_2)/24,$$

$$F^m_{66} = d^3(A_3 + A_4)/12 + bd^2(A_1 + A_2)/4 + b(C_1 + C_2)/3,$$
$$F^m_{67} = \beta bd^3(A_4 - A_3)/24,$$

$$F^m_{77} = \beta^2b^2d^2[b(A_1 + A_2) + d(A_3 + A_4)]/48 + \beta^2[b^3(C_1 + C_2) + d^3(C_3 + C_4)]/144 - \beta[b^3(C_1 + C_2) - d^3(C_3 + C_4)]/72 + [b^3(C_1 + C_2) - d^3(C_3 + C_4)]/144$$

References

[1] Bauld NR, Tzeng LS. A Vlasov theory for fiber-reinforced beams with thin-walled open cross section. Int J Solid Struct 1984;20(3):277–97.
[2] Chandra R, Stemple AD, Chopra I. Thin-walled composite beams under bending, torsion, and extensional load. AIAA J. 1990;27(7):619–26.
[3] Cesnik CES, Hodges DH. VABS: A new concept for composite rotor blade cross section modelling. J Am Helicopter Soc 1997;42(1):27–38.

[4] Kollar LP, Springer GS. Mechanics of Composite Structures. 1st ed. Cambridge University Press; 2003.
[5] Salim HA, Devalos JF. Torsion of open and closed thin-walled laminated composite sections. J Compos Mater 2005;39(6):497–524.
[6] Lee J. Flexural analysis of thin-walled composite beams using shear-deformable beam theory. Compos Struct 2005;70(2):212–22.
[7] Librescu L, Song O. Thin-Walled Composite Beams. 1st ed. Springer; 2006.
[8] Sheikh AH, Thomsen OT. An efficient beam element for the analysis of laminated composite beams. Compos Sci Technol 2008;68:2273–81.
[9] Berdichevsky VL. Variational-asymptotic method of constructing a theory of shell. PMM 1979;43(4):664–87.
[10] Volovoi VV, Hodges DH, Berdichevsky VL, Sutyrin VG. Asymptotic theory for static behaviour of elastic anisotropic I-beams. Int J Solids Struct 1999;36:1017–43.
[11] Volovoi VV, Hodges DH, Cesnik CES, Popescu B. Assessment of beam modelling methods for rotor blade applications. Math Comput Modell 2001;33:1099–112.
[12] Volovoi VV, Hodges DH. Single-and multi-celled composite thin-walled beams. AIAA J 2002;40:960–5.
[13] Volovoi VV, Hodges DH. Theory of anisotropic thin-walled beams. J Appl Mech 2000;67:453–9.
[14] Yu W, Hodges DH, Volovoi VV, Fuchs ED. A generalized Vlasov theory for composite beams. Thin Walled Struct 2005;43:1493–511.
[15] Sheikh AH. New Concept to include shear deformation in a curved beam element. J Struct Eng 2002;128(3):406–10.
[16] Kim N-I, Shin DK, Park Y-S. Dynamic stiffness matrix of thin-walled composite I-beam with symmetric and arbitrary laminations. J Sound Vib 2008;318:364–88.
[17] Vo TP, Lee J. Flexural-torsional coupled vibration and buckling of thin-walled open section composite beams using shear-deformable beam theory. J Mech Sci 2009;51(9–10):631–41.
[18] Vo TP, Lee J, Ahn N. On six fold coupled vibrations of thin-walled composite box beams. Compos Struct 2009;89:524–35.
[19] Vo TP, Lee J. Free vibration of thin-walled composite box beams. Compos Struct 2007;84(1):11–20.
[20] Qin Z, Librescu L. On a shear-deformable theory of anisotropic thin-walled beams: further contribution and validations. Compos Struct 2002;56(4):345–58.
[21] Chopra I, Chandra R. Experimental–theoretical investigation of the vibration characteristics of rotating composite box beams. J Aircraft 1992;29(4):657–64.
[22] Mitra M, Gopalakrishnan S, Bhat MS. A new super convergent thin walled composite beam element for analysis of box beam structures. Int J Solids Struct 2004;41(5–6):1491–518.
[23] Shan L, Qiao P. Flexural–torsional buckling of fiber-reinforced plastic composite open channel beams. Compos Struct 2005;68:211–24.

3. Chapter 3 - Buckling behaviour of thin-walled laminated composite beams having open and closed sections subjected to axial and end moment loading

Journal Paper 2, Submitted

A. Asadi, A.H. Sheikh, O.T. Thomsen, Buckling Behaviour of Thin-Walled Laminated Composite Beams Having Open and Closed Sections Subjected to Axial Load and End Moment, Thin-walled Structures, Submitted, September 2018

Statement of Authorship

Title of Paper	Buckling behaviour of thin-walled laminated composite beams having open and closed sections subjected to axial and end moment loading
Publication Status	☐ Published ☐ Accepted for Publication ☑ Submitted for Publication ☐ Unpublished and Unsubmitted w ork w ritten in manuscript style
Publication Details	A. Asadi, A.H. Sheikh, O.T. Thomsen,Buckling characteristics of thin-walled laminated composite beams having open and closed sections under axial load and end moment, Thin-Walled Structures

Principal Author

Name of Principal Author (Candidate)	Arash Asadi Khansari		
Contribution to the Paper	Developed model, programming, performed all the analyses, prepared Manuscript		
Overall percentage (%)	80%		
Certification:	This paper reports on original research I conducted during the period of my Higher Degree by Research candidature and is not subject to any obligations or contractual agreements with a third party that would constrain its inclusion in this thesis. I am the primary author of this paper.		
Signature		Date	9-Nov-2018

Co-Author Contributions

By signing the Statement of Authorship, each author certifies that:

i. the candidate's stated contribution to the publication is accurate (as detailed above);

ii. permission is granted for the candidate in include the publication in the thesis; and

iii. the sum of all co-author contributions is equal to 100% less the candidate's stated contribution.

Name of Co-Author	Abdul Hamid Sheikh		
Contribution to the Paper	Supervised research, Provided critical manuscript evaluation , Acted as corresponding Author		
Signature		Date	09/11/2018

Name of Co-Author	Ole Thybo Thomsen		
Contribution to the Paper	Provided critical manuscript evaluation		
Signature		Date	13 September 2018

Please cut and paste additional co-author panels here as required.

Buckling behaviour of thin-walled laminated composite beams having open and closed sections subjected to axial and end moment loading

Arash Asadi[1], Abdul Hamid Sheikh[1] and Ole Thybo Thomsen[2]

[1] School of Civil, Environmental and Mining Engineering, the University of Adelaide, Adelaide, Australia
[2] Faculty of Engineering and Physical Sciences, University of Southampton, Highfield, Southampton, United Kingdom

Keywords: Thin-walled composite beams, buckling, shear deformation, warping, finite element modelling

ABSTRACT

An efficient modelling technique based on one dimensional (1D) beam finite element analysis for buckling of thin-walled laminated composite beams having open/closed sections is proposed. The formulation derived has sufficient generality for accommodating arbitrary stacking sequences of the individual beam section walls, and includes all possible couplings between axial, shear, bending and torsional modes of deformation. The effects of transverse shear deformation of the section walls and out-of-plane warping of the beam section are considered where provision exists to restrain or allow warping deformation. The incorporation of shear deformation leads to a problem in the finite element implementation of the proposed beam kinematics, but this is successfully addressed adopting a novel modelling concept. Numerical results obtained for the sample cases of open sections I beams and closed section box beams are presented. The numerical results are benchmarked/compared to data available in open literature, and it is shown that the proposed model performs very well. Finally, a study of the effect of axial and end moment loading, acting alone or in combination, on the buckling response of thin-walled composite beams is presented.

1. INTRODUCTION

1.1. Background

The use of long beam like structural components having a thin-walled construction is common in many real-life engineering products such as wind turbine blades, helicopter rotor blades, aero-structures, ship masts and many other civil engineering applications such as composite beams, columns and reinforcement. In recent years, laminated fibre reinforced composite materials (hereinafter referred to as composites) have gained widespread acceptance and usage as structural materials in various engineering products including the above mentioned structural applications. The rationale is that composites helps to enhance the structural performance significantly due to high specific strength and stiffness in addition to high fatigue resistance and durability. The use of composite structural elements utilising multi-layered composite laminates with arbitrary fibre orientations of the individual layers (plies) provide a high degree of flexibility in tailoring the structural performance, but this can lead to complexities in their behaviour due to couplings between different modes of deformation. Thus, the use of composites introduces additional challenges in the modelling of composite structures of thin-walled construction, which is already inherently complex for thin-walled structures made from isotropic materials due to warping deformation and other characteristic behaviours. In principle, the load-response behaviour of the thin-walled construction composite structural elements of open or closed cross section may be analysed using a 3D modelling strategy based on solid or shell finite elements (FE), but this modelling technique is unfeasible in many cases due to high computational cost and time. To address

this problem previous research available in open literature has proposed to develop alternative modelling techniques, preferably based on 1D FE beam elements, which leads to more efficient and affordable techniques for modelling [e.g. 1-9]. However, a real and significant challenge in developing such reduced order 1D FE models is the inclusion of all relevant physical coupling effects in the condensed (1D) formulation for thin-walled composite beams.

The relevant previous research can be broadly divided into two groups based on the approaches used for determining the constitutive matrix of the beam element. The first approach is based on 'analytical techniques', while the second alternative utilises a two-dimensional (2D) cross-sectional analysis based on a 2D finite element model for calculating the cross-sectional matrices. Hodges et al. [3,10,11] have contributed significantly toward the development of the second approach, which has significant merit in terms of generality, but the 2D finite element analysis needed for the evaluation of cross-sectional stiffness coefficients is a major task. This was experienced and documented in a recent study [12], which is based on a similar approach. On the other hand, the first option (analytical approach), like that presented in Ref. [6], adopted in this paper does not require 2D finite element analysis, nor does it involve the complex mathematical operations involved with the second approach.

1.2. Review of analytical approaches

Vo & Lee et al. studied the behaviour of thin-walled composite beams having open [e.g. 13] and closed [e.g. 14] sections, including buckling analysis. It is observed that their analyses are mostly based on classical lamination theory, thus neglecting the effect of transverse shear deformation of the composite laminated section walls. However, composite laminates are generally weak in transverse shear due to their low shear stiffness and strength relative to the extensional rigidity and strength. Thus, it is important to incorporate the effect of shear deformation to ensure reliable predictive capability for all relevant loading scenarios. In order to address this issue, Vo & Lee [15] incorporated the effect of shear deformation, but the treatment adopted for the finite element implementation of torsional deformations is not promising. They [15] simply extended the concept used for the incorporation of transverse shear deformation in a typical isoparametric FE formulation to express the torsional deformation by introducing an additional parameter. This parameter is analogous to the transverse shear strain but, unfortunately, it does not have any real physical representation. Moreover, the formulation faced the difficulty of breaking down the torsional moment into three components as they attempted to express the beam response behaviour of these beams in terms of stress resultants. With this treatment for the torsion, they [15] succeeded to derive their beam element using an isoparametric formulation for all deformation modes. The element has three nodes thus providing a quadratic interpolation of all (seven) field variables using Lagrangian interpolation functions giving seven degrees of freedom at each node.

Kim et al. [16-18] also considered the effect of shear deformations following the concept introduced by Vo & Lee [15] and encountered similar difficulties. Thus, for the finite element implementation of the beam theory, an isoparametric formulation for all field variables to develop a beam element having C^0 continuous deformations was adopted. The well-known shear locking problem is typically faced in isoparametric elements as this formulation use the same interpolation functions for all field variables. A simple solution of this problem is the application of a reduced integration technique, as adopted by Kim et al. [16-18], but that may lead to spurious zero energy modes for some cases in addition to stress oscillations within the element. Moreover, the reduced integration will affect the evaluation of the stiffness

corresponding to other modes of deformation, including axial and torsion modes and their couplings. Furthermore, it is also difficult to apply a selective reduced integration scheme in this coupled problem. However, Kim et al. [e.g. 16-18] have contributed significantly in this area through investigating various aspects of thin-walled section composite beams.

Piovan and Cortinez [19] developed a shear deformable beam element following a different approach which seems to be interesting. The beam element has also incorporated the effects of warping. In order to avoid shear locking problem, the implementation of shear deformation has been achieved by defining transverse displacement and its derivatives as done in classical beam model, but an additional term been added to the expression for the derivative of transverse displacement. This additional term contributes to the shear deformation, but it is a function of material property and geometry of the element which need to be calculated for individual cases separately. Also, this term seems to be constant over the beam length. The same treatment has also been applied to the torsional deformation of the beam taking torsional rotation and its derivative accompanied with a similar function.

Ascione et al. [20] proposed another interesting approach where different plate elements forming the beam section are taken separately as beams and they are connected at their longitudinal edges using spring elements. This approach helped to accommodate different features including shear deformation, but this model needs more unknowns as it will have multiple nodes at any cross-section.

The formulations presented by both these groups [14,16] are consistent when the contribution of shear deformation is neglected. For this case, the Lagrangian interpolation functions are only used for the axial deformation, whereas other deformation modes, i.e. torsion and bending (bi-axial), are interpolated with Hermitian interpolation functions. Thus, these elements provide C^0 continuity (1 degree of freedom at each node – field variable only) for the axial displacement, and C^1 continuity (2 degrees of freedom at each node – field variable and its derivative) for the other modes of deformation.

1.3. Proposed Model

The aim of this this study is to develop a consistent formulation that includes the effect of shear deformation as composite materials are compliant/weak in shear as mentioned above. In this formulation, the issues associated with the existing modelling approaches e.g. [15,18], discussed in detail above, will be overcome by introducing an alternative approach. The proposed formulation will be applied to study the buckling characteristics of thin-walled composite beams with open or closed cross sections subjected to axial forces, end moments and combinations of these. The different modes of deformation and their coupling included in the formulation include: axial, torsional, bi-axial bending, bi-axial shear as well as warping (for torsion) deformation. The cross-sectional stiffness property matrices are derived in closed-form for both open and closed beam cross sections, including the assumption of both plane stress and plain strain conditions at the lamina level. Once the cross-sectional matrices of these thin-walled composite beams are derived, the remaining part of the analysis is the formulation and solution of the 1D beam problem, which in this study is achieved by adopting a finite element approximation.

Numerical examples of thin-walled composite beams having different cross sections, material configurations, boundary conditions and other features have been analysed by the proposed model, and the results obtained are presented in terms of predicted critical buckling loads (axial and end moment loads) and buckling mode-shapes. A significant amount of the

numerical predictions have been compared and benchmarked against results available in literature, and it is demonstrated that the proposed modelling approach provides a very close match with other model predictions, and that it generally performs very well. New numerical results are also presented for a number of problems that may be beneficial to future research efforts in this area.

2. MODEL FORMULATION

2.1. Finite element formulation – basic concepts

The conventional treatment adopted for incorporating transverse shear deformation in an isoparametric finite element context requires a C^0 continuous formulation, whilst the warping displacement produced by torsion requires a C^1 continuous formulation for the twisting rotation. The C^1 formulation for the torsional deformation is conveniently achieved in this study by using cubic Hermitian interpolation functions, including the angle of twist and its derivative at the two end nodes of the proposed beam element, see Fig. 1. Alternatively, if the C^0 continuous formulation is adopted for the transverse shear deformation, this will require adoption of a reduced integration technique, but its implementation is problematic in the present coupled problem as discussed above. This is a crucial issue, which in this study is addressed adopting the approach proposed by Sheikh [22], which eliminates the need for do reduced integration.

Adopting the above, a three noded beam element as shown in Fig.1 has been developed, where the end nodes have seven degrees of freedom (three displacements, three rotations and the derivative of the torsional rotation), and the middle node has five degrees of freedom (three displacements, two bending rotations). It should be noted that quadratic Lagrangian interpolation functions are used to model the axial deformation taking one degrees of freedom at each node. A computer code was written in MATLAB for the implementation of the formulation.

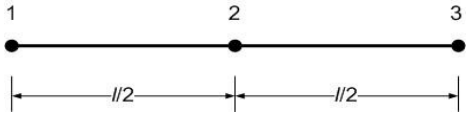

Fig. 1: Schematic of beam finite element

2.2. Kinematics of the beam deformations

Fig. 2 shows part of the cross section of a laminated beam wall segment along with global and local coordinate systems and their corresponding displacement components, which form the basis for the development of the proposed formulation. The curved geometry of the section wall is shown to represent a generic scenario, but the section walls can also be of straight geometry.

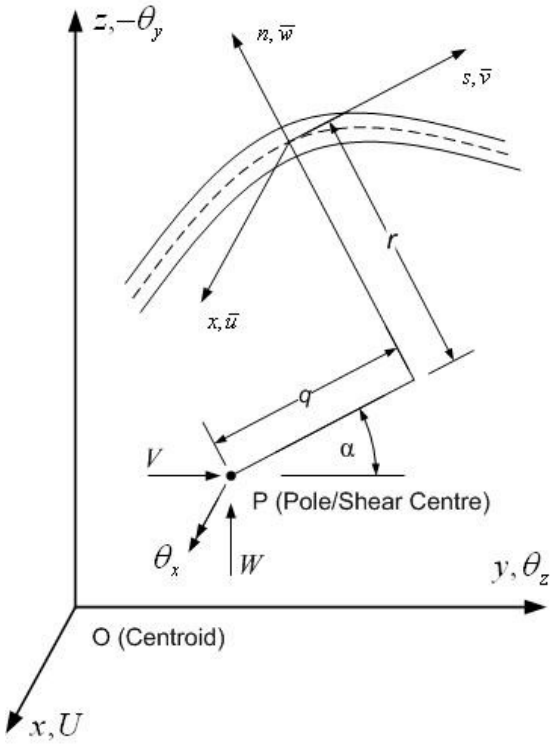

Fig. 2: Cross section of a beam section wall segment with local and global coordinate system and corresponding displacement components

In Fig. 2 *x*-*y*-*z* axes define the global Cartesian coordinate system, where *x* is along the beam axis, passing through the centroid of the complete beam cross section, and y, z define the beam cross section coordinates. The other axes are the local orthogonal coordinate system *x*-*s*-*n*, defined at the mid-plane of a laminated section wall, where *n* is normal to the shell (wall) mid-plane, *s* is the circumference coordinate, and *x* is parallel to global *x* coordinate axis. The displacement components at the mid-plane of the shell wall in the local coordinate system (*x*-*s*-*n*) can be expressed in terms of the global displacements of the beam (Fig. 2) in the form [22]:

$$\begin{aligned} \bar{u} &= U + y\theta_y + z\theta_z + \phi\,\theta_x', \\ \bar{v} &= V\cos\alpha + W\sin\alpha - r(s)\theta_x, \\ \bar{w} &= -V\sin\alpha + W\cos\alpha + q(s)\theta_x, \end{aligned} \tag{1}$$

where θ_y, θ_z are bending rotations (including shear deformations) of the beam cross section relative to the along *y* and *z* axes, respectively, θ_x is the torsional rotation of the beam cross section relative to the *x* axis, and φ is the warping function. *U*, *V* and *W* are the displacement components in the global *x*, *y* and *z* coordinate directions. Defining Ψ_y, Ψ_z as cross-sectional rotations due to shear deformations of the beam section about the *y* and *z* axes, the bending rotations can be expressed as $\theta_y = -V' + \Psi_y$ and $\theta_z = -W' + \Psi_z$, respectively, and V', W' and θ_x' are the derivatives of *V*, *W* and θ_x with respect to *x*.

Although the effects of warping displacement in beams having closed cross sections is generally not as significant as for beams with open cross section [21], the contribution of

warping displacements is incorporated for both types of cross sections to deliver a generic formulation.

The displacement at any point of the shell wall located at a distance *n* from the shell wall mid-plane can be expressed in terms of the bending and transverse shear deformations of the wall as:

$$\begin{aligned} u &= \overline{u} + n\left(-\frac{\partial \overline{w}}{\partial x} + \psi_{xn}\right), \\ v &= \overline{v} + n\left(-\frac{\partial \overline{w}}{\partial s} + \psi_{sn}\right), \\ w &= \overline{w}, \end{aligned} \tag{2}$$

where ψ_{xn} and ψ_{sn} are rotations of the shell wall sections due to shear deformations about *s* and *x*, respectively. Now, ψ_{xn} can be expressed in terms of the corresponding global cross section rotations (Ψ_y, Ψ_z) as $\psi_{xn} = -\Psi_y \sin\alpha + \Psi_z \cos\alpha$, whereas $\psi_{sn} = 0$ based on the restrictive assumption that the overall shape of the beam cross section will not be altered during the deformation of the beam.

Substituting the above expressions for ψ_{xn} and ψ_{sn} as well as Eq. (1) into Eq. (2), the displacements at any point within the shell wall along its local coordinate system (*x*-*s*-*n*) can be expressed in terms of the global displacement components of the 1D beam as follows:

$$\begin{aligned} u &= U + \left(y - n\sin\alpha\right)\theta_y + \left(z + n\cos\alpha\right)\theta_z + \left(\phi - nq(s)\right)\theta_x', \\ v &= V\cos\alpha + W\sin\alpha - \left(r(s) + n\right)\theta_x, \\ w &= -V\sin\alpha + W\cos\alpha + q(s)\theta_x \end{aligned} \tag{3}$$

2.3. Energy systems of the beam

The potential energy (Π) of a beam undergoing buckling caused by an external forces can be expressed in terms of the strain energy (*U*) and the work done by external forces (W_e) as:

$$\Pi = U - W_e \tag{4}$$

Now the strain energy appeared in the above equation can be expressed in terms of stress $\{\sigma\}$ and strain $\{\varepsilon\}$ vectors of the shell walls expressed in their local axis system (*x*-*s*-*n*) as:

$$U = \frac{1}{2}\int \{\varepsilon\}^T \{\sigma\}\, dv \tag{5}$$

The relationship between the above stress and strain vectors for a ply of the laminated shell wall having any orientation can be expressed using its constitutive matrix $[\bar{Q}]$ following 'classical lamination theory' (CLT) as described in texts on mechanics of composite materials [4] as:

$$\{\sigma\}=\begin{Bmatrix}\sigma_x\\ \sigma_s\\ \sigma_{xs}\\ \sigma_{xn}\\ \sigma_{sn}\end{Bmatrix}=\begin{bmatrix}\bar{Q}_{11} & \bar{Q}_{12} & \bar{Q}_{16} & 0 & 0\\ \bar{Q}_{21} & \bar{Q}_{22} & \bar{Q}_{26} & 0 & 0\\ \bar{Q}_{61} & \bar{Q}_{62} & \bar{Q}_{66} & 0 & 0\\ 0 & 0 & 0 & \bar{Q}_{55} & \bar{Q}_{54}\\ 0 & 0 & 0 & \bar{Q}_{45} & \bar{Q}_{44}\end{bmatrix}\begin{Bmatrix}\varepsilon_x\\ \varepsilon_s\\ \varepsilon_{xs}\\ \varepsilon_{xn}\\ \varepsilon_{sn}\end{Bmatrix}=\left[\bar{Q}\right]\{\varepsilon\} \tag{6}$$

The above equation is written in terms of all five stress and strain components typically occurring in a shell element, but some of these components will not be present in the present problem due to the restrictive assumption adopted that the beam cross section will not change shape during deformation. Thus, there will be no bending and shear deformations in the *s-n* plane, which leads to $\psi_{ns}=0$ and $\sigma_s=0$ (usually defined as plane stress condition) or $\varepsilon_s=0$ (plane strain condition). By incorporating this the above equation reduces to:

$$\{\sigma\}=\begin{Bmatrix}\sigma_x\\ \sigma_{xs}\\ \sigma_{xn}\end{Bmatrix}=\begin{bmatrix}\tilde{Q}_{11} & \tilde{Q}_{16} & 0\\ \tilde{Q}_{61} & \tilde{Q}_{66} & 0\\ 0 & 0 & \tilde{Q}_{55}\end{bmatrix}\begin{Bmatrix}\varepsilon_x\\ \varepsilon_{xs}\\ \varepsilon_{xn}\end{Bmatrix}=\left[\tilde{Q}\right]\{\varepsilon\} \tag{7}$$

where $\tilde{Q}_{11}=\bar{Q}_{11}$, $\tilde{Q}_{16}=\bar{Q}_{16}$, $\tilde{Q}_{66}=\bar{Q}_{66}$ and $\tilde{Q}_{55}=\bar{Q}_{55}$ for plane strain condition ($\varepsilon_s=0$); and $\tilde{Q}_{11}=\bar{Q}_{11}-\bar{Q}_{12}\bar{Q}_{12}/\bar{Q}_{22}$, $\tilde{Q}_{16}=\bar{Q}_{16}-\bar{Q}_{12}\bar{Q}_{26}/\ \bar{Q}_{22}$, $\tilde{Q}_{66}=\bar{Q}_{66}-\bar{Q}_{16}\bar{Q}_{16}/\bar{Q}_{22}$ and $\tilde{Q}_{55}=\bar{Q}_{55}$ for plane stress ($\sigma_s=0$) condition.

The substitution of the expressions for the local displacement components, at any point of the shell wall in terms of the global displacement components (Eq. 3), into the reduced strain vector (Eq. (7)), leads to:

$$\{\varepsilon\}=\begin{Bmatrix}\partial u/\partial x\\ \partial u/\partial s+\partial v/\partial x\\ \psi_{xn}\end{Bmatrix}=\begin{Bmatrix}U'+\left(y-n\sin\alpha\right)\theta_y'+\left(z+n\cos\alpha\right)\theta_z'+\left(\phi-nq\right)\theta_x''\\ \Psi_y\cos\alpha+\Psi_z\sin\alpha-\left(2n+r-\partial\phi/\partial s\right)\theta_x'\\ -\Psi_y\sin\alpha+\Psi_z\cos\alpha\end{Bmatrix} \tag{8}$$

The local strain vector can now be decoupled in terms of the cross section stiffness matrix ($[H]$) and strain vector of the beam ($\{\bar{\varepsilon}\}$) which contains global displacement parameters for 1D beam as :

$$\{\varepsilon\}=[H]\{\bar{\varepsilon}\} \tag{9}$$

where

$$\{\bar{\varepsilon}\}=\left\{U' \quad \theta_y' \quad \theta_z' \quad \theta_x'' \quad \theta_x' \quad V'+\theta_y \quad W'+\theta_z\right\}^T$$

$$[H]=\begin{bmatrix}1 & y-n\sin\alpha & z+n\cos\alpha & \phi-nq & 0 & 0 & 0\\ 0 & 0 & 0 & 0 & -\left(2n+r-\phi_{,s}\right) & \cos\alpha & -\sin\alpha\\ 0 & 0 & 0 & 0 & 0 & \sin\alpha & \cos\alpha\end{bmatrix} \tag{10}$$

By substitution of Eqs. (7-9) into Eq. (5), the strain energy of the system can be expressed as:

$$U = \frac{1}{2}\int \{\varepsilon\}^T \{\sigma\}\, dv = \frac{1}{2}\int \{\bar{\varepsilon}\}^T [H]^T \left[\tilde{Q}\right] [H] \{\bar{\varepsilon}\}\, dnds dx = \frac{1}{2}\int \{\bar{\varepsilon}\}^T [D] \{\bar{\varepsilon}\}\, dx \tag{11}$$

where

$$[D] = \int \left(\int [H]^T \left[\tilde{Q}\right] [H]\, dn \right) ds = \int [C]\, ds \tag{12}$$

All individual elements of the matrix [*C*] are derived explicitly in closed form. Similarly, all elements of the cross sectional stiffness matrix [*D*] are derived specifically and in closed form for open I section and closed box section profiles having generic geometric configurations, as depicted in Fig. 3. This includes general specification of cross section dimensions, and arbitrary lay-up (stacking sequence) of the cross section walls in terms of choice of material, number of plies, and ply orientations. The explicit expressions for the components of [*C*] and [*D*] are derived in a previous article by the authors [23].

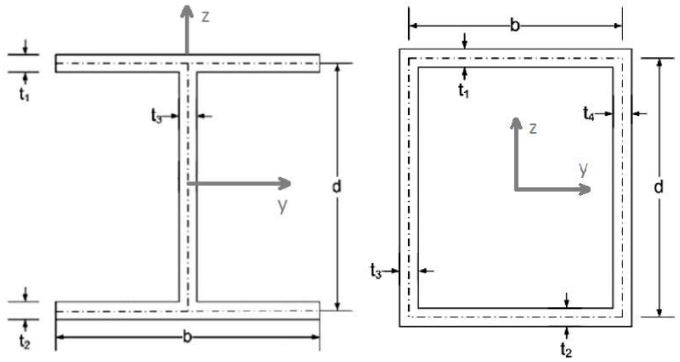

Fig. 3: Thin-walled beam having open and closed section

For the purpose of this study the warping function φ used in the above equations are taken as:

$$\phi = \int r ds - 2A_c \delta_s / \delta \tag{13}$$

where $\delta_s = \int \frac{ds}{\tilde{Q}_{66}}$, $\delta = \oint \frac{ds}{\tilde{Q}_{66}}$. For a closed beam cross section profile A_c is the cross-sectional area enclosed by the wall mid-plane line/contour. For an open section profile, the warping function may be simply obtained by dropping the second term associated with secondary warping, thus giving $\phi = \int r ds$.

The external forces considered in this study, which will be causing the buckling of the thin-walled composite beams are axial force (P_0) and end moment (M_0) loading. Both these forces induce only one stress component, the axial stress (σ_x), which can be expressed in simple form and used to formulate the problem conveniently, i.e.:

$$\sigma_x = \frac{P_\circ}{A} + \frac{M_0^y}{I_y} z \tag{14}$$

where A and I_y are cross-sectional area and moment of inertia of the beam cross sectional area. It should be noted that the above equation will give a stress that can be defined as an equivalent stress. The aim here to estimate this stress in a simple way without affecting the results significantly rather than undertaking a detailed analysis for predicting the stress distribution over the individual layers precisely. The work done (W_e) by the external forces P_0 and M_0 can be expressed as:

$$W_e = \frac{1}{2}\int_V \sigma_x (v'^2 + w'^2)\, dv = \frac{1}{2}\int_V \{v' \quad w'\}\, \sigma_x \begin{Bmatrix} v' \\ w' \end{Bmatrix} dv = \frac{1}{2}\int_V \{\varepsilon_g\}^T\, \sigma_x \{\varepsilon_g\}\, dv \tag{15}$$

Using Eq. (3), the geometric strain vector $\{\boldsymbol{\varepsilon}_g\}$ in the above equation can be written as

$$\{\varepsilon_g\} = \begin{Bmatrix} v' \\ w' \end{Bmatrix} = \begin{bmatrix} cos\,\alpha & sin\,\alpha & -(r+n) \\ -sin\,\alpha & cos\,\alpha & q \end{bmatrix} \begin{Bmatrix} V' \\ W' \\ \theta_x' \end{Bmatrix} = [H_g]\{\bar{\varepsilon}_g\}. \tag{16}$$

Eqs. (14) and (16) may be substituted into Eq. (15) leading to:

$$\begin{aligned} W_e &= \frac{P_0}{2A}\int_V \{\varepsilon_g\}^T \{\varepsilon_g\}\, dv + \frac{M_0}{2I_y}\int_L \{\varepsilon_g\}^T z \{\varepsilon_g\}\, dv \\ &= \frac{P_0}{2A}\int_L \{\bar{\varepsilon}_g\}^T \left[F_g^P\right]\{\bar{\varepsilon}_g\}\, dx + \frac{M_0}{2I_y}\int_L \{\bar{\varepsilon}_g\}^T \left[F_g^M\right]\{\bar{\varepsilon}_g\}\, dx \end{aligned} \tag{17}$$

where

$$\begin{aligned} \left[F_g^P\right] &= \int_A \left[H_g\right]^T \left[H_g\right] ds\, dn = \int \left(\int \left[H_g\right]^T \left[H_g\right] dn\right) ds = \int \left(\left[C_g^P\right]\right) ds \\ \left[F_g^M\right] &= \int_A \left[H_g\right]^T z \left[H_g\right] ds\, dn \end{aligned} \tag{18}$$

The individual elements of the matrices $\left[C_g^P\right]$ are derived explicitly and provided in Appendix A. Also, all elements of the matrices $\left[F_g^P\right]$ and $\left[F_g^M\right]$ are derived for the considered generic I (open) and box (closed) beam sections and given in Appendix B.

2.4. Finite element formulation

For the 1D finite element implementation of the thin-walled beam theory based on the energy expressions presented in the previous section, quadratic Lagrangian interpolation functions are used for the axial deformation, while cubic Hermitian interpolation functions are used for the torsional deformation. This ensures the desired C^1 continuity of the torsional rotation (θ_x) as the strain vector (Eq. 8) contains second derivative of θ_x. As mentioned earlier, the bending deformations along with the shear deformations are treated in a different

manner following the approach introduced in [21] to eliminate the difficulties faced by other existing formulations [13-15], [16-18]. According to [21], the cross-sectional rotations Ψ_y and Ψ_z due to shear deformations are adopted as field variables instead of θ_y and θ_z in addition to the bending displacements *V* and *W*. adopting a linear approximation of Ψ_y, Ψ_z, and a cubic approximation of *V* and *W*, these field variables (*V*, *W*, Ψ_y and Ψ_z) along with the remaining two field variables (*U* and θ_x) can be expressed in the form:

$$\begin{aligned} U &= a_1 + a_2 x + a_3 x^2 \\ V &= a_4 + a_5 x + a_6 x^2 + a_7 x^3 \\ W &= a_8 + a_9 x + a_{10} x^2 + a_{11} x^3 \\ \Psi_y &= a_{12} + a_{13} x \\ \Psi_z &= a_{14} + a_{15} x \\ \theta_x &= a_{16} + a_{17} x + a_{18} x^2 + a_{19} x^3 \end{aligned} \tag{19}$$

It should be noted that Ψ_y and Ψ_z are defined as field variables, but they are not used as nodal degrees of freedom in the finite element formulation. The corresponding nodal degrees of freedom correspond to θ_y and θ_z which can be expressed in the following form θ_y and θ_z by invoking the above Eqs. (19):

$$\begin{aligned} \theta_y &= \Psi_y - V' = a_{12} + a_{13} x - a_5 - 2a_6 x - 3a_7 x^2 \\ \theta_z &= \Psi_z - W' = a_{14} + a_{15} x - a_9 - 2a_{10} x - 3a_{11} x^2 \end{aligned}, \tag{20}$$

The unknown constants (a_1, a_2, a_3 ..... a_{19}) appearing in Eqs. (19) can be replaced in terms of the nodal displacement vector $\{\delta\}$ by substitution of U, V, W (from Eqs. 19), $\boldsymbol{\theta}_y$ and $\boldsymbol{\theta}_z$ (from Eq. (20)) at all three nodes of the beam element (see Fig. 1), and θ_x (from Eqs. (19)) and its derivative θ_x' $\left(= a_{17} + 2a_{18} x + 3a_{19} x^2\right)$ at the two end nodes, thus giving:

$$\{\delta\} = [R]\{a\} \text{ or } \{a\} = [R]^{-1}\{\delta\} \tag{21}$$

where $\{a\}^T = \begin{bmatrix} a_1 & a_2 & a_3 & \cdots & a_{19} \end{bmatrix}$, $[R]$ consists of the coordinates (*x* values) of the three nodes and

$$\{\delta\} = \begin{Bmatrix} U_1 & V_1 & W_1 & \theta_{x1} & \theta_{y1} & \theta_{z1} & \theta'_{x1} & U_2 & V_2 & W_2 & \theta_{y2} & \theta_{z2} & U_3 & V_3 & W_3 & \theta_{x3} & \theta_{y3} & \theta_{z3} & \theta'_{x3} \end{Bmatrix}^T.$$

Using Eqs. (19-21), the strain vector of the beam $\{\bar{\varepsilon}\}$ as appearing in Eq. (9) can be expressed in terms of the nodal displacement vector $\{\delta\}$ as:

$$\begin{aligned} \{\bar{\varepsilon}\} &= \begin{Bmatrix} U' & \theta'_y & \theta'_z & \theta''_x & \theta'_x & V' + \theta_y & W' + \theta_z \end{Bmatrix}^T \\ &= [S(x)]\{a\} = [S(x)][R]^{-1}\{\delta\} = [B]\{\delta\} \end{aligned} \tag{22}$$

The above equation can be substituted into Eq. (11) and it is rewritten to get the stiffness matrix [*K*] of the beam element as

$$U = \frac{1}{2}\int \{\bar{\varepsilon}\}^T [D]\{\bar{\varepsilon}\}\, dx = \frac{1}{2}\{\delta\}^T \int [B]^T [D][B] dx \{\delta\} = \frac{1}{2}\{\delta\}^T [k]\{\delta\} \tag{23}$$

Again Eqs. (19 - 21) can be substituted into the vector $\{\bar{\varepsilon}_g\}$ as found in Eq. (16) and it can further be expressed in terms of $\{\delta\}$ as:

$$\{\bar{\varepsilon}_g\} = \begin{bmatrix} V' & W' & \theta_x' \end{bmatrix}^T = [S_g(x)]\{a\} = [S_g(x)][R]^{-1}\{\delta\} = [B_g]\{\delta\} \tag{24}$$

The above equation is substituted into Eq. (17) and rewritten in the form:

$$\begin{aligned} W_e &= \frac{P_0}{2A}\int_L \{\delta\}^T \left[B_g\right]^T \left[F_g^P\right]\left[B_g\right]\{\delta\}\, dx + \frac{M_0}{2I_y}\int_L \{\delta\}^T \left[B_g\right]^T \left[F_g^M\right]\left[B_g\right]\{\delta\}\, dx \\ &= \frac{P_0}{2}\{\delta\}^T \left[k_g^P\right]\{\delta\} + \frac{M_0}{2}\{\delta\}^T \left[k_g^M\right]\{\delta\} \end{aligned} \tag{25}$$

where $\left[k_g^P\right] = \frac{1}{A}\int_L \left[B_g\right]^T \left[F_g^P\right]\left[B_g\right] dx$ and $\left[k_g^M\right] = \frac{1}{I_y}\int_L \left[B_g\right]^T \left[F_g^M\right]\left[B_g\right] dx$ are the geometric stiffness matrix of the beam element corresponding to axial (P_0) and end moment (M_0) loads, respectively.

Now the strain energy (Eq. (23)) and the work done by the external forces (Eq. (25)) for all elements are substituted into the potential energy of the structural system (Eq. (4)), followed by minimisation with respect to the nodal displacements of the structure $\{\Delta\}$, to obtain the final governing equation of the thin-walled cross section beam as:

$$\left([K] - P_0\left[K_g^P\right] - M_0^y\left[K_g^M\right]\right)\{\Delta\} = 0 \tag{26}$$

where $[K]$ is the stiffness matrix of the structure, and $\left[K_g^P\right]$ and $\left[K_g^M\right]$ are the geometric stiffness matrices for the axial (*P*) and end moment (M_y) load cases, respectively. These are obtained by assembling their corresponding components of the individual elements.

Eq. (26) can be reduced to a simple Eigen-value problem by taking $M_0^y = 0$ or $P_0 = 0$, and this can be solved to obtain the critical value of the axial load (P_{CR}) or the critical value of the end moment (M_{CR}) as the Eigen value. For a beam subjected to combined axial force and end moments and displaying interaction between these loads, one of the load parameters should be specified (i.e. $M_0^y = M_0 < M_{CR}$ or $P_0 < P_{CR}$), whilst and the other parameter will be the unknown Eigen value that will be solved to obtain its critical value (i.e. P_{cr}^i or M_{cr}^i). A

given thin-walled beam problem can display multiple buckling modes that will provide multiple Eigen values as well as multiple Eigen vectors and mode shapes, which will be extracted from $\{\Delta\}$.

3. RESULTS AND DISCUSSION

In this section, numerical examples of thin-walled composite beams having I and box sections are analysed using the developed modelling approach. Initially, the results predicted are compared and benchmarked against analytical and numerical results available in literature to show the performance of the model proposed herein. After this, the results of parametric studies are presented to demonstrate the effect of different parameters on the buckling behaviour of the considered thin-walled cross section beams.

3.1. Benchmarking against results from literature

3.1.1. Buckling of a simply supported doubly symmetric I-section beam subjected to axial compression

A thin-walled laminated composite beam having a span of 6 m is studied assuming plane stress conditions ($\sigma_s = 0$) in the plies. A doubly symmetric I beam cross section is chosen with a flange width (b) of 600 mm and a depth (d) of 600 mm for its web. All flange and web plates are assumed to be made of four plies of 7.5 mm thickness (so $t_1 = t_2 = t_3 = 30$ mm - total thickness), and they are assumed to have identical stacking sequence. Five different stacking sequence configurations (Table 1) are considered to investigate the five different cases of the thin-walled I-beam. All plies are assumed to be made of graphite/epoxy with the following properties: E_1=144 GPa, E_2=9.65 GPa, G_{12}= G_{13}=4.14 GPa, G_{23}=3.45 GPa, ν_{12}=0.3. To show the convergence of the proposed model with respect to element size, a specific case having the stacking sequence of $[0/90]_S$ is considered and the results are presented in Fig. 4.

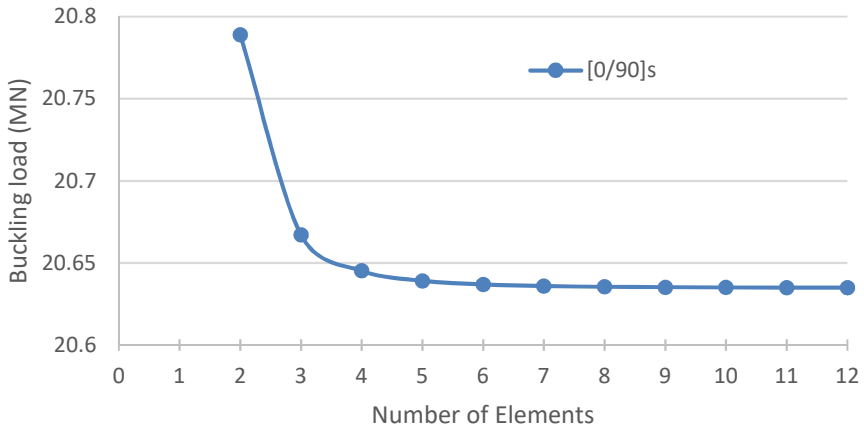

Fig. 4: Predicted buckling load of a simply supported double symmetric composite I-section ($[0/90]_S$) beam vs. number of elements

Fig. 4 shows that the predicted buckling load converges when the number of elements is 8 or more. Based on this observation, all other composite beams studied ahead are analysed with 10 elements unless mentioned otherwise.

The critical buckling loads predicted by the modelling approach developed in this study is shown in Table 1 for all five composite lay-up cases (outer right column). Table 1 also shows the corresponding buckling loads predicted by Vo & Lee [17], Machado & Cortinez [24], and Back & Will [25]. Considering the results predicted by the detailed 3D finite element model [25] (ABAQUS - high computational cost) as reference results in terms of accuracy, the proposed 1D beam element model (high computational efficiency) performed comparatively better than other modes. Though the model of Vo & Lee [15] performed well, the problem of their formulation for accommodating shear deformation has been explained in Section 1.

Table 1: Critical buckling load (in MN) of a simply supported doubly symmetric composite I-section beam

Lay-ups	Machado & Cortinez [24]		Back & Will [25]		Vo & Lee [15]	Present model
	No shear	Incl. shear	ABAQUS	Incl. shear	With shear	Incl. shear
$[0]_4$	42.11	33.18	30.78	28.85	30.38	30.93
$[\pm 30]_S$	-	-	13.06	13.17	13.17	13.16
$[\pm 45]_S$	4.45	4.44	4.41	4.41	4.41	4.41
$[\pm 60]_S$	-	-	2.89	2.89	2.88	2.88
$[0/90]_S$	22.57	19.84	20.41	20.63	20.63	20.63

3.1.2. Buckling of a cantilever mono-symmetric I-section beam subjected to axial compression

A cantilever mono-symmetric I section beam length of 1.0 m is investigated for seven different wall stacking sequences (see Table 2) assuming identical lay-up for all section walls in each case. The web of the beam is assumed to be 50 mm deep, and the top and bottom flanges are 30 mm and 50 mm wide, respectively. The web and flange walls/plates are made of 16 layers/plies each 0.13 mm thick with a symmetrical $[\pm\theta]_{4S}$ lay-up. The material assumed for all the layers is glass/epoxy with the following elastic properties E_1=53.78 GPa, E_2=17.93 GPa, G_{12}= G_{13}=8.96GPa, G_{23}=3.45, GPa, ν_{12}=0.25. The I-section beam has been analysed with the model proposed herein, and the critical buckling loads obtained for the seven different stacking sequences are presented in Table 2 along with numerical results reported by Kim et al. [16], and Vo & Lee [15]. The comparison of the results demonstrates an excellent match between the predictions obtained using the element proposed here and the results from [15, 16].

3.1.3. Buckling of a simply supported I-section beam under axial load and end moments

A composite I-section beam having a span of l = 8 m is analysed adopting a plane stress condition ($\sigma_s = 0$) for the plies. Both flanges are assumed to be 100 mm wide (b), and the section is assumed to be 200 mm deep (d). All section walls are made of two plies each 2.5 mm thick (total thickness: t = 5mm) with unidirectional $[0]_2$ lay-up for the top flange and the web, while the bottom flange is assumed to have a $[\pm\theta]$ lay-up. The material used for all the layers is assumed to have the following (normalised) elastic parameters: E_1/E_2=25, G_{12}/E_2=0.6, G_{13}=G_{23} =G_{12}, ν_{12}=0.25. The I-beam is first analysed with the proposed model to obtain the critical buckling load (P_{cr}) when the end moment is zero. Then, under the action of

three different values of the axial force ($P_0 < P_{cr}$), the critical end buckling moments (M_{cr}^i) corresponding to each of the different value of P_0 interactive scenarios are calculated. Note that $M_{cr}^i = M_{cr}$ for the case of no axial preload, i.e. $P_0 = 0$. These results, expressed in non-dimensional form ($\bar{P}_{cr} = P_{cr} l^2 / (d^3 t E_2)$; $\bar{M}_{cr}^i = M_{cr}^i l / (d^3 t E_2)$), are presented in Table 3 along with results obtained from Vo & Lee [14]. Table 3 shows that the predictions of the modelling approach proposed here show a good correlation with the results of [14]. Further, the effect of shear deformation is observable for the cases of end moment loading (only included in present model).

Table 2: Critical buckling load (N) of a mono-symmetric cantilever composite I-section beam with a symmetrical layup $[\pm\theta]_{4S}$

Lay-ups	Kim et al. [16]	Vo & Lee [15]	Present model
	No Shear	Incl. shear	Incl. shear
$[0]_{16}$	2998.2	2993.2	2994.5
$[\pm 15]_{4S}$	2811.8	2803.6	2803.3
$[\pm 30]_{4S}$	2199.7	2184.7	2185.1
$[\pm 45]_{4S}$	1561.9	1546.0	1547.2
$[\pm 60]_{4S}$	1241.3	1227.8	1229.0
$[\pm 75]_{4S}$	1134.5	1126.7	1127.9
$[0/90]_{4S}$	2113.9	2100.6	2101.8

Table 3: Critical buckling load $\bar{P}_{cr}$ and end moment $\bar{M}_{cr}^i$ with axial preload of a composite I-beam (bottom flange: $[\pm\theta]$, web and top flange: $[0]_2$)

$\frac{P_0}{P_{cr}}$	Critical Load	Reference	Fiber Angle θ (degree)						
			0	15	30	45	60	75	90
	$\bar{P}_{cr}$	Vo & Lee [14] *	5.153	4.565	2.771	1.631	1.259	1.140	1.112
		Present +	5.139	4.492	2.780	1.576	1.242	1.134	1.109
-0.5	$\bar{M}_{cr}^i$	Vo & Lee [14] *	10.175	9.233	6.071	4.265	3.655	3.448	3.397
		Present +	10.183	9.405	6.160	4.427	3.650	3.469	3.374
0	$\bar{M}_{cr}^i$	Vo & Lee [14] *	7.370	6.883	4.895	3.597	3.117	2.948	2.905
		Present +	7.372	6.885	4.833	3.540	3.184	2.821	2.821
0.5	$\bar{M}_{cr}^i$	Vo & Lee [14] *	4.451	4.042	2.498	1.819	1.621	1.553	1.536
		Present +	4.446	4.244	2.456	1.866	1.688	1.612	1.416

* Shear effects not included + Shear effects included

3.1.4. Buckling of a simply supported I-section beam under eccentric axial compression

The behaviour of a 5 m long I-section beam subjected to eccentric axial loading as shown in Fig. 5 is investigated. The application of a compression load with a constant known eccentricity (e) will induce a proportional end moment ($M_0 = P_0 e$). This enabled Eq. (26) to be expressed in terms of a single unknown load parameter (P_0), and the solution of this

equation provides the critical value of this load (P_{cr}^{i}) as the eigenvalue. For this sample case, all the section walls (including the web plate) are assumed to be 50 mm wide and made of 16 layers each 0.13 mm thick with a symmetrical $[\pm\theta]_{4S}$ lay-up. The material for all the layers is glass/epoxy assuming the following elastic properties: E_1=53.78 GPa, E_2=17.93 GPa, G_{12}= G_{13}=8.96 GPa, G_{23}=3.45 GPa, ν_{12}=0.25.

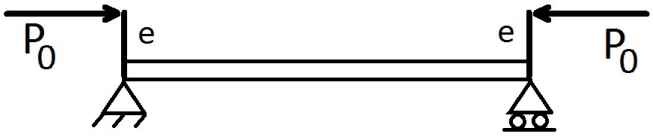

Fig. 5: Simply supported beam under eccentric axial load

The I-section beam has been analysed using the proposed model for three distinct values of the eccentricity; e = 0, h/4 and h/2, where h is the depth of the beam. The predicted values of P_{cr}^{i} by the proposed model are presented in Table 4 along with the results of Vo & Lee [14] and Kim et al. [26]. Again, it is found that predictions of the present model are in good agreement with the results obtained from ABAQUS [26] (a detailed 3D shell based finite element model using the commercial software Abaqus) as well as the predictions of [14].

Table 4: Effect of eccentricities on critical buckling loads (N) of a composite I-beam with a symmetrical $[\pm\theta]_{4S}$ lay-up for all walls

e	Reference	Layups					
		$[0]_{16}$	$[\pm15]_{4S}$	$[\pm30]_{4S}$	$[\pm45]_{4S}$	$[\pm60]_{4S}$	$[\pm75]_{4S}$
0	Vo & Lee [14] +	920.80	832.00	617.80	427.60	338.40	311.70
	Present +	920.56	831.76	617.68	427.60	338.33	311.69
$\frac{h}{4}$	Kim et al. [26] ABAQUS		809.20	608.10	423.50	335.50	308.60
	Kim et al. [26] Analytical *		810.70	608.70	423.70	335.60	308.60
	Vo & Lee [14] +	890.30	810.50	608.00	422.90	334.90	308.30
	Present +	890.63	810.69	608.63	423.36	334.64	308.03
$\frac{h}{2}$	Vo & Lee [14] +	818.60	757.50	582.20	410.00	325.30	298.80
	Present +	820.02	758.38	581.55	411.59	326.39	297.98

* Shear effects not included + Shear effects are included

3.1.5. Buckling of a simply supported box-section beam under axial load and end moments

The effect of different predefined axial loads on the critical end moments causing buckling of an 8 m long beam having a box section has been investigated as well. The box section is assumed to be of width b = 100 mm and depth d = 200mm, and different lay-up sequences are studied. All section walls are assumed to be made of two layers, each having a thickness of 2.5 mm (total thickness: t = 5mm), and with (relative) elastic properties of E_1/E_2=25, G_{12}/E_2=0.6, G_{13}=G_{23} =G_{12}, ν_{12}=0.25. The top and bottom flanges are assumed to have unidirectional $[0]_2$ lay-ups, and the webs have $[\pm\theta]$ lay-ups.

Initially, the box section beam is analysed using the method presented herein to estimate the critical buckling loads (P_{cr}) with no end moments being applied. Following this, the critical end moments (M^i_{cr}) are calculated for three different values of axial preloads; $P_0 = -0.5P_{cr}$, $P_0 = 0$, and $P_0 = +0.5P_{cr}$. The results are expressed in non-dimensional form, $\overline{P}_{cr} = P_{cr}l^2/(d^3tE_2)$ and $\overline{M}^i_{cr} = M^i_{cr}l/(d^3tE_2)$, and presented in Table 5 along with results reported by Vo et al. [13].

Table 5: Critical buckling load $\overline{P}_{cr}$ and moment $\overline{M}^i_{cr}$ with axial preload of a composite box-beam (flanges: $[0]_2$, webs: $[\pm\theta]$)

$\frac{P_0}{P_{cr}}$	Critical Load	Reference	Fiber Angle θ (degree)						
			0	15	30	45	60	75	90
	$\overline{P}_{cr}$	Vo et al. [13]*	36.009	29.245	13.549	7.858	6.67	6.419	6.375
		Present +	35.510	28.917	13.479	7.834	6.653	6.403	6.359
-0.5	$\overline{M}^i_{cr}$	Vo et al. [13]*	3.309	4.571	3.374	2.111	1.633	1.441	1.386
		Present +	3.269	4.519	3.324	2.098	1.611	1.428	1.379
0	$\overline{M}^i_{cr}$	Vo et al. [13]*	2.688	3.725	2.753	1.722	1.332	1.175	1.131
		Present +	2.660	3.681	2.711	1.712	1.315	1.165	1.125
0.5	$\overline{M}^i_{cr}$	Vo et al. [13]*	1.891	2.629	1.945	1.217	0.941	0.830	0.798
		Present +	1.874	2.597	1.915	1.210	0.929	0.823	0.795

* Shear effects not included + Shear effects are included

To study the effects of varying the stacking sequences of the section of the section walls further, the same box section beam is analysed in an exactly the same manner assuming $[\theta]_2$ stacking sequence for the top flange and the left web, and $[0]_2$ for the right web and the bottom flange. The coupling between the different loads will be more pronounced for the case of unsymmetrical stacking sequence scheme in comparison with the previous case (Table 5). The results predicted by the proposed model are presents in Table 6 along with results presented in. [13]. Table 5 and Table 6 show a good agreement between the results.

Table 6: Critical buckling load $\overline{P}_{cr}$ and moment $\overline{M}^i_{cr}$ with axial preload of a composite box-beam (top flange and left web: $[\theta]_2$, bottom flange and right web: $[0]_2$)

$\frac{P_0}{P_{cr}}$	Critical Load	Reference	Fiber Angle θ (degree)						
			0	15	30	45	60	75	90
	$\overline{P}_{cr}$	Vo & Lee [13]*	36.009	30.210	17.015	9.899	7.918	7.454	7.370
		Present +	35.510	29.964	16.820	9.808	7.870	7.415	7.304
-0.5	$\overline{M}^i_{cr}$	Vo & Lee [13]*	3.309	3.366	2.834	2.133	1.743	1.571	1.523
		Present +	3.283	3.346	2.842	2.133	1.742	1.570	1.519
0	$\overline{M}^i_{cr}$	Vo & Lee [13]*	2.688	2.741	2.322	1.748	1.427	1.285	1.246
		Present +	2.673	2.713	2.303	1.731	1.416	1.277	1.236
0.5	$\overline{M}^i_{cr}$	Vo & Lee [13]*	1.891	1.922	1.625	1.232	1.008	0.909	0.881
		Present +	1.884	1.897	1.605	1.209	0.991	0.895	0.867

* Shear effects not included + Shear effects included

3.2. Parametric Study

3.2.1. Buckling of a fully clamped I-section beam subjected to axial compression loading

A clamped I-section beam subjected to axial compression loading is considered. The effect of different fibre orientations (θ) of the bottom flange ($[\theta]_2$) with unaltered laminate lay-up ($[0/45]$) for the top flange and the web on the buckling behaviour is studied for different slenderness ratios (l/d) of the beam (l is length and d is the depth). The beam section is 300 mm deep and its flanges are 200mm wide. All section walls are assumed to be made of two layers having a thickness of 2.5mm giving a total wall thickness (t) of 5 mm, and the normalised elastic properties of these layers are specified to: E_1/E_2=25, G_{12}/E_2=0.6, G_{13}=G_{23} =G_{12}, ν_{12}=0.25. The asymmetry with respect to the top and bottom flange laminations is responsible for producing nonzero off-diagonal terms in the cross-sectional stiffness matrix (F_{13}, F_{16}, F_{24}, F_{35}, see Appendix B [23]), which in turn introduces coupling of different deformation modes. The variation of the critical axial load, as predicted by the proposed model, for varying values of θ, ranging from 0 to 90^0, is presented in Fig. 6 as a non-dimensional buckling load parameter ($\bar{P} = P_{cr} l^2 / (d^3 t E_2)$) taking l/d = 5 (short beam), 10 and 25 (long beam). It is seen that the critical buckling load decreased monotonically with increasing fibre angle (θ), where the effect is visibly pronounced when θ is ranging between 20^0 and 50^0. It is further observed that the effect of varying the slenderness ratio (l/d) is most prominent when θ is varied between 0 and 20^0, reduces gradually with increasing values of θ , to become negligible beyond 50^0. In order to show the contribution of shear deformation, the present formulation is amended to exclude the shear deformation by dropping the terms Ψ_y and Ψ_z. The amended formulation without shear deformation is used to produce in a similar manner and included in Fig. 6. Though a similar trend of results is obtained by the two formulations, but the contribution of shear deformation is found to be significant for l/d = 5 (short beam) specifically for lower range of θ and it is reduced with the increase of l/d ratio. It is also clear from the figure that the non-dimensional buckling load for all l/d ratios without shear deformation are identical and very close to shear deformable results for a long beam (l/d = 25).

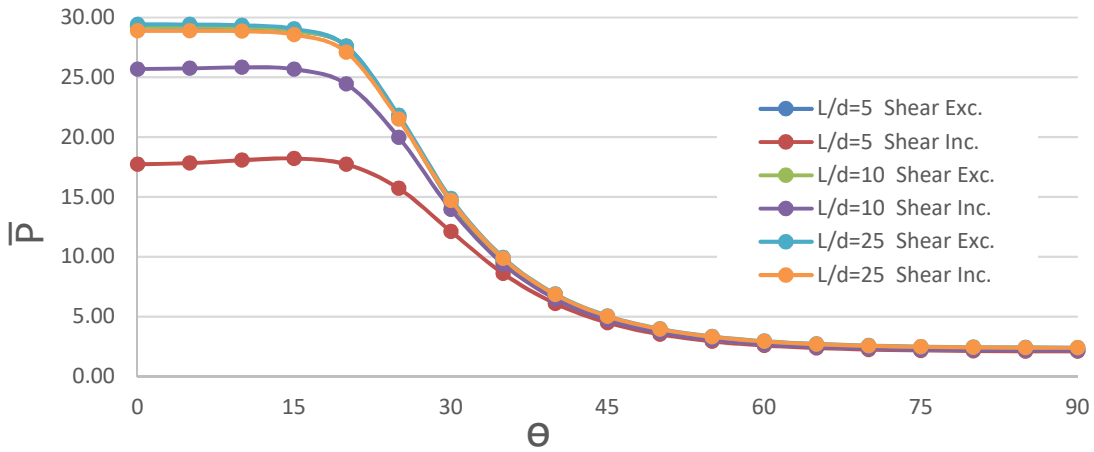

Fig. 6: Variation of buckling load parameter ($\bar{P}$) of a clamped I-section composite beam with respect to fibre angle (θ) of its bottom flange

The mode shapes the lateral displacements v and the torsional rotation θ_x (beam twist) corresponding to the specific parametric case of the beam; $\theta = 75°$, $l/d = 25$, $\bar{P}_1 = 2.48$, are plotted in Fig. 7, which shows a very pronounced coupled buckling response displaying combined bending and twist.

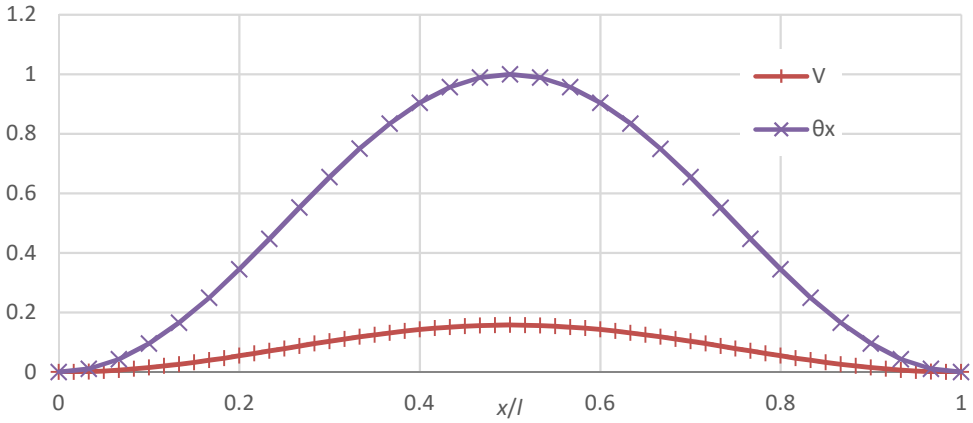

Fig. 7: Typical buckling mode shapes of a clamped I-section composite beam

3.2.2. Buckling of a simply supported I-section composite beam subjected to eccentric axial compression and end moment preloading

The case of a simply supported I-section composite beam subjected to combined eccentric axial compression and end moment loading is considered, see Fig. 8. It is assumed that the beam has the same material properties and geometry as discussed in section 3.1.4.

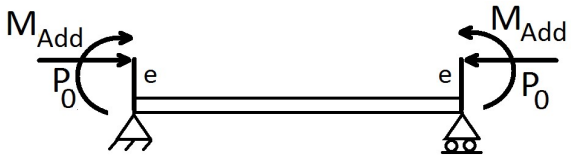

Fig. 8: Simply supported beam subjected to eccentric axial compression and end moment loading

In addition to the eccentric axial compression load P_0, additional end moments M_{Add} are applied as a preload, which are combined with the bending moments induced by the eccentric axial load as explained in section 3.1.4. Initially, the value of the axial load P_0 is taken as zero and the critical value of the end moment, $M_{Add} = M_{cr}$, is then calculated. Following this, different values of the end moment, $M_{Add} < M_{cr}$, are applied as preloading, and the critical value of the eccentric axial load P_{cr}^i is calculated. Utilising these results, the interaction curves for the eccentric axial force, $P_0 = P_{cr}^i$, and the preloading end moment, $M_{Add} = M_{cr}^i$, which produce buckling of the I-section beam, is plotted in Fig. 9 for three different eccentricities, e = 0, h/2 and h, and three different fibre angles, $\theta = 0, 30°$ and $60°$, for all section walls having $[\pm\theta]_{4s}$ lay-up.

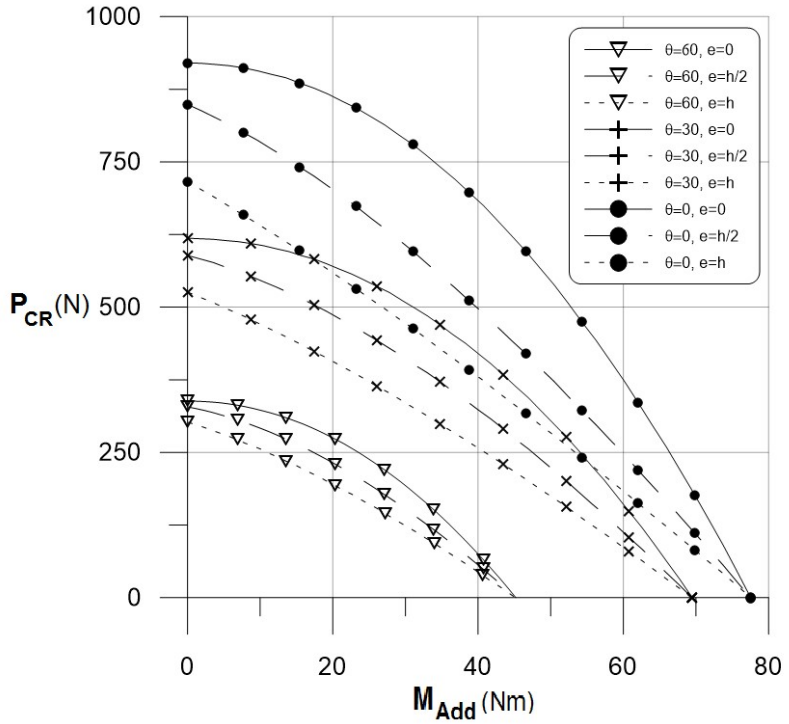

Fig. 9: Interaction between the eccentric axial loads and preloaded end moments for the buckling of a composite I-section beam

Fig. 9 shows that both the critical values of the axial force P_{cr}^{i} and the end moment M_{Add}^{i} decrease with increasing fibre angle θ. The reason for this is that the cross section stiffness reduces when the fibre angle θ is increased. Further, it is observed that the critical values of the axial loads and end moments are reduced when the loading eccentricity ***e*** is increased as expected.

3.2.3. Buckling of a cantilever I-section composite beam subjected to axial and end moment loadings

A cantilever I-section beam subjected to axial and end moment loading is considered, with a focus of investigating a wide range of interactions between the axial compression and the end moment loads. The following beam dimensions are assumed; span l = 8 m, flange width b=100 mm, web depth d = 200 mm. It is further assumed that all laminated section walls are of $[\pm\theta]_3$ lay-up, and that each ply is 1.25 mm thick (total thickness t = 7.5 mm). The following normalised material properties are assumed: E_1/E_2=25, G_{12}/E_2=0.6, G_{13}=G_{23} =G_{12}, ν_{12}=0.25. Initially the I-section beam is first analysed assuming only axial loading (i.e. no end moment) to determine the critical value, P_{cr}, and following that the case of pure end moment loading (i.e. no axial compression load) is analysed to evaluate M_{cr}. In the next stage, a parametric study is conducted in which the axial force P_0 is applied as a preload and varied over a wide range from $P_0 / P_{cr} = 0.8$ to $P_0 / P_{cr} = -0.8$ (axial tension) in increments of 0.2, followed by calculation of the critical end moment M_{cr}^{i} for each value of the axial preload. The results are expressed in non-dimensional form $\bar{M}_{cr}^{i} = M_{cr}^{i} l / (d^3 t E_2)$ and presented in Table 7 for different values of θ ranging from 0 to 90^0 with increments of 15^0. The results show that there is a stabilizing effects of axial tension on the buckling of the member for all

values of θ. Also, for all preload values, it is observed that $\bar{M}^i_{cr}$ increases while θ increases from 0 to 15^0 whereas $\bar{M}^i_{cr}$ decreases monotonically as θ increases beyond 15^0.

Table 7: Critical end moment $\bar{M}^i_{cr}$ for buckling of axially preloaded cantilever composite I-section beam with $[\pm\theta]_3$ lay-up in all section walls

$\frac{P_0}{P_{cr}}$	Fiber Angle θ (degree)						
	0	15	30	45	60	75	90
-0.8	12.8825	13.5666	7.5088	3.2986	1.9903	1.5811	1.4801
-0.6	11.7575	12.5667	7.0303	3.0983	1.8704	1.4853	1.3901
-0.4	10.6225	11.5416	6.5300	2.8873	1.7439	1.3843	1.2953
-0.2	9.4740	10.4841	6.0025	2.6629	1.6092	1.2769	1.1945
0.0	8.3064	9.3833	5.4398	2.4216	1.4641	1.1614	1.0862
0.2	7.1103	8.2217	4.8298	2.1576	1.3051	1.0349	0.9677
0.4	5.8683	6.9689	4.1516	1.8612	1.1265	0.8929	0.8347
0.6	4.5429	5.5639	3.3641	1.5137	0.9166	0.7263	0.6788
0.8	3.0263	3.8429	2.3605	1.0661	0.6459	0.5116	0.4780

Similarly, a parametric study is conducted in which the end moment M_0 is applied as a preload and varied over the range from $M_0 / M_{cr} = 0$ to 0.9 in increments of 0.1, followed by calculation of the critical axial load P^i_{cr} for each value of the end moment preload. The results are presented in Table 8 expressed in non-dimensional form $\bar{P}^i_{cr} = P^i_{cr} l / (d^3 t E_2)$ for the same range of fibre orientations θ. Results shows that the value of $\bar{P}^i_{cr}$ decreases monotonically with the increase of θ for all preload values.

3.2.4. Buckling of a simply supported I-section composite beam subjected to axial and end moment loadings

In this section the behaviour of a 10 m long I-section beam is studied in a similar manner as in the previous example analysing four different values of the flange width (*b*) and web height (*d*), while maintaining same cross-sectional area and wall thickness for all four cases. Fixed ply orientation ($\left[0/30^0/-30^0/90^0\right]_S$) is assumed for the web and flange plates, where each ply is assumed to 1.25 mm with the following normalised elastic properties: E_1/E_2=25, G_{12}/E_2=0.6, $G_{13}=G_{23}=G_{12}$, ν_{12}=0.25. The variation of critical axial load for the buckling of the four I-section beam cases subjected to preloading end moments are plotted in Fig. 10. Similarly, Fig. 11 presents the variation of the critical end moments causing buckling of I section beams when subjected to axial preloads. Both these figures (Figs. 10 and 11) show that the buckling resistance of these beams having same mass enhances with the increase of b/d ratio of the beam section i.e., a wide flanged beam performs better. In this case, the beam section with highest b/d ratio $(b=0.175, d=0.150)$ outperformed the other sections in terms of axial load and end moment buckling capacity.

Table 8: Critical axial force $\bar{P}_{cr}^{i}$ for buckling of end moment preloaded cantilever composite I-section beam with $[\pm\theta]_3$ lay-up for all walls under preloaded end moments

$\frac{M_0}{M_{cr}}$	Fiber Angle θ (degree)						
	0	15	30	45	60	75	90
0.0	5.1552	4.0337	1.4082	0.4551	0.2562	0.2141	0.2068
0.1	5.0673	3.9833	1.3930	0.4504	0.2536	0.2119	0.2046
0.2	4.8156	3.8341	1.3476	0.4362	0.2456	0.2052	0.1982
0.3	4.4289	3.5912	1.2725	0.4126	0.2324	0.1942	0.1875
0.4	3.9399	3.2625	1.1683	0.3799	0.2140	0.1787	0.1726
0.5	3.3767	2.8572	1.0361	0.3380	0.1905	0.1591	0.1535
0.6	2.7603	2.3849	0.8771	0.2872	0.1620	0.1352	0.1304
0.7	2.1055	1.8551	0.6924	0.2277	0.1285	0.1072	0.1034
0.8	1.4228	1.2762	0.4837	0.1598	0.0903	0.0753	0.0726
0.9	0.7193	0.6557	0.2524	0.0838	0.0474	0.0395	0.0381

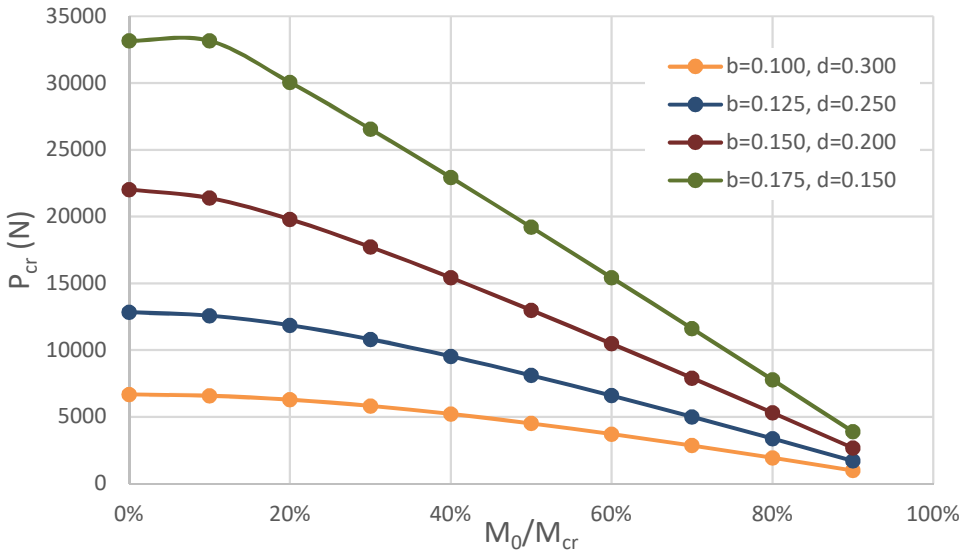

Fig. 10: Variation of buckling loads of composite I-section beams having the same cross section with different sectional parameters subjected to different end moment preloading

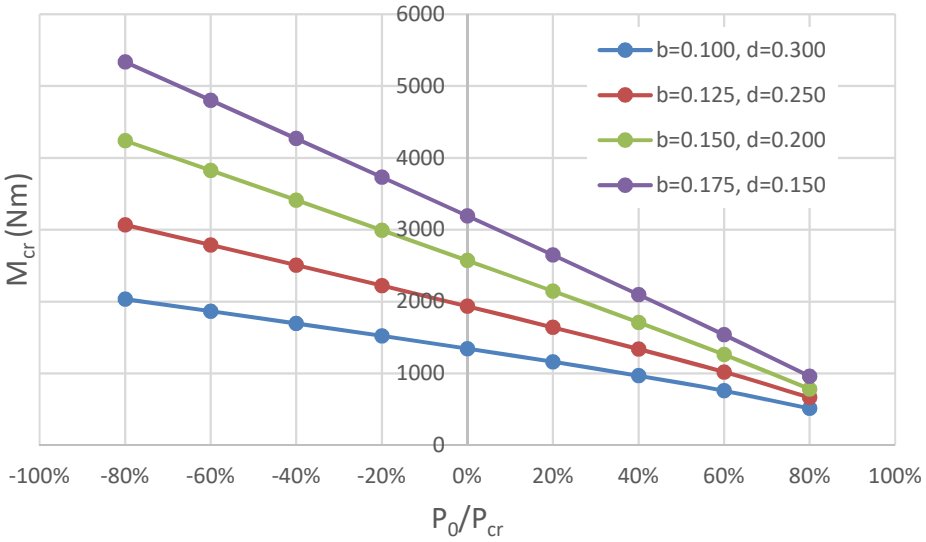

Fig. 11: Variation of end critical moment loading causing buckling of composite I-section beams having the same cross section with different sectional parameters subjected to different axial preloads

3.2.5. Buckling of a simply supported box-section composite beam subjected to axial and end moment loadings

In this section a simply supported composite box section beam subjected axial and end moment loading is considered. The beam is assumed to be of span l = 8 m with flanges of width of b=100 mm, and depth of the webs d = 200 mm. The analyses conducted focus on the interactions between the axial and end moment loadings in a similar manner as shown in the previous sections. It is assumed that laminated sections are of $[\pm\theta]_2$ lay-up, with each ply assumed to be 1.25 mm thick, and assuming the following normalised elastic material properties: E_1/E_2=25, G_{12}/E_2=0.6, G_{13}=G_{23} =G_{12}, ν_{12}=0.25. Table 9 presents the variation of the non-dimensional critical end moments causing buckling of the box section beams subjected to axial preloads. Similarly, it is observed for all axial preloading values that $\bar{M}^i_{cr}$ increases with the increase of θ from 0 to 15^0 while $\bar{M}^i_{cr}$ decreases monotonically as θ increases from 15^0 to 90^0. Also, Table 10 presents the variation of the non-dimensional critical axial load for the buckling of the box section beams when subjected to preloaded end moments. The table shows that the value of $\bar{P}^i_{cr}$ decreases monotonically with the increase of θ for all moment preloading values.

3.2.6. Buckling of a simply supported optimized box-section beam subjected to axial and end moment loading

Similar to the previous example, the behaviour of a 8 m long composite box-section beam is investigated considering four different values of flange width (b) and web height (d), while maintaining the same cross-sectional area and section wall thickness for all four cases. In this case, a fixed ply orientation ($[\pm 60]_2$) is used for the all the laminated section walls where each ply is 1.25 mm thick and assuming the following normalised elastic properties: E_1/E_2=25, G_{12}/E_2=0.6, G_{13}=G_{23} =G_{12}, ν_{12}=0.25.

The variation of critical axial load for the buckling of the four different box-beam cases when subjected to varying preload end moments is shown in Fig. 12. In the same way, Fig. 13 presents the variation of critical end moments causing buckling of the four different box-beam cases when subjected to varying levels of axial preloading. Fig. 12 shows that the resistance in terms of axial buckling load capacity of the beam with square section $(b=0.200, d=0.200)$ is superior over rectangular beams sections having same cross-sectional area. The buckling load capacity is found to deteriorate with the increase of aspect ratio of the cross-section. This is due to the buckling characteristic of box-section beams which undergo lateral buckling in the weakest direction. It is found to be different for I-section beams (Figs. 10 and 11) as they undergo lateral-torsion buckling where a wide flange beam (lower d/b ratio) is beneficial. On the other hand, Fig. 13 shows that the rectangular beam section having the highest aspect ratio (d/b) $(b=0.125, d=0.275)$ provides the highest resistance for end buckling moment and this behaviour is just opposite to that of I-section beam (Fig. 11).

Table 9: Critical buckling moment $\bar{M}^{i}_{cr}$ of a simply supported composite box-section beam with $[\pm\theta]_2$ lay-up in all section walls and subjected to different axial preloads P_0/P_{cr}

$\frac{P_0}{P_{cr}}$	Fiber Angle θ (degrees)						
	0	15	30	45	60	75	90
-0.8	226.70	348.48	226.18	102.07	61.31	48.37	45.14
-0.6	213.47	328.47	213.24	96.23	57.81	45.60	42.56
-0.4	199.44	307.17	199.46	90.02	54.07	42.66	39.81
-0.2	184.41	284.30	184.65	83.34	50.06	39.49	36.86
0.0	168.14	259.46	168.56	76.08	45.70	36.05	33.65
0.2	150.20	232.01	150.76	68.05	40.88	32.25	30.09
0.4	129.92	200.87	130.56	58.93	35.40	27.93	26.06
0.6	105.94	163.96	106.59	48.12	28.91	22.80	21.28
0.8	74.82	115.91	75.37	34.03	20.44	16.12	15.05

Table 10: Critical axial buckling load $\bar{P}^{i}_{cr}$ of a simply supported composite Box-section beam having $[\pm\theta]_2$ lamination for all walls and subjected to different end moment preloads M_0/M_{CR}

$\frac{M_0}{M_{cr}}$	Fiber Angle θ (degree)						
	0	15	30	45	60	75	90
0.0	44.4808	35.0107	12.2659	3.9677	2.2344	1.8671	1.8033
0.1	44.0305	34.6596	12.1432	3.9280	2.2120	1.8485	1.7853
0.2	42.6802	33.6066	11.7751	3.8090	2.1450	1.7924	1.7312
0.3	40.4320	31.8519	11.1616	3.6106	2.0333	1.6991	1.6410
0.4	37.2893	29.3962	10.3028	3.3329	1.8769	1.5684	1.5148
0.5	33.2567	26.2402	9.1986	2.9758	1.6758	1.4004	1.3525
0.6	28.3404	22.3849	7.8492	2.5394	1.4301	1.1950	1.1541
0.7	22.5476	17.8317	6.2545	2.0236	1.1396	0.9523	0.9197
0.8	15.8866	12.5820	4.4147	1.4285	0.8045	0.6722	0.6492
0.9	8.3672	6.6374	2.3298	0.7539	0.4246	0.3548	0.3426

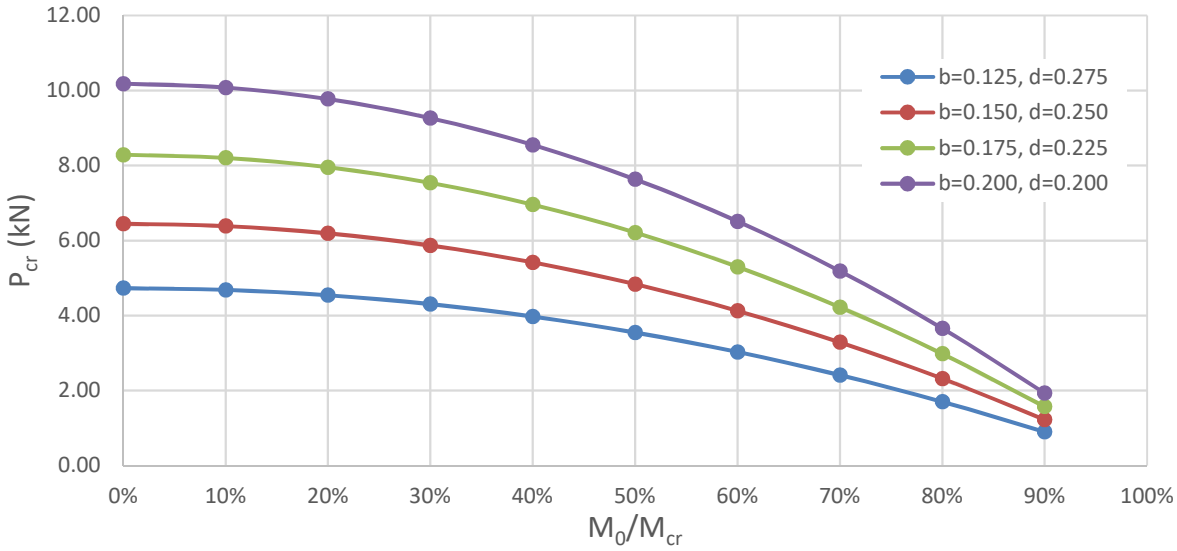

Fig. 12: Variation of buckling loads of composite box-section beams having the same cross section with different flange widths (b) and web heights (d) and subjected to different levels of preload end moments

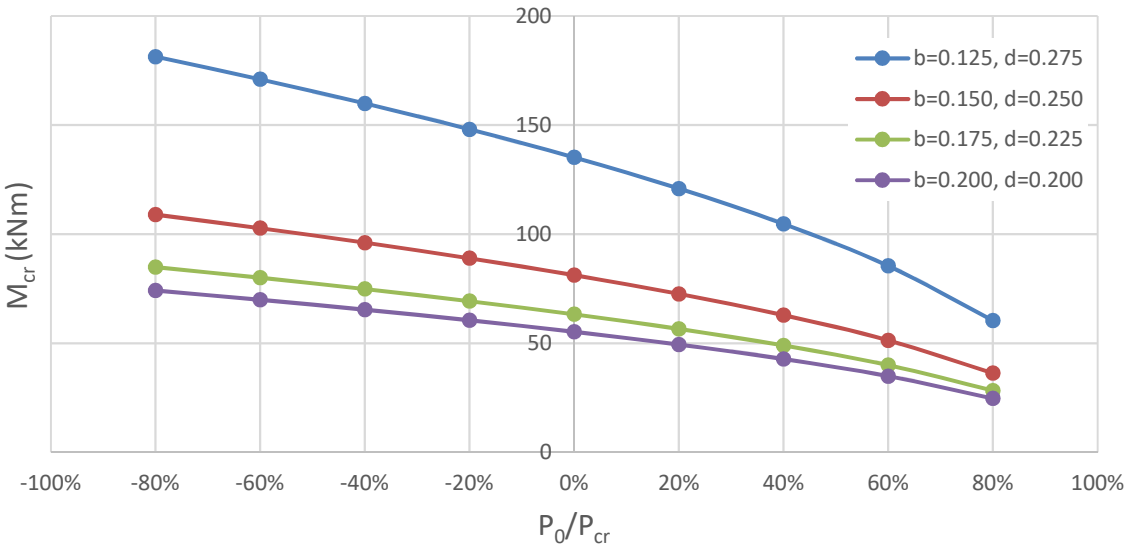

Fig. 13: Variation of critical end moment causing buckling of composite box-section beams having the same cross section with different flange widths (b) and web heights (d) and subjected to different levels of axial preloading

4. CONCLUSIONS

A new technique for the buckling analysis of thin-walled composite beams subjected to axial forces and end moment loading has been presented. The new technique is based on one-dimensional beam element formulation that helped to improve the computation efficiency significantly in contrast with a typical full-blown three-dimensional finite element model using solid or shell elements. The proposed model is valid for thin-walled open and closed section beams, and is especially well-suited for the analysis of the load response and buckling behaviour of composite beams displaying complex mode interactions. The formulation is general, includes axial deformation, torsion, bi-axial bending and transverse shear deformation as well as out of plane cross-sectional warping. The cross-sectional matrices of the beams are derived analytically and includes all the possible couplings between the abovementioned modes of deformation. The effect of shear deformation of the beam section walls is included in the formulation, which typically demands a C^0 continuous finite element formulation for the bending deformations of the beam element coupled with transverse shear deformations. Previous attempts [16-18] to include cross-sectional warping effects within the framework of C^0 continuity have displayed susceptibility to shear locking problems, which have typically been circumvented by using the reduced integration technique which supresses the problematic terms related to shear energy. However, this affects the solution accuracy, including stress oscillations and other related issues due to inadequate integration of other terms of the strain energy of the structural system. Moreover, a consistent implementation of cross-sectional warping demands a C^1 continuous formulation for the torsional deformation due to the appearance of second order derivatives of the torsional rotation (twist) in the strain vector. To overcome this in a C^0 continuous formulation requires inclusion of fictitious nodal parameters that cannot be attributed any physical meaning [15]. To overcome these difficulties a C^1 continuous formulation is adopted in this research, which includes full integration to achieve correct evaluation of the strain energy. The model proposed overcomes the crucial obstacles by adopting a different formulation for the coupled bending and shear deformations of the beam element which permits the use of full integration. The new modelling technique is used to solve numerical examples of thin-walled laminated composite beams having open (I) and closed (box) sections assuming different boundary conditions, laminated section wall stacking sequences, and different loading conditions. The results produced are thoroughly benchmarked and validated against analytical and numerical results available in literature, and it is shown that the proposed model performs very well in terms of both accuracy and computational efficiency. Finally, the new finite element is used to conduct extensive parametric studies to demonstrate the effect of varying different parameters on the buckling characteristics of composite thin-walled beams subjected to different loading scenarios involving the interactions between axial and end moment loads. It is anticipated that these new results can prove to be useful as benchmarks for future research in this area.

REFERENCES

[1] N.R. Bauld, L.S. Tzeng, A Vlasov theory for fibre-reinforced beams with thin-walled open cross section, Int. J. of Solid and Struc. 20(3) (1984) 277–97.

[2] R. Chandra, A.D. Stemple, I. Chopra, Thin-walled composite beams under bending, torsion, and extensional load, AIAA Journal 27(7) (1990) 619-626.

[3] C.E.S Cesnik, D.H. Hodges, VABS: A new concept for composite rotor blade cross section modelling, J. of the American Helicopter Society 42(1) (1997) 27–38.

[4] L.P. Kollar, Springer GS. Mechanics of Composite Structures, Cambridge University Press, 2003.

[5] H.A. Salim, J.F. Devalos, Torsion of open and closed thin-walled laminated composite sections, J. of compos. Mat. 39(6) (2005) 497-524.

[6] J. Lee, Flexural analysis of thin-walled composite beams using shear-deformable beam theory, Compos. Struc. 70(2) (2005) 212-222.

[7] L. Librescu, O. Song, Thin-walled Composite Beams, Springer, 2006.

[8] H.X. Nguyen, J. Lee, T.P. Vo, D. Lanc, Vibration and lateral buckling optimisation of thin-walled laminated composite channel-section beams, Compos. Struc. 143(2016) 84–92.

[9] L. Shang, P. Xia, D.H. Hodges, Geometrically exact nonlinear analysis of pre-twisted composite rotor blades, Chinese J. of Aeronautics 31(2) (2018) 300–309.

[10] M. Gupta, D.H. Hodges, Modelling Thin-Walled Beams using VAM, Structural Dynamics, and Materials Conference, AIAA SciTech Forum, (AIAA 2017-1832), 2017. https://doi.org/10.2514/6.2017-1832.

[11] D. Harursampath, A.B. Harish, D. H. Hodges, Model reduction in thin-walled open-section composite beams using variational asymptotic method. Part I: Theory, Thin-Walled Struc. 117 (2017) 356-366.

[12] K. Kashefi, A.H. Sheikh, MS.M. Ali, MC. Griffith, An efficient modelling approach based on a rigorous cross-sectional analysis for analysing box girder bridge superstructures, Adv. in Struc. Eng. 19(3) (2016) 513–528.

[13] T.P. Vo, J. Lee, Interaction curves for vibration and buckling of thin-walled composite box beams under axial loads and end moments, App. Math. Modelling 34(2010) 3412-3157.

[14] T.P. Vo, J. Lee, Vibration and Buckling of thin-walled composite I-Beams with Arbitrary Lay-ups under axial Loads and End Moments, Mech. of Adv. Mat. and Struc. 20(8) (2013) 652-665.

[15] T.P. Vo, J. Lee, On Sixfold coupled buckling of thin-walled composite beams, Compos. Struc. 90 (2009) 295-303.

[16] N.-I. Kim, D. K. Shin, and M.-Y. Kim, Flexural-Torsional buckling loads for spatially coupled stability analysis of thin-walled composite columns, Adv. in Eng. Softw. 39 (2008) 949-961.

[17] N.-I. Kim, D. K. Shin, and Y.-S. Park, Coupled stability analysis of thin-walled composite beams with closed cross section, Thin-walled Struc. 48 (2010) 581-596.

[18] N.-I. Kim, C.K. Jeon, Coupled Static and Dynamic Analyses of Shear Deformable Composite Beams with Channel-Sections, Mech. Based Design of Struc. and Mach., 2013, https://doi.org/10.1080/15397734.2013.797332.

[19] M.T. Piovan, V.H. Cortinez, Mechanics of shear deformable thin-walled beams made of composite materials, Thin-Walled structures, 45 (2007) 37-62.

[20] F. Ascione, M.Lamberti, G.Razaqpur, Modifications of standard GFRP sections shape and proportions for improved stiffness and lateral-torsional stability, Composite Structures, 132 (2015) 265-289.

[21] A.H. Sheikh, New Concept to include shear deformation in a curved beam element, J. of Struc. Eng. 128(3) (2002) 406-410.
[22] N.R. Bauld, L.S. Tzeng, A Vlasov theory for fibre-reinforced beams with thin-walled open cross section, Int. J. of Sol. and Struc. 20(3) (1984) 277–97.
[23] A.H. Sheikh, O.T. Thomsen, An efficient beam element for the analysis of laminated composite beams, Compos. Sci. and Tech. 68(2008) 2273–2281.
[24] SP. Machado, VH. Cortinez, Non-linear model for stability of thin-walled composite beams with shear deformation, Thin-Walled Struct. 43(10) (2005) 1615–45.
[25] S.Y. Back, K.M. Will, Shear-flexible thin-walled element for composite I-beams, Eng. Struc. 30(5) (2007) 1447-1458.
[26] N.-I. Kim, D. K. Shin, M.-Y. Kim, Improved flexural-torsional stability analysis of thin-walled composite beam and exact stiffness matrix, I. J. of Mech. Sci. 49(2007) 950-969.

APPENDIX A

The non-zero elements appearing in the upper triangle of the symmetric matrix $[C_g]$ (Eq. (18)) are presented in their explicit form as follows (applicable for I and box sections).

$C_{11}^{gP} = C_{22}^{gP} = A$, $C_{13}^{\mathrm{gP}} = -B\cos\alpha - A(q\sin\alpha + r\cos\alpha)$

$C_{23}^{gP} = -B\sin\alpha + A(q\cos\alpha - r\sin\alpha)$, $C_{33}^{gP} = C + 2rB + A(q^2 + r^2)$

Where $(A, B, D, F) = \int_t (1, n, n^2, n^3)dn$

APPENDIX B

The non-zero elements appeared in the upper triangle of the symmetric matrix $\left[F_g^P\right]$ and $\left[F_g^M\right]$ (Eq. (18)) are presented in their explicit form as follows (applicable for I section, Fig. 3(a)).

$$F_{11}^{gP} = F_{22}^{g} = b_1A_1 + b_2A_2 + dA_3,\ F_{13}^{gP} = -b_1(A_1d/2 + B_1) + b_2(A_2d/2 + B_2),\ F_{23}^{gP} = -B_3d$$
$$F_{33}^{gP} = b_1^3A_1/12 + b_1(0.25A_1d^2 + B_1d + D_1) + b_2^3A_2/12 + b_2(0.25A_2d^2 + B_2d + D_2) + A_3d^3/12 + D_3d$$

and

$$F_{11}^{gM} = F_{22}^{gM} = b_1(0.5A_1d + B_1) - b_2(0.5A_2d + B_2),$$
$$F_{13}^{gM} = -b_1(0.25A_1d^2 + B_1d + D_1) - b_2(0.25A_2d^2 + B_2d + D_2) - A_3d^3/12,$$
$$F_{33}^{gM} = b_1(b_1^2dA_1 + 2b_1^2B_1 + 3d^3A_1 + 18d^2B_1 + 36dD_1/2 + 24F_1)/24$$
$$-b_2(b_2^2dA_2 + 2b_2^2B_2 + 3d^3A_2 + 18d^2B_2 + 36dD_2/2 + 24F_2)/24$$

The non-zero elements appeared in the upper triangle of the symmetric matrix $\left[F_g^P\right]$ and $\left[F_g^M\right]$ (Eq. (18)) are presented in their explicit form as follows (applicable for box section, Fig. 3(b)).

$F_{11}^{gP} = F_{22}^{gP} = b(A_1 + A_2) + d(A_3 + A_4)$, $F_{13}^{gP} = bd(A_2 - A_1)/2 - b(B_2 - B_1)$,

$$F_{23}^{gP} = bd(A_4 - A_3)/2 + d(B_4 - B_3),$$
$$F_{33}^{gP} = b^3(A_1 + A_2)/12 + bd^2(A_1 + A_2)/4 + b^2d(A_3 + A_4)/4 + bd(B_1 + B_2 + B_3 + B_4)$$
$$+b(C_1 + C_2) + d^3(A_3 + A_4)/12 + d(C_3 + C_4)$$

and

$$F_{11}^{gM} = F_{22}^{gM} = bd(A_1 - A_2)/2 + b(B_1 - B_2),$$
$$F_{13}^{gM} = -bd^2(A_1 + A_2)/4 - bd(B_1 + B_2) - b(D_1 + D_2) + d^3(A_3 + A_4)/12,$$
$$F_{33}^{gM} = b^3d(A_1 - A_2)/24 + b^3(B_1 - B_2)/12 + bd^3(A_1 - A_2)/8 + 3bd^2(B_1 - B_2)/4$$
$$+3bd(D_1 - D_2)/2 + b(F_1 - F_2)$$

4. Chapter 3a - Bucking and Vibration Characteristics of Thin-Walled Laminated Composite Beams Having Open and Closed Sections

Seminar Paper 2 –Presented

ICCM20 - 20th International Conference on Composite Materials
Event: Conference
Duration: 19 - 24 July 2015
City: Copenhagen
Country: Denmark
Degree of recognition: International event

BUCKING AND VIBRATION CHARACTERISTICS OF THIN-WALLED LAMINATED COMPOSITE BEAMS HAVING OPEN AND CLOSED SECTIONS

Arash Asadi[1], Abdul Hamid Sheikh[*1] and Ole Thybo Thomsen[2, 3]

[1]School of Civil, Environmental and Mining Engineering, University of Adelaide, Adelaide, Australia

[2]Engineering and the Environment, University of Southampton, Southampton, United Kingdom

[3]Department of Mechanical and Manufacturing, Aalborg University, Aalborg, Denmark

Keywords: Buckling Analysis, Finite element model, Thin-walled Composite beams, Vibration Frequency

ABSTRACT

An efficient modelling technique based on one dimensional beam finite element analysis for buckling and vibration of thin-walled laminated composite beams having open/closed sections is proposed in this paper. For the vibration analysis, the effect of axial load is also incorporated. The formulation is generalised so as to accommodate any stacking sequence of individual walls and consider all possible couplings between different modes of deformation. The effect of transverse shear deformation of walls and out of plane warping of the beam section is considered where the warping can be restrained or free. The incorporation of shear deformation in the finite element formulation of the beam has imposed a difficulty which is successfully addressed using a concept proposed by one of the authors. Numerical examples of open section I beams and closed section box beams are solved by the proposed approach and the results are compared with those available in literature to show the performance of the proposed method.

1 INTRODUCTION

Modelling of thin-walled laminated composite beams having open and closed cross-sections as a condensed one dimensional beam model has drawn considerable attentions of many researchers in recent years. It leads to the development of a number of modelling techniques and their advancements which helped to have a better understanding of the behaviour of such beams under complex loading and boundary conditions. References 1-8 are simply few recent representative samples of these models. One of the early applications of this approach is found in the modelling and analysis of helicopter blades which is then followed by analysis of pultruded composite profiles, wind turbine blades and some similar structures.

The previous studies may be divided into two major categories based on the approach used for calculating the cross-section stiffness coefficients of these composite beams. The first approach is based on ‘analytical technique’ while the other approach utilizes a two-dimensional (2D) cross-sectional analysis based on a (2D) finite element model to calculate the cross-section matrices.

Hodges and co-workers [3] have significantly contributed toward the development of the second approach where the three dimensional (3D) elasticity problem defining the deformation of these beams is systematically divided into a one-dimensional beam problem and a two dimensional cross-sectional problem. This method is generally referred to as variational asymptotic beam section analysis (VABS) which is based on variational asymptotic method (VAM) [9]. This approach is also suitable for modelling solid and the thick walled cross-sections. The same group ([10-14]) have also attempted to solve the 2D cross-sectional problem defined within the framework of VAM analytically but this approach involves rigorous mathematical treatments to evaluate the cross-sectional stiffness coefficients.

In the present study, the analytical approach (first approach) is adopted for the determination of the cross-sectional matrices as the objective of this paper is to analyse thin-walled composite beams. Moreover, the 2D finite element analysis or a complex mathematical treatment involved with the other approach can be avoided in the present approach. Specifically, the current study has adopted the analytical approach proposed by Sheikh and Thomsen [8] and extended to buckling and vibration with/without axial load of these structures. The different modes of deformation and their coupling considered in the development of the present closed-form analytical solution are axial, torsion, bi-axial bending, bi-axial shear as well as warping for the torsional deformation. The cross-sectional matrices are explicitly derived for the open I section and closed box section. The present formulation considered both plane stress and plain strain conditions of a lamina. The 1D beam problem is solved by the finite element approximations. The out of plane warping displacement requires a C^1 continuous finite element formulation for the twisting rotation, which is accommodated using Hermetian interpolation functions. On the other hand, the usual treatment of the transverse shear deformation requires a C^0 formulation. This needs the reduced integration technique to avoid any shear locking problem. The different degrees of continuity for the different modes of deformation and their coupling impose a problem for their implementation. This problem is addressed satisfactorily utilising the concept proposed by Sheikh [15] which does not require the reduced integration technique. For the 1D beam finite element analysis, a three node beam element as shown in Fig.1 has been developed.

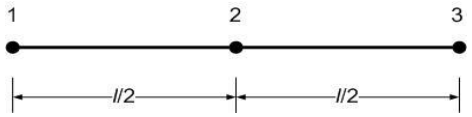

Figure 1: A typical beam element

A computer code is written in FORTRAN to implement present formulation. Numerical examples of thin-walled composite beams having different cross sections and other conditions are analysed by the proposed model and the results obtained in the form of buckling loads and vibration frequencies and validated with the available results in literature. These results demonstrate a very good performance of proposed finite element model.

1 FORMULATION

Figure 2 shows a segment of the composite beam shell wall where *x*-*y*-*z* is taken as the global Cartesian coordinate system and *x* is directed along the beam axis which is passing through the centroid of the beam section. A local orthogonal coordinate system *x*-*s*-*n* is also defined where *x*-*n* plane passes through the tangential plane of beam wall mid plane (local *x*-axis is parallel to the global *x*-axis) and *n* is directed along the wall thickness. The displacement components at the mid-plane of the shell wall in the local coordinate system (*x*-*s*-*n*) can be expressed in term of the global displacement components of the beam [1] as

$$\begin{aligned} \bar{u} &= U + y\theta_y + z\theta_z + \varphi\theta_x', \\ \bar{v} &= V\cos\alpha + W\sin\alpha - r\theta_x, \\ \bar{w} &= -V\sin\alpha + W\cos\alpha + q\theta_x, \end{aligned} \tag{1}$$

where φ is the warping function, θ_x is the torsional rotation and θ_y, θ_z are bending rotations of the cross-section of the beam along *x* and *y*, respectively. These bending rotations can again be expressed as $\theta_y = -V' + \Psi_y$ and $\theta_z = -W' + \Psi_z$, where Ψ_y, Ψ_z are shear rotations of the beam section about *z* and *y*, respectively, and V', W' and θ_x' are respectively the derivatives of *V*, *W* and θ_x with respect to *x*.

It has been observed that the warping displacement of a closed section beam is relatively less than that of an open section beam [14] but the present formulation has considered the effect of warping in

all cases. Considering the effects of bending and transverse shear deformation of the beam shell wall, the displacements at any point of the shell wall away from its mid-plane may be expressed as

$$u = \bar{u} + n\left(-\frac{\partial \bar{w}}{\partial x} + \psi_{xn}\right), \quad v = \bar{v} + n\left(-\frac{\partial \bar{w}}{\partial s} + \psi_{sn}\right), \quad w = \bar{w}, \tag{2}$$

where ψ_{xn} and ψ_{sn} are shear rotations of the shell wall section about *s* and *x* , respectively. It is assumed that $\psi_{sn} = 0$ whereas ψ_{xn} can be expresses in terms of the corresponding global components (Ψ_y and Ψ_z) as $\psi_{xn} = -\Psi_y \sin\alpha + \Psi_z \cos\alpha$.

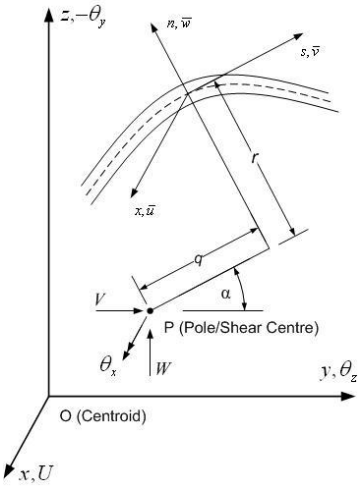

Figure 2: Cross-section of a portion of beam shell wall with local and global coordinate system and displacement component

Substituting this and as well as Equation (1) in the above equation (2), the displacements at any point within the shell wall along its local coordinate system (*x*-*s*-*n*) can be expressed in terms of the global displacement components of the 1D beam as

$$u = U + (y - n\sin\alpha)\,\theta_y + (z + n\cos\alpha)\,\theta_z + (\varphi - nq)\theta_x', \quad v = V\cos\alpha + W\sin\alpha - (r+n)\,\theta_x, \quad w = -V\sin\alpha + W\cos\alpha + q\theta_x . \tag{3}$$

With the beam kinematics (3), the governing equation of the axially loaded vibration beam can be derived from its total energy utilising Hamilton's principle. The total energy of a structure consists of strain energy (*U*), strain energy due to axial force (U_g) and kinetic energy (*T*) which can be used to derive the stiffness matrix $[K]$, geometric stiffness matrix $[K_g]$ and mass matrix $[M]$, respectively in a finite element analysis of the structure. As the derivation of the stiffness matrix $[K]$ has already been shown elsewhere [8], it is not repeated here. For a beam under an axial force ($P = \sigma A$) acting uniformly over its entire cross-sectional area (*A*), the strain energy due to the axial force may be written as

$$U_g = \frac{1}{2}\int_V \sigma(v'^2 + w'^2)\,dv \tag{4}$$

$$U_g = \frac{P}{2A}\int_V (v'^2 + w'^2)\,dv = \frac{P}{2A}\int_V \{v' \quad w'\}\begin{Bmatrix} v' \\ w' \end{Bmatrix} dv = \frac{P}{2A}\int_V \{\varepsilon_g\}^T \{\varepsilon_g\}\,dv .$$

Using equation (3), the geometric strain vector $\{\varepsilon_g\}$ in the above equation can be written as

$$\{\varepsilon_g\} = \begin{Bmatrix} v' \\ w' \end{Bmatrix} = \begin{bmatrix} \cos\alpha & \sin\alpha & -(r+n) \\ -\sin\alpha & \cos\alpha & q \end{bmatrix} \begin{Bmatrix} V' \\ W' \\ \theta_x' \end{Bmatrix} = [H_g]\{\bar{\varepsilon}_g\}. \tag{5}$$

The above equation (5) may be substituted in equation (4) and it leads to

$$U_g = \frac{P}{2A}\int_V \{\varepsilon_g\}^T \{\varepsilon_g\} dv = \frac{P}{2A}\int_L \{\bar{\varepsilon}_g\}^T [F_g]\{\bar{\varepsilon}_g\} dx \tag{6}$$

where $[F_g] = \int_A [H_g]^T [H_g] ds dn = \int \left(\int [H_g]^T [H_g] dn\right) ds = \int ([C_g]) ds$.

The above equation can be used to derive the geometric stiffness matrix conveniently using finite element approximation of the geometric strain vector $\{\varepsilon_g\}$. The individual elements of the matrices $[F_g]$ and $[C_g]$ for I and box sections are explicitly given in Appendix A and Appendix B, respectively.

Now the kinetic energy of the beam having a harmonic motion may be written as

$$T = \frac{1}{2}\int_V \{\dot{U}\}^T \rho\{\dot{U}\} dv = -\frac{\omega^2}{2}\int_V \{U\}^T \rho\{U\} dv. \tag{7}$$

where ρ is the mass density of the material, ω is the vibration frequency, $\{U\}^T = [u \quad v \quad w]$ (equation 3) is the displacement vector and $\{\dot{U}\} = d\{U\}/dt$ is the velocity vector. In a similar manner, the displacement vector (equation 3) can be written as

$$\{U\} = [H_m]\{\bar{u}\}. \tag{8}$$

where $[H_m]$ contains sectional parameters (x, y, n, r, q, α) whereas $\{\bar{u}\}$ contains global parameters (U, V, W, θ_z, θ_y and θ_z) of the 1D beam. After substitution of the above equation (8) in equation (7), it can be written as

$$T = -\frac{\omega^2}{2}\int_V \{U\}^T \rho\{U\} dv = -\frac{\omega^2}{2}\int_L \{\bar{u}\}^T [F_m]\{\bar{u}\} dx \tag{9}$$

where $[F_m] = \int_A [H_m]^T \sigma[H_m] ds dn = \int \left(\int [H_m]^T \sigma[H_m] dn\right) ds = \int ([C_m]) ds$.

For I and box section beams, all elements of the above matrices $[F_m]$ and $[C_m]$ are explicitly derived which are given in Appendix C and Appendix D.

For finite element implementation of the beam, quadratic Lagrangian interpolation functions are used for the axial deformation while cubic Hermetian interpolation functions are used for torsional deformation which will ensure the desired C^1 continuity of torsional rotation (θ) as the displacement field (equation 3) contains derivative of θ. As mentioned earlier, the bending deformations which are coupled with shear deformations and these are treated in a different manner following the concept of Sheikh [15] where the shear rotations Ψ_y and Ψ_z are adopted as field variables instead of θ_y and θ_z in addition to the bending displacements V and W. Taking a linear approximation of Ψ_y, Ψ_z and a cubic approximation of V and W, the field variables can be written as

$$U = a_1 + a_2 x + a_3 x^2$$
$$V = a_4 + a_5 x + a_6 x^2 + a_7 x^3$$
$$W = a_8 + a_9 x + a_{10} x^2 + a_{11} x^3 \tag{10}$$
$$\Psi_y = a_{12} + a_{13} x \ , \ \Psi_z = a_{14} + a_{15} x$$
$$\theta_x = a_{16} + a_{17} x + a_{18} x^2 + a_{19} x^3$$

Though Ψ_y and Ψ_z are taken as field variables, they are not used as nodal degrees of freedom. Interestingly, the corresponding nodal degrees of freedom are θ_y and θ_z which are introduced with the help of bending deformations which may be expressed using the above equations as

$$\theta_y = \Psi_y - V' = a_{12} + a_{13} x - a_5 - 2a_6 x - 3a_7 x^2 , \tag{11}$$
$$\theta_z = \Psi_z - W' = a_{14} + a_{15} x - a_9 - 2a_{10} x - 3a_{11} x^2 .$$

The unknown constants (a_1, a_2, a_3 ..... a_{19}) found in Equations (10) can be replaced in terms of nodal displacement parameters by substitution of U, V, W, θ_y and θ_z (Equations 10 and 11) at all three nodes of the beam element (Fig. 1), and θ_x (Equation 10) and its derivative θ_x' at the two end nodes as

$$\{\delta\} = [R]\{a\} \text{ or } \{a\} = [R]^{-1}\{\delta\} \tag{12}$$

where $\{a\}^T = [a_1 \quad a_2 \quad a_3 \quad \cdots \quad a_{19}]$, [$R$] consists of coordinates (x values) of the 3 nodes and $\{\delta\}^T = [U_1 \ V_1 \ W_1 \ \theta_{x1} \ \theta_{y1} \ \theta_{z1} \ \theta'_{x1} \ U_2 \ V_2 \ W_2 \ \theta_{y2} \ \theta_{z2} \ U_3 \ V_3 \ W_3 \ \theta_{x3} \ \theta_{y3} \ \theta_{z3} \ \theta'_{x3}]$ is the nodal displacement vector.

With the help of Equations (10) and (12), the vector $\{\bar{\varepsilon}_g\}$ as defined in Equation (5) may be expressed in terms of nodal displacement vector $\{\delta\}$ as

$$\{\bar{\varepsilon}_g\} = [V' \quad W' \quad \theta_x']^T = [S_g]\{a\} = [S_g][R]^{-1}\{\delta\} = [B_g]\{\delta\}. \tag{13}$$

The above equation is substituted in Equation (6) and it is rewritten as

$$U_g = \frac{P}{2A}\int_L \{\bar{\varepsilon}_g\}^T [F_g]\{\bar{\varepsilon}_g\} dx = \frac{P}{2A}\int_L \{\delta\}^T [B_g]^T [F_g][B_g]\{\delta\} dx = \frac{P}{2}\{\delta\}^T [K_g]\{\delta\} \tag{14}$$

where $[K_g] = \frac{1}{A}\int_L [B_g]^T [F_g][B_g]\, dx$ is the geometric stiffness matrix of a beam element.

Similarly, the vector $\{\bar{u}\}$ as defined in Equation (9) may be expressed in terms of $\{\delta\}$ with the help of Equations (10) (11) and (12) as

$$\{\bar{u}\} = [S_m]\{a\} = [S_m][R]^{-1}\{\delta\} = [B_m]\{\delta\}. \tag{15}$$

Again this equation is substituted in Equation (9) and it is rewritten as

$$T = -\frac{\omega^2}{2}\int_L \{\bar{u}\}^T [F_m]\{\bar{u}\} dx = -\frac{\omega^2}{2}\int_L \{\delta\}^T [B_m]^T [F_m][B_m]\{\delta\} dx = -\frac{\omega^2}{2}\{\delta\}^T [m]\{\delta\} \tag{16}$$

where $[M] = \int_L [B_m]^T [F_m][B_m]\, dx$ is the mass matrix of an element.

The stiffness, geometric stiffness and mass matrices of all elements are assembled together to form the form these matrices of the whole beam. Taking same notations of these assembled matrices, the governing equation of the axially loaded (P = axial compression) vibrating beams may be expressed as

$$\left([K]-P[K_g]\right)\{\delta\}=\omega^2[M]\{\delta\} \tag{17}$$

This is an Eigen-value problem which is solved to get the vibration frequencies as Eigen values and modes of vibration as Eigen vectors. The buckling of these beams can also be solved by the above equation by simply dropping the mass matrix and can be rewritten as

$$[K]\{\delta\}=P_{cr}[K_g]\{\delta\} \tag{18}$$

where P_{cr} is the critical value of the axial compression P for the buckling of the beam.

2 RESULTS AND DISCUSSION

In the section, numerical examples of thin-walled composite beams having I and Box sections are solved using proposed model and the results obtained are validated with the analytical and numerical results available in literature.

Example 1: The problem of a simply supported thin-walled laminated composite beam having a span of 6m is studied using plane stress condition ($\sigma_s = 0$) of the plies. The beam has a double symmetric I section where both the flanges are 600mm wide and the web is 600mm deep. All the flange and web plates are made of 4 plies each 7.5mm thick (30mm total thickness) which are having 5 different ply orientations. The material used for all the plies is Graphite-epoxy and its properties are: E_1=144GPa, E_2=9.65GPa, G_{12}= G_{13}=4.14GPa, G_{23}=3.45GPa, υ_{12}=0.3. The beam is analysed with the proposed technique using diffident number of elements and it is observed that the results are converged when the number of elements is 10 or more which is used to generate results in all cases. The critical buckling loads predicted by the proposed technique are presented in Table 1 along with those produced by other investigators who studied this problem earlier with their approach. The table shows that the present results have good agreement with the existing results.

Lay-ups	Machado & Cortinez [16]		Back & Will [17]		Vo and Lee [18]	Present
	No shear	With shear	ABAQUS	With shear	With shear	With shear
$[0]_4$	42.11	33.18	30.78	28.85	30.38	35.51
$[30/-30]_s$	-	-	13.06	13.17	13.17	13.16
$[45/-45]_s$	4.45	4.44	4.41	4.41	4.41	4.41
$[60/-60]_s$	-	-	2.89	2.89	2.88	2.88
$[0/90]_s$	22.57	19.84	20.41	20.63	20.63	20.52

Table 1: Critical buckling load (MN) of a simply supported doubly-symmetric composite I-beam

Example 2: The behaviour of a 1m long cantilever beam having a mono-symmetric I section is investigated for 7 different stacking sequences for its laminated walls. The web of the beam is 50mm deep whereas the breadths of its top and bottom flanges are 30mm and 50mm, respectively. The web and flanges are made of 16 layers each 0.13mm thick with a symmetrical layup. The material used for all the layers is glass-epoxy having the following properties: E_1=53.78GPa, E_2=17.93GPa, G_{12}= G_{13}=8.96GPa, G_{23}=3.45GPa, υ_{12}=0.25. The beam is analysed with the proposed approach and the critical buckling loads obtained for different ply orientations are presented in Table 2 along with those reported by Kim et al. [19], and Vo and Lee [18]. The comparison of the results shows a very good performance of the proposed element.

Lay-ups	Kim et al. [19]		Vo and Lee[18]	Present
	Abaqus	No Shear	With shear	With shear
$[0]_{16}$	2969.7	2998.2	2993.2	2994.5
$[15/-15]_{4s}$	2790.9	2811.8	2803.6	2803.3
$[30/-30]_{4s}$	2190.6	2199.7	2184.7	2185.1
$[45/-45]_{4s}$	1558.9	1561.9	1546.0	1547.2
$[60/-60]_{4s}$	1239.4	1241.3	1227.8	1229.0
$[75/-75]_{4s}$	1132.2	1134.5	1126.7	1127.9
$[0/90]_{4s}$	2101.5	2113.9	2100.6	2101.8

Table 2: Critical buckling load (N) of a cantilever mono-symmetric composite I-beam

Example 3: A double symmetric I section beam clamped at its two ends is taken to study the effect of fibre orientations of one of its laminated flanges for different values of the beam length (l) with respect to the depth (d) of the web. The web and flanges are made of 2 layers where each layer has a thickness of 2.5mm (total thickness t=5mm) and the following material properties: E_1/E_2=25, G_{12}/E_2=0.6, $G_{13}=G_{23}=G_{12,}$ υ_{12}=0.25. The layup of the top flange and the web is $[0/45^0]$ and that of the bottom flange is $[\theta]_2$ where the value of θ is varies from 0 to 90 degrees. The asymmetric laminated configuration found in this situation produces nonzero off-diagonal terms of the cross sectional stiffness matrix (F_{13}, F_{16}, F_{24}, F_{35}) which is responsible for coupling of different deformation modes. The variation of normalized critical buckling load $\overline{P} = P_{cr} l^2/(d^3 t E_2)$ with respect to θ as predicted by the proposed model is presented in Fig. 3 for three different values of (l/d) ratio. Figure 3 shows that the critical buckling load decreases monolithically with the increase of fiber angle (θ). However, there is a small increasing tendency of this buckling load parameter ($\overline{P}$) for low span-to-depth ratios (l/d) when the fiber angle is ranging from 0 to 15 degrees. Also, the mode shapes for different displacement components corresponding to $\overline{P}_1 = 2.48$ (θ=75°, l/d=25) are plotted in Fig.4.

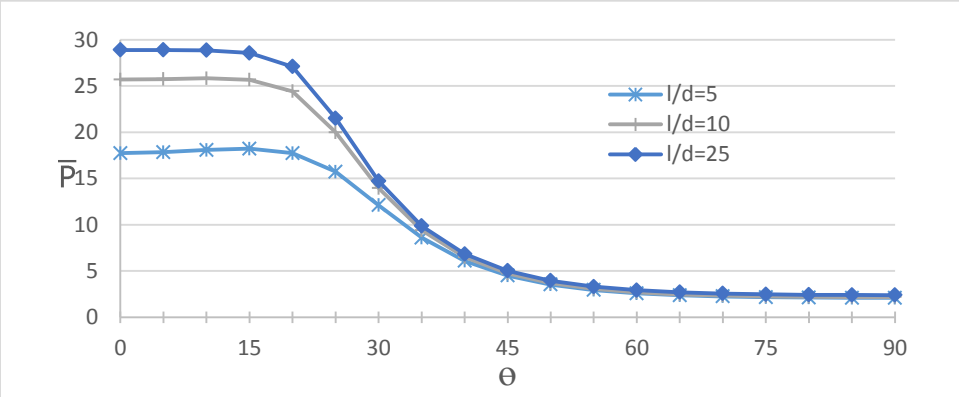

Figure 3: Variation of buckling load parameter ($\overline{P}$) of a clamped composite I-beam with respect to fiber angle (θ) of its bottom flange

Example 4: The buckling characteristics of a 12m long simply supported beam having a box section (300mm wide and 600mm deep) is studied for different stacking sequences of its laminated walls. In all these cases, the four laminated walls of this box section beam consist of 4 layers each having a thickness of 7.5mm. The material used for these layers is Graphite-Epoxy (AS4/3501) which is having the following properties: E_1=144GPa, E_2=9.65GPa, $G_{12}=G_{13}$=4.14GPa, G_{23}=3.45GPa, υ_{12}=0.3. The lamination schemes used for all the beam walls are $[0]_4$, $[0/90]_{2s}$ and $[45/-45]_{2s}$. The critical buckling loads predicted by the proposed model are presented in Table 3 along with those of

Cortinez and Piovan [20] and Kim et al. [11] (based on two techniques) which show a very good correlation between the results obtained by different techniques.

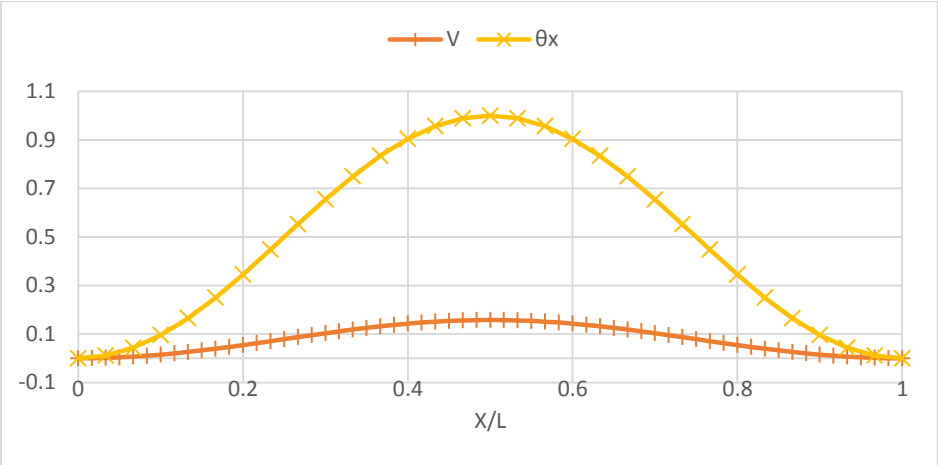

Figure 4: Mode shapes of a clamped I section composite beam (θ=75° and l/d=25)

Lay-ups	Cortinez and Piovan [20] (no shear)	Kim et al. [21]		Present
		30 H-Beam elements (with shear)	SMM (with shear)	
[0/0/0/0]	9.33	9.35	9.35	9.00
[45/-45/-45/45]	0.97	0.97	0.97	0.97
[0/90/90/0]	4.97	5.02	5.02	4.94

Table 3: Critical buckling load (MN) of a simply supported composite box-beam

Example 5: An 8m long simply supported beam having a box section (100mm width and 200mm deep) is used to study its buckling and vibration characteristics. The four walls of the beam are made of two layers each having a thickness of 2.5mm and the following material properties: E_1/E_2=25, G_{12}/E_2=0.6, υ_{12}=0.25. The flanges have a stacking sequence of $[0]_2$ and that of the webs is $[\theta/-\theta]$ where the value of θ is varied from 0 to 90^0 with an increment of 15^0. The non-dimensional critical buckling load $\overline{P} = P_{cr}l^2/(b^3tE_2)$ evaluated by the proposed technique and presented with those of Vo and Lee [22] in Table 4 which shows a good agreement between them.

Fiber angle	Vo and Lee [22] (with shear)	Present
0	36.009	35.509
15	29.245	28.916
30	13.549	13.479
45	7.858	7.834
60	6.670	6.653
75	6.419	6.403
90	6.375	6.359

Table 4: Normalized critical buckling load $\overline{P}$ of a simply supported composite box-beam

The vibration analysis of this beam subjected axial load is also carried out by the proposed model where the axial load is varied from $-P_{cr}$ to P_{cr}. The variation of natural frequency for the fundamental mode with respect to the axial load is plotted in Fig. 5 for different values of θ. Figure 5 clearly shows a monotonic decrease of the vibration frequency with the increase of axial compression as expected.

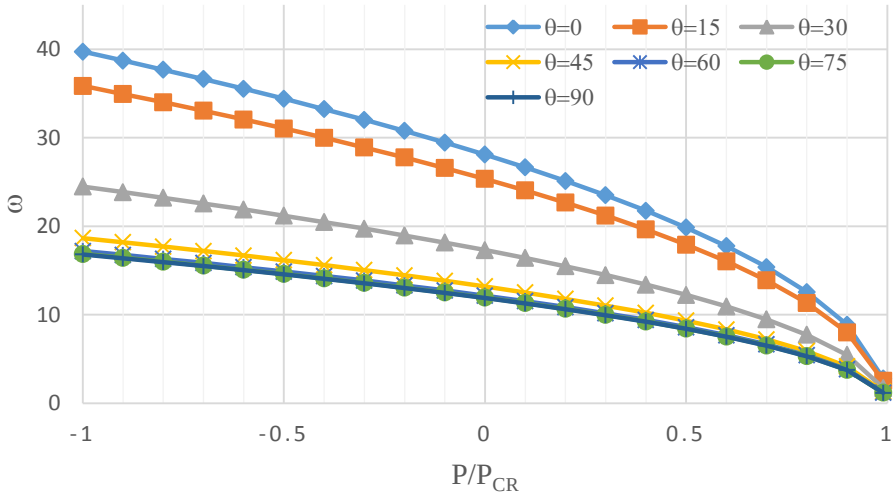

Figure 5: Effects on axial load on vibration frequency of a composite box- beam

3 CONCLUSIONS

An efficient one dimensional beam element is developed for buckling and vibration analysis of thin-walled composite beams of open and closed cross sections considering axial displacement, torsion, bi-axial bending and transverse shear deformations as well as out of plane sectional warping. The cross-sectional matrices required for the formulation of geometric stiffness and mass matrices of the beam are derived analytically where all possible couplings between the abovementioned modes of deformation are considered. The effect of shear deformation of the beam walls is included which requires a C^0 continuous finite element formulation of the bending deformation coupled with the shear deformation. On the other hand, the torsional deformation requires a C^1 continuous FE formulation due to the incorporation of warping deformation. The difficulty associated with the implementation of both these formulations in the present coupled problem is successfully overcome by using a novel concept proposed by of one of the authors. The proposed analysis technique is used to solve numerical examples of thin-walled laminated composite beams having open I and closed box sections taking different boundary conditions and stacking sequences of the beam walls. For the vibration analysis of beams, the effect of axial force on the frequency of vibration is also studied. In many cases, the results predicted by the proposed technique are validated with the analytical and/or numerical results available in literature. The agreement between the results is found to be very good in most of the cases which ensures the reliability and range of applicability of the proposed element. New results are also presented in this paper which should be useful to future researchers.

REFERENCES

[1] N.R. Bauld and L.S. Tzeng, A Vlasov theory for fiber-reinforced beams with thin-walled open cross section, *International Journal of Solid and Structures*, 20(3), 1984, pp. 277–97.

[2] R. Chandra, A.D. Stemple and I, Chopra, Thin-walled composite beams under bending, torsion, and extensional load. *AIAA Journal*, 27(7), 1990, pp 619-626.

[3] C.E.S. Cesnik, D.H. Hodges, VABS: A new concept for composite rotor blade cross section modelling, *Journal of the American Helicopter Society* 42(1), 1997, pp. 27–38.

[4] L.P.Kollar and G.S. Springer, *Mechanics of composite structures*, 1st edition, Cambridge University Press, 2003.
[5] H.A. Salim and J.F. Devalos J.F., Torsion of open and closed thin-walled laminated composite sections, *Journal of composite materials*, 39(6), 2005, pp 497-524.
[6] J. Lee, Flexural analysis of thin-walled composite beams using shear-deformable beam theory, *Composite Structures*, 70(2), 2005, pp 212-222.
[7] L. Librescu, and O. Song, *Thin-walled composite beams*, 1st edition, Springer, 2006.
[8] A.H. Sheikh and O.T. Thomsen, An efficient beam element for the analysis of laminated composite beams, *Composites Science and Technology*, 68, 2008, pp. 2273–2281.
[9] V.L. Berdichevsky, Variational-asymptotic method of constructing a theory of shell, *PMM*, 43(4), 1979, pp. 664–87.
[10] V.V. Volovoi, , D.H. Hodges, V.L. Berdichevsky, and V.G. Sutyrin, Asymptotic theory for static behaviour of elastic anisotropic I-beams, *International Journal of Solids and Structures*. 36, 1999, pp.1017-1043.
[11] V.V. Volovoi, D.H. Hodges, C.E.S. Cesnik, and B. Popescu, Assessment of beam modelling methods for rotor blade applications, *Mathematical and Computer Modelling*, 33, 2001, pp.1099-1112.
[12] V.V. Volovoi and D.H. Hodges, Single-and multi-celled composite thin-walled beams, *AIAA Journal*, 40, 2002, pp. 960–965.
[13] V.V. Volovoi and D.H. Hodges, Theory of anisotropic thin-walled beams, *Journal of Applied Mechanic*, 67, 2000, pp.453–459.
[14] W. Yu, D.H. Hodges, V.V. Volovoi and E.D. Fuchs, A generalized Vlasov theory for composite beams, *Thin Walled Structures*, 43, 2005, pp.1493–511.
[15] A.H. Sheikh, New Concept to include shear deformation in a curved beam element, *Journal of structural engineering*, 2002, 128(3), pp. 406-410.
[16] S.P. Machado, and V.H. Cortinez, Lateral buckling of thin-walled composite bisymmetric beams with prebuckling and shear deformation, *Engineering Structures*, 27, 2005, pp.1185-1196.
[17] S.Y. Back and K.M. Will, Shear-flexible thin-walled element for composite I-beams, *Engineering Structures*, 30, 2008, pp. 1447-1458.
[18] T.P. VO and J. Lee, On sixfold coupled buckling of thin-walled composite beams, *Composite Structures*, 90, 2009, pp.295-303.
[19] N-I. Kim, D.K. Shin, and M-Y. Kim, Flexural–torsional buckling loads for spatially coupled stability analysis of thin-walled composite columns, *Advances in Engineering Software*, 39, 2008, pp.949-961.
[20] V.H. Cortinez and M.T. Piovan, Vibration and buckling of composite thin-walled beams with shear deformability, *Journal of Sound and Vibration*, 258(4), 2002, pp. 701-723.
[21] N-I. Kim, D.K. Shin and Y-S. Park, Coupled stability analysis of thin-walled composite beams with closed cross-section, *Thin-Walled Structures*, 48, 2010, p.581–596.
[22] T.P. VO, and J. Lee, Interaction curves for vibration and buckling of thin-walled composite box beams under axial loads and end moments. *Applied Mathematical Modelling*. 34, 2010, pp.3142-3157.

APPENDIX A

The non-zero elements appeared in the upper triangle of the symmetric matrix [C_g] (Equation 6) are presented in their explicit form as follows (applicable for I and box sections).

$$C_{11}^g = C_{22}^g = A_{11},\ C_{13}^g = -B_{11}\cos\alpha - A_{11}(q\sin\alpha + r\cos\alpha)$$
$$C_{23}^g = -B_{11}\sin\alpha + A_{11}(q\cos\alpha - r\sin\alpha),\ C_{33}^g = C_{11} + 2rB_{11} + A_{11}(q^2 + r^2)$$

APPENDIX B

The non-zero elements appeared in the upper triangle of the symmetric matrix [F_g] (Equation 6) are presented in their explicit form as follows (applicable for I section, Fig. 6a).

$$F_{11}^g = F_{22}^g = b(A_{11}^1 + A_{11}^2) + dA_{11}^3,\ F_{13}^g = bd(A_{11}^2 - A_{11}^1)/2 - b(B_{11}^2 - B_{11}^1),\ F_{23}^g = -dB_{11}^3$$
$$F_{33}^g = b^3(A_{11}^1 + A_{11}^2)/12 + bd^2(A_{11}^1 + A_{11}^2)/4 + bd(B_{11}^1 + B_{11}^2) + b(C_{11}^1 + C_{11}^2) + d^3A_{11}^3/12 + dC_{11}^3/12$$

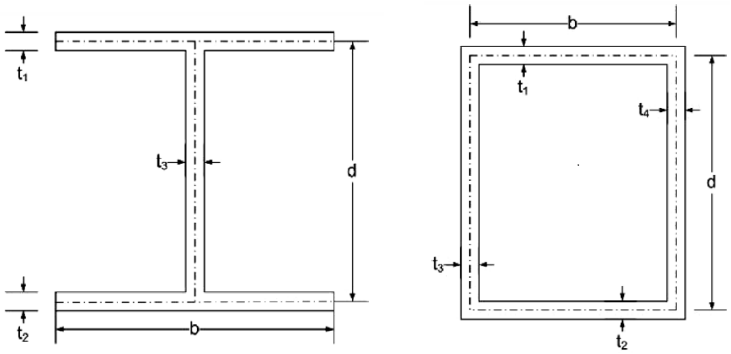

Figure 6: Thin-walled beam having open and closed section

The non-zero elements appeared in the upper triangle of the symmetric matrix [F_g] (Equation 6) are presented in their explicit form as follows (applicable for box section, Fig. 6b).

$$F_{11}^g = F_{22}^g = b(A_{11}^1 + A_{11}^2) + d(A_{11}^3 + A_{11}^4),\ F_{13}^g = bd(A_{11}^2 - A_{11}^1)/2 - b(B_{11}^2 - B_{11}^1),$$
$$F_{23}^g = bd(A_{11}^4 - A_{11}^3)/2 + d(B_{11}^4 - B_{11}^3),$$
$$F_{33}^g = b^3(A_{11}^1 + A_{11}^2)/12 + bd^2(A_{11}^1 + A_{11}^2)/4 + b^2d(A_{11}^3 + A_{11}^4)/4 + bd(B_{11}^1 + B_{11}^2 + B_{11}^3 + B_{11}^4)$$
$$+ b(C_{11}^1 + C_{11}^2) + d^3(A_{11}^3 + A_{11}^4)/12 + d(C_{11}^3 + C_{11}^4)$$

APPENDIX C

The non-zero elements appeared in the upper triangle of the symmetric matrix [C_m] (Equation 6) are presented in their explicit form as follows (applicable for I and box sections).

$$C_{11}^m = C_{22}^m = C_{33}^m = A,\ C_{15}^m = Ay\ ,\ C_{16}^m = Az\ ,\ C_{17}^m = A\phi,\ C_{24}^m = -A(q\sin\alpha + r\cos\alpha),$$
$$C_{34}^m = A(q\cos\alpha - r\sin\alpha),\ C_{44}^m = A(q^2 + r^{\wedge 2}) + C/12\ ,\ C_{55}^m = Ay^2 + C\sin^2\alpha/12,$$
$$C_{56}^m = Ayz - C\sin(2\alpha)/24\ ,\ C_{57}^m = Ay\phi + Cq\sin\alpha/12,\ C_{66}^m = Az^2 + C\cos^2\alpha/12,$$
$$C_{67}^m = Az\phi - Cq\cos\alpha/12,\ C_{77}^m = A\phi^2 + Cq^2/12$$

where $A = \sum t_i\rho_i$, $B = \sum t_i^2\rho_i$ and $C = \sum t_i^3\rho_i$

APPENDIX D

The non-zero elements appeared in the upper triangle of the symmetric matrix $[F_m]$ (Equation 9) are presented in their explicit form as follows (applicable for I section, Fig. 6a).

$$F_{11}^m = F_{22}^g = F_{33}^g = b_1A_1 + b_2A_2 + dA_3,\ F_{16}^m = -F_{24}^m = d(b_1A_1 - b_2A_2)/2,$$
$$F_{44}^m = (b_1^3A_1 + b_2^3A_2 + d^3A_3)/12 + d^2(b_1A_1 + b_2A_2)/4 + (b_1C_1 + b_2C_2 + dC_3)/12,$$
$$F_{55}^m = (b_1^3A_1 + b_2^3A_2)/12 + dC_3/3,\ F_{57}^m = d(b_1^3A_1 - b_2^3A_2)/24,$$
$$F_{66}^m = d^3A_3/12 + d^2(b_1A_1 + b_2A_2)/4 + (b_1C_1 + b_2C_2)/3,\ F_{77}^m = d^2(b_1^3A_1 + b_2^3A_2)/48 + d^3C_3/36$$

The non-zero elements appeared in the upper triangle of the symmetric matrix $[F_m]$ (Equation 9) are presented in their explicit form as follows (applicable for box section, Fig. 6b).

$$F_{11}^m = F_{22}^g = F_{33}^g = b(A_1 + A_2) + d(A_3 + A_4),\ F_{15}^m = F_{34}^m = bd(A_4 - A_3)/2,$$
$$F_{16}^m = -F_{24}^m = bd(A_1 - A_2)/2,$$
$$F_{44}^m = [b^3(A_1 + A_2) + d^3(A_3 + A_4)]/12 + bd[d(A_1 + A_2) + b(A_3 + A_4)]/4 + [b(C_1 + C_2) + d(C_3 + C_4)]/12,$$
$$F_{55}^m = b^3(A_1 + A_2)/12 + b^2d(A_3 + A_4)/4 + d(C_3 + C_4)/3,\ F_{57}^m = b^3d(A_1 - A_2)/24,$$
$$F_{66}^m = d^3(A_3 + A_4)/12 + bd^2(A_1 + A_2)/4 + b(C_1 + C_2)/3,\ F_{67}^m = \beta bd^3(A_4 - A_3)/24,$$
$$F_{77}^m = \beta^2b^2d^2[b(A_1 + A_2) + d(A_3 + A_4)]/48 + \beta^2[b^3(C_1 + C_2) + d^3(C_3 + C_4)]/144$$
$$- \beta[b^3(C_1 + C_2) - d^3(C_3 + C_4)]/72 + [b^3(C_1 + C_2) - d^3(C_3 + C_4)]/144$$

5. Chapter 4 - Vibration and dynamic stability of thin-walled laminated composite beams subjected to axial and end moment loads

Journal Paper 3, Submitted

A. Asadi, A.H. Sheikh, O.T. Thomsen, Vibration and dynamic stability of thin-walled laminated composite beams subjected to axial and end moment loads, Journal of Sound and Vibration, Submitted, November 2018

Statement of Authorship

Title of Paper	Vibration and dynamic stability of thin-walled laminated composite beams under axial load and end moments
Publication Status	☐ Published ☐ Accepted for Publication ☑ Submitted for Publication ☐ Unpublished and Unsubmitted w ork w ritten in manuscript style
Publication Details	A. Asadi, A.H. Sheikh, O.T. Thomsen,Vibration and dynamic stability of thin-walled laminated composite beams subjected to axial and end moment loading, Journal of Sound and Vibration

Principal Author

Name of Principal Author (Candidate)	Arash Asadi Khansari
Contribution to the Paper	Developed model, programming, performed all the analyses, prepared Manuscript
Overall percentage (%)	80%
Certification:	This paper reports on original research I conducted during the period of my Higher Degree by Research candidature and is not subject to any obligations or contractual agreements with a third party that would constrain its inclusion in this thesis. I am the primary author of this paper.
Signature	Date 9-Nov-2018

Co-Author Contributions

By signing the Statement of Authorship, each author certifies that:

i. the candidate's stated contribution to the publication is accurate (as detailed above);

ii. permission is granted for the candidate in include the publication in the thesis; and

iii. the sum of all co-author contributions is equal to 100% less the candidate's stated contribution.

Name of Co-Author	Abdul Hamid Sheikh
Contribution to the Paper	Supervised research, Provided critical manuscript evaluation
Signature	Date 09/11/2018

Name of Co-Author	Ole Thybo Thomsen
Contribution to the Paper	Provided critical manuscript evaluation, Acted as corresponding Author
Signature	Date 13 September 2018

Please cut and paste additional co-author panels here as required.

Vibration and dynamic stability of thin-walled laminated composite beams subjected to axial and end moment loads

Arash Asadi[1], Abdul Hamid Sheikh*[1] and Ole Thybo Thomsen[2]

[1] School of Civil, Environmental and Mining Engineering, the University of Adelaide, Adelaide, Australia

[2] Faculty of Engineering and Physical Sciences, University of Southampton, Highfield, Southampton, United Kingdom

Keywords: Buckling Analysis, Vibration Analysis, Axial and End Moment Preload, Finite element model, Thin-walled Composite beams, Dynamic Stability

ABSTRACT

An efficient technique based on a one dimensional beam finite element model for dynamic stability and vibration of thin-walled laminated composite beams having open/closed sections and subjected to axial loading and end moment preloads is proposed in this paper. The formulation accommodates for arbitrary stacking sequence of the individual section walls and includes all possible couplings between axial, shear, bending and torsional modes of deformation of the beam. The effects of transverse shear deformation of the section walls and out-of-plane warping are also included, where provision is made to either restrain or allow cross-sectional warping. Shear deformation is included in the finite element formulation of the beam by means of a novel concept proposed by the authors. A number of numerical examples involving open sections I beams and closed section box beams are analysed using the proposed approach, and it is shown that the new model performs very well when benchmarked against model results available in literature and finite element analysis results obtained using the software package Abaqus. Further, a parametric study is performed to elucidate the effects of axial load, end moments preload, and the combination of both loading actions on the vibration response and dynamic stability of various thin-walled composite beams.

1. INTRODUCTION

The use of long and slender beam like structural components having a thin-walled construction is very common in many real-life engineering products such as wind turbine

blades, helicopter rotor blades, civil engineering construction and other applications. In recent years, laminated fibre reinforced polymer materials (referred to as composite materials or just composites) have gained widespread use as structural materials in such structures. The motivation for this is the high specific stiffness and strength (stiffness and strength relative to mass/weight), which provides for more efficient structures with improved performance characteristics in many cases. Composites also display other desirable properties of high importance for many engineering applications, including high fatigue resistance and environmental durability to mention some.

The use of composite structural elements utilising multi-layered composite laminates with arbitrary fibre orientations of the individual layers (plies) provide a high degree of flexibility in tailoring the structural performance, but this can lead to complex in their behaviour due to couplings between different modes of deformation. Thus, the use of composites introduces additional challenges in the modelling of composite structures of thin-walled construction, which is already inherently complex for thin-walled structures made from isotropic materials due to warping deformation and other characteristic behaviours. In principle, the load-response behaviour of the thin-walled construction composite structural elements of open or closed cross section may be analysed using a 3D modelling strategy based on solid or shell finite elements (FE), but this modelling technique is unfeasible in many cases due to high computational cost and time. To address this problem previous research available in open literature has proposed to develop alternative modelling techniques, preferably based on 1D FE beam elements, which leads to more efficient and affordable techniques for modelling [e.g. 1-9].

The relevant previous research can be broadly divided into two groups based on the approaches used for determining the constitutive matrix of the beam element. The first approach is based on ‘analytical techniques’, while the second alternative utilises a two-dimensional (2D) cross-sectional analysis based on a 2D finite element model for calculating the cross-sectional matrices. Hodges et al. [3,10,11] have contributed significantly toward the development of the second approach, which has significant merit in terms of generality, but the 2D finite element analysis needed for the evaluation of cross-sectional stiffness coefficients is a major task. This was experienced and documented in a recent study [12], which is based on a similar approach. On the other hand, the first option (analytical approach), like presented in e.g. [6], adopted in this paper does not require 2D finite element

analysis, nor does it involve the complex mathematical operations involved with the second approach.

Vo & Lee et al. studied the behaviour of thin-walled composite beams having closed [e.g. 13] and open [e.g. 14, 15] sections, including buckling analysis. It is observed that their analyses are mostly based on classical lamination theory, thus neglecting the effect of transverse shear deformation of the composite laminated section walls. However, composite laminates are generally weak/compliant in transverse shear due to their low shear stiffness and strength relative to the extensional rigidity and strength. Thus, it is important to incorporate the effect of shear deformation to ensure reliable predictive capability for all relevant loading scenarios. In order to address this issue, Vo & Lee [16] incorporated the effect of shear deformation, by simply extending the concept used for the incorporation of transverse shear deformation in a typical isoparametric FE formulation to express the torsional deformation by introducing an additional parameter. This parameter is analogous to the transverse shear strain but, unfortunately, it does not have any real physical representation. Moreover, following this formulation it is difficult to resolve the torsional moment into three components to express the beam response in terms of stress resultants. However, by adopting this treatment of torsion loading, is was shown in [16] to be possible to derive an operational beam element using an isoparametric formulation for all deformation modes. The element has three nodes thus providing a quadratic interpolation of all (seven) field variables using Lagrangian interpolation functions giving seven degrees of freedom at each node.

Kim et al. [18-20] also considered the effect of shear deformations following the concept introduced by Vo & Lee [16] and encountered similar difficulties. Thus, for the finite element implementation of the beam theory, an isoparametric formulation for all field variables to develop a beam element having C^0 continuous deformations was adopted. The well known shear locking problem is typically faced in isoparametric elements as this formulation use the same interpolation functions for all field variables. A simple solution of this problem is the application of a reduced integration technique, as adopted by Kim et al. [18-20], but that may lead to spurious zero energy modes for some cases in addition to non-physical stress oscillations within the element. Moreover, the reduced integration will affect the evaluation of the stiffness corresponding to other modes of deformation, including axial and torsion modes and their couplings. Furthermore, it is also difficult to apply a selective reduced integration scheme in this coupled problem. However, Kim et al. [e.g. 18-22] have contributed

significantly in this area through investigating various aspects of thin-walled section composite beams.

The formulations presented by both these groups [13-16, 18-20] are consistent when the contribution of shear deformation is neglected. For this case, the Lagrangian interpolation functions are only used for the axial deformation, whereas other deformation modes, i.e. torsion and bending (bi-axial), are interpolated with Hermitian interpolation functions. Thus, these elements provide C^0 continuity (1 degree of freedom at each node – field variable only) for the axial displacement, and C^1 continuity (2 degrees of freedom at each node – field variable and its derivative) for the other modes of deformation. Machado et al. [23-30] also included the effect of shear deformation in their modelling of thin-walled composite beams in a series of studies. These are mostly based on the use of the Ritz method to develop analytical solutions that are applied to symmetrically balanced laminates or special layups to decouple the equations for simplicity. The models were also employed for the analysis of dynamic stability problems of thin-walled composite beams subjected to periodic transverse and axial loads [27,28]. Furthermore, a finite element model for simulating vibration and dynamic stability was proposed in [31] considering the effect of shear deformation and cross-sectional warping due to torsion. As mentioned above, the finite element formulation for torsional deformation typically requires C^1 continuity for the angle of twist (θ_x)due to the presence of the derivative of the twist (θ_x') in the expression for the displacement fields of the beam. However, θ_x and θ_x' were treated as independent variables, thus enabling the derivation of a C^0 continuous element having linear interpolations for all displacement field variables. However, ass θ_x' is not physically independent of θ_x, this approach can be expected to display physically inconsistent results in some cases.

The literature review shows that a limited number of studies have been conducted on dynamic stability and vibration of thin-walled composite beams with arbitrary cross sections and arbitrary laminate layups subjected to preloading (axial force and/or end moments). Thus, the focus of this paper is to propose a new and efficient finite element based modelling approach to address the analysis of such composite beam structures and ensuring a high level of generality. The model proposed includes the effect of shear deformation since composites are compliant in shear as mentioned above. However, the problems associated with existing techniques, e.g. [16,20], will be overcome by introducing an alternative formulation.

The new formulation will be applied to thin-walled composite beams with both open and closed cross sections subjected to axial forces, end moments and combinations of these applied as preloads. The model addresses all the different modes of deformation and their coupling including axial, torsional, bi-axial bending, bi-axial shear as well as warping (for torsion) deformations. The cross-sectional property matrixes are derived explicitly in closed form for open and closed cross sections for both plane stress and plane strain conditions of the laminae.

Based on the evaluation of the components of the cross-sectional matrixes of a thin-wall composite beam, the analysis is achieved through the solution of the 1D finite element formulation of the beam problem. The usual approach adopted for incorporating the transverse shear deformation in an isoparametric FE model framework requires a C^0 continuous formulation, whilst the warping displacement produced by torsion requires a C^1 continuous formulation for the twisting rotation. The C^1 formulation for the torsional deformation is conveniently achieved in this study by using cubic Hermitian interpolation functions for the angle of twist and its derivative at the two end nodes of the proposed beam element (Fig. 1). If the conventional C^0 continuous formulation is adopted for the transverse shear deformation, this will require the need for reduced integration, but the implementation of this is problematic for the considered coupled beam problem as discussed above. This is a crucial issue, which can be circumvented conveniently by utilising the modelling concept proposed by Sheikh [32] that eliminates the need for reduced integration.

For the 1D beam finite element analysis, a three-node beam element as shown in Fig. 1 has been developed, where the two end nodes have seven degrees of freedom (three displacements, three rotations and the derivative of the twist) and the middle node has five degrees of freedom (three displacements, two bending rotations). It should be noted that quadratic Lagrangian interpolation functions are used to model the axial deformation taking one degrees of freedom at each node.

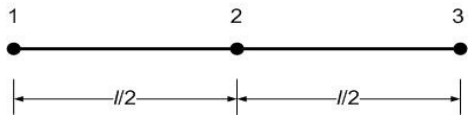

Fig. 1: A typical beam element

A computer code was written in MATLAB for the implementation of the formulation. Numerical examples of thin-walled composite beams having different cross sections, material configurations, boundary conditions and other features are analysed by the proposed model. The results obtained are presented in the form of preloaded vibrational and dynamic stability regions, and the predictions are compared to and benchmarked against data available in open literature. It is shown that the present finite element model formulations performs very well in comparison with other published models. Finally, the new model has been used to investigate a number of cases of special interest, which generate results that are considered to be beneficial benchmarks for future research in this area.

2. FORMULATION

2.1. Kinematics of the Beam Deformations

Fig. 2 shows part of the cross section of a laminated beam wall segment along with global and local coordinate systems and their corresponding displacement components, which form the basis for the development of the proposed formulation. The curved geometry of the section wall is shown to represent a generic scenario, but the section walls can also be of straight geometry.

In Fig. 2, the *x*-*y*-*z* axes define the global Cartesian coordinate system, where *x* is along the beam axis, passing through the centroid of the complete beam cross section, and y, z define the beam cross section coordinates. The other axes in Fig. 2 are the local orthogonal coordinate system *x*-*s*-*n*, defined at the mid-plane of a laminated section wall, where *n* is normal to the shell (wall) mid-plane, *s* is the circumference coordinate, and *x* is parallel to global *x* coordinate axis. The displacement components at the mid-plane of the shell wall in the local coordinate system (*x*-*s*-*n*) can be expressed in terms of the global displacements of the beam (Fig. 2) in the form [1]:

$$\begin{aligned} \bar{u} &= U + y\theta_y + z\theta_z + \phi\,\theta_x', \\ \bar{v} &= V\cos\alpha + W\sin\alpha - r(s)\theta_x, \\ \bar{w} &= -V\sin\alpha + W\cos\alpha + q(s)\theta_x, \end{aligned} \tag{1}$$

where θ_y, θ_z are bending rotations (including shear deformations) of the beam cross section relative to the along *y* and *z* axes, respectively, θ_x is the torsional rotation of the beam cross section relative to the *x* axis, and φ is the warping function. *U*, *V* and *W* are the displacement

components in the global *x*, *y* and *z* coordinate directions. Defining Ψ_y, Ψ_z as cross-sectional rotations due to shear deformations of the beam section about the *y* and *z* axes, the bending rotations can be expressed as $\theta_y = -V' + \Psi_y$ and $\theta_z = -W' + \Psi_z$, respectively, and V', W' and θ_x' are the derivatives of *V*, *W* and θ_x with respect to *x*.

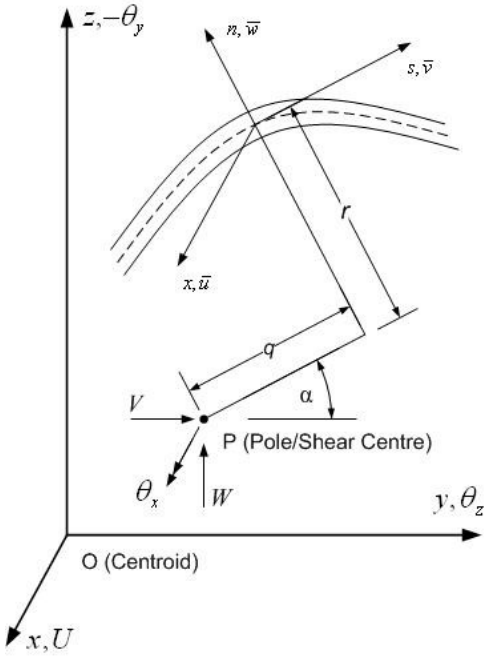

Fig. 2: Cross section of a beam section wall segment with local and global coordinate system and corresponding displacement components

Although the effects of warping displacement in beams having closed cross sections is generally not as significant as for beams with open cross section, the contribution of warping displacements is incorporated for both types of cross sections to deliver a generic and complete formulation.

The displacement at any point of the shell wall located at a distance *n* from the shell wall mid-plane can be expressed in terms of the bending and transverse shear deformations of the wall as:

$$u = \bar{u} + n\left(-\frac{\partial \bar{w}}{\partial x} + \psi_{xn}\right),$$
$$v = \bar{v} + n\left(-\frac{\partial \bar{w}}{\partial s} + \psi_{sn}\right), \quad (2)$$
$$w = \bar{w},$$

where ψ_{xn} and ψ_{sn} are rotations of the shell wall sections due to shear deformations about *s* and *x*, respectively. Now, ψ_{xn} can be expressed in terms of the corresponding global cross section rotations (Ψ_y, Ψ_z) as $\psi_{xn} = -\Psi_y \sin\alpha + \Psi_z \cos\alpha$, whereas $\psi_{sn} = 0$ based on the restrictive assumption that the overall shape of the beam cross section will not be altered during the deformation of the beam.

Substituting the above expressions for ψ_{xn} and ψ_{sn} as well as Eq. (1) into Eq. (2), the displacements at any point within the shell wall along its local coordinate system (*x*-*s*-*n*) can be expressed in terms of the global displacement components of the 1D beam as follows:

$$\begin{aligned} u &= U + \left(y - n\sin\alpha\right)\theta_y + \left(z + n\cos\alpha\right)\theta_z + \left(\phi - nq(s)\right)\theta_x', \\ v &= V\cos\alpha + W\sin\alpha - \left(r(s) + n\right)\theta_x, \\ w &= -V\sin\alpha + W\cos\alpha + q(s)\theta_x \end{aligned} \tag{3}$$

2.2. Energy Systems for the Composite Beam

The potential energy (Π) of a beam undergoing buckling caused by an external forces can be expressed in terms of the strain energy (*U*), Kinetic energy (*T*), and the work done by external forces (W_e) as:

$$\Pi = U + T - W_e, \tag{4}$$

Now the strain energy appearing in the above equation can be expressed in terms of stress $\{\sigma\}$ and strain $\{\varepsilon\}$ vectors of the shell walls expressed in their local axis system (*x*-*s*-*n*) as:

$$U = \frac{1}{2}\int \{\varepsilon\}^T \{\sigma\}\, dv \tag{5}$$

The relationship between the stress and strain vectors for a ply of the laminated shell wall having any orientation can be expressed using its constitutive matrix $\left[\bar{Q}\right]$ following the 'classical lamination theory' (CLT) as described in text books on mechanics of composite materials [4] as:

$$\{\sigma\} = \begin{Bmatrix} \sigma_x \\ \sigma_s \\ \sigma_{xs} \\ \sigma_{xn} \\ \sigma_{sn} \end{Bmatrix} = \begin{bmatrix} \bar{Q}_{11} & \bar{Q}_{12} & \bar{Q}_{16} & 0 & 0 \\ \bar{Q}_{21} & \bar{Q}_{22} & \bar{Q}_{26} & 0 & 0 \\ \bar{Q}_{61} & \bar{Q}_{62} & \bar{Q}_{66} & 0 & 0 \\ 0 & 0 & 0 & \bar{Q}_{55} & \bar{Q}_{54} \\ 0 & 0 & 0 & \bar{Q}_{45} & \bar{Q}_{44} \end{bmatrix} \begin{Bmatrix} \varepsilon_x \\ \varepsilon_s \\ \varepsilon_{xs} \\ \varepsilon_{xn} \\ \varepsilon_{sn} \end{Bmatrix} = \left[\bar{Q}\right]\{\varepsilon\} \tag{6}$$

Eq (6) above is expressed in terms of all five stress and strain components typically occurring in a shell element, but some of these components will not be present in the present problem due to the restrictive assumption adopted that the beam cross section will not change shape during deformation. Thus, there will be no bending and shear deformations in the *s*-*n* plane, which leads to $\psi_{ns} = 0$ and $\sigma_s = 0$ (usually defined as a plane stress condition) or $\varepsilon_s = 0$ (i.e. a plane strain condition). By incorporating this the above equation reduces to:

$$\{\sigma\} = \begin{Bmatrix} \sigma_x \\ \sigma_{xs} \\ \sigma_{xn} \end{Bmatrix} = \begin{bmatrix} \tilde{Q}_{11} & \tilde{Q}_{16} & 0 \\ \tilde{Q}_{61} & \tilde{Q}_{66} & 0 \\ 0 & 0 & \tilde{Q}_{55} \end{bmatrix} \begin{Bmatrix} \varepsilon_x \\ \varepsilon_{xs} \\ \varepsilon_{xn} \end{Bmatrix} = \left[\tilde{Q}\right]\{\varepsilon\} \tag{7}$$

where $\tilde{Q}_{11} = \overline{Q}_{11}$, $\tilde{Q}_{16} = \overline{Q}_{16}$, $\tilde{Q}_{66} = \overline{Q}_{66}$ and $\tilde{Q}_{55} = \overline{Q}_{55}$ for plane strain condition (ε_s = 0); and $\tilde{Q}_{11} = \overline{Q}_{11} - \overline{Q}_{12}\overline{Q}_{12} / \overline{Q}_{22}$, $\tilde{Q}_{16} = \overline{Q}_{16} - \overline{Q}_{12}\overline{Q}_{26} / \overline{Q}_{22}$, $\tilde{Q}_{66} = \overline{Q}_{66} - \overline{Q}_{16}\overline{Q}_{16} / \overline{Q}_{22}$ and $\tilde{Q}_{55} = \overline{Q}_{55}$ for the plane stress (σ_s = 0) condition.

The substitution of the expressions for the local displacement components, at any point of the shell wall in terms of the global displacement components (Eq. (3)), into the reduced strain vector (Eq. (7)), leads to:

$$\{\varepsilon\} = \begin{Bmatrix} \partial u/\partial x \\ \partial u/\partial s + \partial v/\partial x \\ \psi_{xn} \end{Bmatrix} = \begin{Bmatrix} U' + (y - n\sin\alpha)\theta_y' + (z + n\cos\alpha)\theta_z' + (\phi - nq)\theta_x'' \\ \Psi_y \cos\alpha + \Psi_z \sin\alpha - (2n + r - \partial\phi/\partial s)\theta_x' \\ -\Psi_y \sin\alpha + \Psi_z \cos\alpha \end{Bmatrix} \tag{8}$$

where

$$\phi = \int r ds - 2A_c\delta_s / \delta \tag{9}$$

where $\delta_s = \int \frac{ds}{\tilde{Q}_{66}}$, $\delta = \oint \frac{ds}{\tilde{Q}_{66}}$. For a closed beam cross section profile A_c is the cross-sectional area enclosed by the wall mid-plane line/contour. For an open section profile, the warping function may be simplified to $\phi = \int r ds$.

Eq. (8) can now be rearranged as multiplication of the cross section stiffness matrix ($[H]$) and the strain vector of the beam ($\{\bar{\varepsilon}\}$) which contains global displacement parameters for 1D beam as:

$$\{\varepsilon\} = [H]\{\bar{\varepsilon}\} \tag{10}$$

where

$$\{\bar{\varepsilon}\} = \left\{U' \quad \theta_y' \quad \theta_z' \quad \theta_x'' \quad \theta_x' \quad V'+\theta_y \quad W'+\theta_z\right\}^T$$

$$[H] = \begin{bmatrix} 1 & y-n\sin\alpha & z+n\cos\alpha & \phi-nq & 0 & 0 & 0 \\ 0 & 0 & 0 & 0 & -\left(2n+r-\phi_{,s}\right) & \cos\alpha & -\sin\alpha \\ 0 & 0 & 0 & 0 & 0 & \sin\alpha & \cos\alpha \end{bmatrix} \tag{11}$$

By substitution of Eqs. (7, 8, 10) into Eq. (5), the strain energy of the system can be expressed as:

$$U = \frac{1}{2}\int \{\varepsilon\}^T \{\sigma\}\, dv = \frac{1}{2}\int \{\bar{\varepsilon}\}^T [H]^T \left[\tilde{Q}\right][H]\{\bar{\varepsilon}\}\, dnds dx = \frac{1}{2}\int \{\bar{\varepsilon}\}^T [D]\{\bar{\varepsilon}\}\, dx \tag{12}$$

where

$$[D] = \int\left(\int [H]^T \left[\tilde{Q}\right][H] dn\right) ds = \int [C] ds \tag{13}$$

All individual elements of the matrix [*C*] are derived explicitly in closed form. Similarly, all elements of the cross sectional stiffness matrix [*D*] are derived specifically and in closed form for open I section and closed box section profiles having generic geometric configurations. This includes general specification of cross section dimensions, and arbitrary lay-up (stacking sequence) of the cross section walls in terms of choice of material, number of plies, and ply orientations. The explicit expressions for the components of [*C*] and [*D*] are derived in a previous article by the authors [33].

The kinematic energy can be expressed in terms of derivative of the displacement vector ($\{\dot{u}\}$) and mass density of the laminate material (ρ) as:

$$T = \frac{1}{2}\int \{\dot{u}\}^T \{\rho\}\{\dot{u}\}\, dv \tag{14}$$

Using Eq. (3) the displacement vector $\{u\}$ may be expressed in the form:

$$\{u\} = \begin{Bmatrix} u \\ v \\ w \end{Bmatrix} = [H_m]\{\bar{\delta}\} \tag{15}$$

where

$$[H_m] = \begin{bmatrix} 1 & 0 & 0 & 0 & y-n\sin\alpha & z+n\cos\alpha & \phi-nq(s) \\ 0 & \cos\alpha & \sin\alpha & -r(s)-n & 0 & 0 & 0 \\ 0 & -\sin\alpha & \cos\alpha & q(s) & 0 & 0 & 0 \end{bmatrix} \tag{16}$$

$$\{\bar{\delta}\}^T = \left\{U \quad V \quad W \quad \theta_x \quad \theta_y \quad \theta_z \quad \theta'\right\}$$

Taking the derivative of Eq. (15) with respect to regards to time (*t*) yields:

$$\{\dot{u}\} = [H_m]\left\{\dot{\bar{\delta}}\right\} \tag{17}$$

And substituting Eq. (17) into Eq. (14), the kinetic energy can be expressed as

$$T = \frac{1}{2}\int \left\{\dot{\bar{\delta}}\right\}^T [H_m]^T \{\rho\}[H_m]\left\{\dot{\bar{\delta}}\right\} dv = \frac{1}{2}\int \left\{\dot{\bar{\delta}}\right\}^T [F_m]\left\{\dot{\bar{\delta}}\right\} dx \tag{18}$$

where

$$[F_m] = \int_A [H_m]^T \{\boldsymbol{\rho}\}[H_m] dsdn = \int \left(\int [H_m]^T \{\boldsymbol{\rho}\}[H_m] dn\right) ds = \int [C_m] ds \tag{19}$$

The individual elements of the matrices $[C_m]$ and $[F_m]$ have been derived in explicit form and are presented in a previous paper by the authors [34].

The external forces considered in this study, which will be causing the buckling of the thin-walled composite beams, are axial force (P_0) and end moment (M_0) loading. Both these forces induce only one stress component, the axial stress (σ_x), which can be expressed in simple form and used to formulate the problem conveniently, i.e.:

$$\sigma_x = \frac{P_\circ}{A} + \frac{M_0^y}{I_y} z \tag{20}$$

where A and I_y are cross-sectional area and moment of inertia of the beam cross sectional area. It should be noted that the above equation will give a stress that can be defined as an equivalent stress. The aim here to estimate this stress in a simple way without affecting the results significantly rather than undertaking a detailed analysis for predicting the stress distribution over the individual layers precisely. The work done (W_e) by the external forces P_0 and M_0 can be expressed as:

$$W_e = \frac{1}{2}\int_V \sigma_x (v'^2 + w'^2) dv = \frac{1}{2}\int_V \{v' \quad w'\} \sigma_x \begin{Bmatrix} v' \\ w' \end{Bmatrix} dv = \frac{1}{2}\int_V \left\{\varepsilon_g\right\}^T \sigma_x \left\{\varepsilon_g\right\} dv \tag{21}$$

Using Eq. (3), the geometric strain vector $\left\{\boldsymbol{\varepsilon}_g\right\}$ in the above equation can be written as

$$\left\{\varepsilon_g\right\} = \begin{Bmatrix} v' \\ w' \end{Bmatrix} = \begin{bmatrix} \cos\alpha & \sin\alpha & -(r+n) \\ -\sin\alpha & \cos\alpha & q \end{bmatrix} \begin{Bmatrix} V' \\ W' \\ \theta_x' \end{Bmatrix} = [H_g]\left\{\bar{\varepsilon}_g\right\}. \tag{22}$$

Eqs. (14) and (16) may be substituted into Eq. (15) leading to:

$$W_e = \frac{P_0}{2A}\int_V \{\varepsilon_g\}^T \{\varepsilon_g\} dv + \frac{M_0}{2I_y}\int_L \{\varepsilon_g\}^T z \{\varepsilon_g\} dv$$
$$= \frac{P_0}{2A}\int_L \{\bar{\varepsilon}_g\}^T \left[F_g^P\right] \{\bar{\varepsilon}_g\} dx + \frac{M_0}{2I_y}\int_L \{\bar{\varepsilon}_g\}^T \left[F_g^M\right] \{\bar{\varepsilon}_g\} dx \quad (23)$$

where

$$\left[F_g^P\right] = \int_A \left[H_g\right]^T \left[H_g\right] dsdn = \int \left(\int \left[H_g\right]^T \left[H_g\right] dn\right) ds = \int \left(\left[C_g^P\right]\right) ds$$
$$\left[F_g^M\right] = \int_A \left[H_g\right]^T z \left[H_g\right] dsdn \quad (24)$$

The individual elements of the matrices $\left[C_g^P\right]$ are derived explicitly and provided in Appendix A. Also, all elements of the matrices $\left[F_g^P\right]$ and $\left[F_g^M\right]$ are derived for the considered generic I (open) and box (closed) beam sections and given in Appendix B.

2.3. Finite Element Formulation

For the 1D finite element implementation of the thin-walled beam theory based on the energy expressions presented in the previous section, quadratic Lagrangian interpolation functions are used for the axial deformation, while cubic Hermitian interpolation functions are used for the torsional deformation. This ensures the desired C^1 continuity of the torsional rotation (θ_x) as the strain vector (Eq. (8)) contains second derivative of θ_x. As mentioned earlier, the bending deformations along with the shear deformations are treated in a different manner following the approach introduced in [32] to eliminate the difficulties faced by other existing formulations. Accordingly, the cross-sectional rotations Ψ_y and Ψ_z due to shear deformations are adopted as field variables instead of θ_y and θ_z in addition to the bending displacements V and W. adopting a linear approximation of Ψ_y, Ψ_z, and a cubic approximation of V and W, these field variables (V, W, Ψ_y and Ψ_z) along with the remaining two field variables (U and θ_x) can be expressed in the form:

$$
\begin{aligned}
U &= a_1 + a_2 x + a_3 x^2 \\
V &= a_4 + a_5 x + a_6 x^2 + a_7 x^3 \\
W &= a_8 + a_9 x + a_{10} x^2 + a_{11} x^3 \\
\Psi_y &= a_{12} + a_{13} x \\
\Psi_z &= a_{14} + a_{15} x \\
\theta_x &= a_{16} + a_{17} x + a_{18} x^2 + a_{19} x^3
\end{aligned}
\tag{25}
$$

It should be noted that Ψ_y and Ψ_z are taken as field variables, but that they are not used as nodal degrees of freedom. Rather, the corresponding nodal degrees of freedom correspond to θ_y and θ_z utilising the following equations for θ_y and θ_z obtained by invoking Eqs. (25):

$$
\begin{aligned}
\theta_y &= \Psi_y - V' = a_{12} + a_{13} x - a_5 - 2a_6 x - 3a_7 x^2, \\
\theta_z &= \Psi_z - W' = a_{14} + a_{15} x - a_9 - 2a_{10} x - 3a_{11} x^2
\end{aligned}
\tag{26}
$$

The unknown constants (a_1, a_2, a_3 ..... a_{19}) appearing in Eqs. (25) can be replaced by the nodal displacement vector $\{\delta\}$ by substitution of U , V , W (from Eqs. 25), θ_y and θ_z (Eq. (26)) at all three nodes of the beam element (Fig. 1), and θ_x (from Eq. 25) and its derivative $\theta_x' \left(= a_{17} + 2a_{18} x + 3a_{19} x^2\right)$ at the two end nodes as:

$$
\{\delta\} = [R]\{a\} \text{ or } \{a\} = [R]^{-1}\{\delta\} \tag{27}
$$

where $\{a\}^T = \begin{bmatrix} a_1 & a_2 & a_3 & \cdots & a_{19} \end{bmatrix}$, $[R]$ consists of coordinates (x values) of the three element nodes, and $\{\delta\} = \begin{Bmatrix} U_1 & V_1 & W_1 & \theta_{x1} & \theta_{y1} & \theta_{z1} & \theta'_{x1} & U_2 & V_2 & W_2 & \theta_{y2} & \theta_{z2} & U_3 & V_3 & W_3 & \theta_{x3} & \theta_{y3} & \theta_{z3} & \theta'_{x3} \end{Bmatrix}^T$.

Utilising Eqs. (25-27), the strain vector of the beam $\{\bar{\varepsilon}\}$ appearing in Eq. (9) can be expressed in terms of nodal displacement vector $\{\delta\}$ in the form:

$$
\begin{aligned}
\{\bar{\varepsilon}\} &= \begin{Bmatrix} U' & \theta_y' & \theta_z' & \theta_x'' & \theta_x' & V' + \theta_y & W' + \theta_z \end{Bmatrix}^T \\
&= [S(x)]\{a\} = [S(x)][R]^{-1}\{\delta\} = [B]\{\delta\}
\end{aligned}
\tag{28}
$$

The above equation is substituted into Eq. (11) and rewritten to obtain the stiffness matrix [K] of the beam element as:

$$U = \frac{1}{2}\int \{\bar{\varepsilon}\}^T [D]\{\bar{\varepsilon}\}\, dx = \frac{1}{2}\{\delta\}^T \int [B]^T [D][B] dx \{\delta\} = \frac{1}{2}\{\delta\}^T [k]\{\delta\} \tag{29}$$

Similarly, using of Eqs. (25-27), the vector $\{\bar{\delta}\}$ appearing in Eq. (15) can be expressed in terms of $\{\delta\}$ as:

$$\{\bar{\delta}\} = [S_m(x)][R]^{-1}\{\delta\} \tag{30}$$

By taking the derivative of Eq. (30) with respect to time (t), $\{\dot{\bar{\delta}}\}$ may be expressed as:

$$\{\dot{\bar{\delta}}\} = [S_m(x)][R]^{-1}\{\dot{\delta}\} \tag{31}$$

Eq. (31) is then substituted into Eq. (18) and regrouped to get:

$$T = \frac{1}{2}\{\dot{\delta}\}^T \int [R]^{-T}[S_m(x)]^T [F_m]^T [S_m(x)][R]^{-1} dv \{\dot{\delta}\} = \frac{1}{2}\{\dot{\delta}\}^T [M]\{\dot{\delta}\}^T \tag{32}$$

Again Eqs. (25-27) can be substituted into the vector $\{\bar{\varepsilon}_g\}$ appearing in Eq. (16) and it can be expressed in terms of $\{\delta\}$ as:

$$\{\bar{\varepsilon}_g\} = \begin{bmatrix} V' & W' & \theta_x' \end{bmatrix}^T = [S_g(x)]\{a\} = [S_g(x)][R]^{-1}\{\delta\} = [B_g]\{\delta\}. \tag{33}$$

Eq. (33) is now substituted into Eq. (23) which can be regrouped to yield:

$$\begin{aligned} W_e &= \frac{P_0}{2A}\int_L \{\delta\}^T \left[B_g\right]^T \left[F_g^P\right]\left[B_g\right]\{\delta\}\, dx + \frac{M_0}{2I_y}\int_L \{\delta\}^T \left[B_g\right]^T \left[F_g^M\right]\left[B_g\right]\{\delta\}\, dx \\ &= \frac{P_0}{2}\{\delta\}^T \left[k_g^P\right]\{\delta\} + \frac{M_0}{2}\{\delta\}^T \left[k_g^M\right]\{\delta\} \end{aligned} \tag{34}$$

where $\left[k_g^P\right] = \frac{1}{A}\int_L \left[B_g\right]^T \left[F_g^P\right]\left[B_g\right] dx$, and $\left[k_g^M\right] = \frac{1}{I_y}\int_L \left[B_g\right]^T \left[F_g^M\right]\left[B_g\right] dx$ are the geometric stiffness matrices of the beam element corresponding to axial loading and end moment loading, respectively.

Now the strain energy (Eq. (29)), the kinetic energy (Eq. (32)) and the work done by external loads (Eq. (34)) for all elements are substituted into the expression for the total potential energy of the structural system (Eq. (4)). This is then minimised with respect to the nodal displacements of the structure $\{\Delta\}$ to obtain the final governing equation of the beam in the form:

$$\left([K] - P_0\left[K_g^P\right] - M_0^y\left[K_g^M\right]\right)\{\Delta\} + [M]\{\ddot{\Delta}\} = 0 \tag{35}$$

where $[K]$ is the stiffness matrix of the structure, $[M]$ is the mass matrix of the structure, and $[K_g^P]$ and $[K_g^M]$ are the geometric stiffness matrices for the axial load (P) and the end moments (M_y), respectively, which are obtained by assembling their corresponding components of the individual elements.

Eq. (35) can be reduced to a simple Eigenvalue problem by taking $M_0^y = 0$ or $P_0 = 0$ in addition to $[M] = 0$, and the equation can be solved to obtain the critical value of the axial load (P_{CR}) or the critical value of end moment (M_{CR}) (the Eigen value). Eq. (35) can also be reduced to a simple Eigenvalue problem by assigning preload values $M_0^y = 0$ and $P_0 = 0$, and following this solving the equation to obtain the natural vibration frequencies of the system as the Eigen values. Furthermore, for a composite beam subjected to static axial force and/or end moments ($M_0^y < M_{CR}$ and $P_0 < P_{CR}$) the equation can be solved to obtain vibration frequencies of the preloaded system as the Eigen values. The composite beam problem exhibits multiple vibrational modes that will provide multiple Eigen values, as well as multiple Eigen vectors as mode shapes that can be extracted from $\{\Delta\}$.

So far, the axial force and end moments have been considered as static actions but in many practical problems, they are often found to include a dynamic component varying over time in addition to the static component. For such scenarios, a special type of instability can occur where even the algebraic summation of the static and dynamic (peak) components will be less than the static critical buckling load. This phenomenon is typically referred to as dynamic instability, and it occurs when the frequency of the dynamic load element exerts a significant influence on the structural response. This will be addressed in the following section.

2.4. Dynamic Stability Formulation

The axial force can be expressed as the sum of a static and a dynamic part, which can further be expressed in terms of critical the static buckling load (P_{CR}) in the form:

$$P_0 = P_{ST} + P_{Dyn} = P_{CR}(\alpha + \beta\cos(\Omega t)) \tag{36}$$

where the dynamic load part is assumed to be a simple harmonic excitation with a frequency of Ω for simplicity. In the absence of end moments, Eq. (36) can be substituted into Eq. (35) and written as:

$$\left([K]-P_{CR}(\alpha+\beta\cos(\Omega t))[K_g^P]\right)\{\Delta\}+[M]\{\ddot{\Delta}\}=0 \tag{37}$$

Eq. (37) has the form of a so-called Mathieu-Hill equation, and is a mathematical representation of the instability behaviour of a composite beam subjected to periodic axial loading [35] The region of instability is determined by using periodic solutions of the response with a period of T and $2T$ where $T=2\pi/\Omega$. With this, the solution for the displacement vector can be expressed as [35]:

$$\{\Delta\}=\sum_{k=1,3,5,\ldots}^{\infty}\left(\{a_k\}\sin\frac{k\Omega t}{2}+\{b_k\}\cos\frac{k\Omega t}{2}\right) \tag{38}$$

After substitution of Eq. (38) into Eq. (37), and considering only the first term in the series expansion only [35], the following is obtained:

$$\left([K]-P_{CR}(a\mp 0.5\beta)[K_g^P]-0.25\Omega^2[M]\right)\{\Delta_{ab}\}=0 \tag{39}$$

Eq. (39) is a standard Eigenvalue problem and it is solved twice corresponding to positive and negative signs of β to determine the two frequencies indicating the boundaries of the instability region.

Similarly, the end moment can be written as the sum of a static and a dynamic part, which can further be expressed in terms of the critical static buckling load (M_{CR}) as:

$$M=M_{ST}^{y}+M_{Dyn}^{y}=M_{CR}^{y}(\eta+\lambda\cos(\Upsilon t)) \tag{40}$$

where it is assumed, for simplicity, that the dynamic loading part can be modelled as a simple harmonic excitation with frequency of Υ . In the absence of axial force, the above equation can be substituted into Eq. (35) and rewritten as:

$$\left([K]-M_{CR}^{y}(\eta+\lambda\cos(\Upsilon t))[K_g^M]\right)\{\Delta\}+[M]\{\ddot{\Delta}\}=0 \tag{41}$$

Similarly, the regions of instability for Eq. (41) can be determined using periodic solutions with the Period T and 2T where $T=2\pi/Y$. With this, the solution for the displacement vector can be expressed as [35]:

$$\{\Delta\}=\sum_{k=1,3,5,\ldots}^{\infty}\left(\{c_k\}\sin\frac{k\Upsilon t}{2}+\{d_k\}\cos\frac{k\Upsilon t}{2}\right) \tag{42}$$

After substitution of Eq. (38) into Eq. (37) and considering only the first term in the series expansion [35] the following relation is obtained:

$$\left([K]-M_{CR}^{y}(\eta\mp 0.5\lambda)[K_g^M]-0.25\Upsilon^2[M]\right)\{\Delta_{cd}\}=0 \tag{43}$$

As before, Eq. (43) is a standard Eigenvalue problem and it is solved twice corresponding to positive and negative signs of λ to determine the two frequencies indicating the boundaries of the instability region.

3. RESULTS AND DISCUSSION

In this section, numerical examples of thin-walled composite beams having I and box sections are presented based on solutions obtained using the proposed model. Firstly, the vibration behaviour of composite beams preloaded with axial force and/or end moments is presented. Secondly, the predictive results are benchmarked and compared against results available in open literature. Finally, predictions regarding dynamic instability of composite beams are presented and discussed.

3.1. Vibration of Preloaded Composite Beams

3.1.1. Vibration of a cantilever mono-symmetric I section beam under axial preload

The behaviour of a 1 m long cantilever beam having a mono-symmetric I section is investigated for different stacking sequences for its laminated walls. The web of the beam is 50 mm deep and the width of its top and bottom flanges are 30 mm and 50 mm, respectively. The web and flanges are made of 16 plies, each 0.13 mm thick, with a symmetrical lay-up $[\pm\theta]_{4S}$. The material used for all the layers is glass-epoxy having the following properties: E_1=53.78GPa, E_2=17.93GPa, G_{12}=G_{13}=8.96GPa, G_{23}=3.45GPa, ν_{12}=0.25, ρ=1968.9 kg/m^3. To show the convergence behaviour of the proposed model with respect to element size, a specific design case from Table 1 having the stacking sequence of $[\pm 45]_{4S}$ and subjected to an axial preload of -781.2 N (see Table 1, $\theta = 45^0$) is considered and the results are presented in Fig. 3. Figure shows that the analyses have converged with eight elements or more along the length of the beam. Based on this observation, all subsequent analyses of composite beams are analysed with 10 elements unless mentioned otherwise.

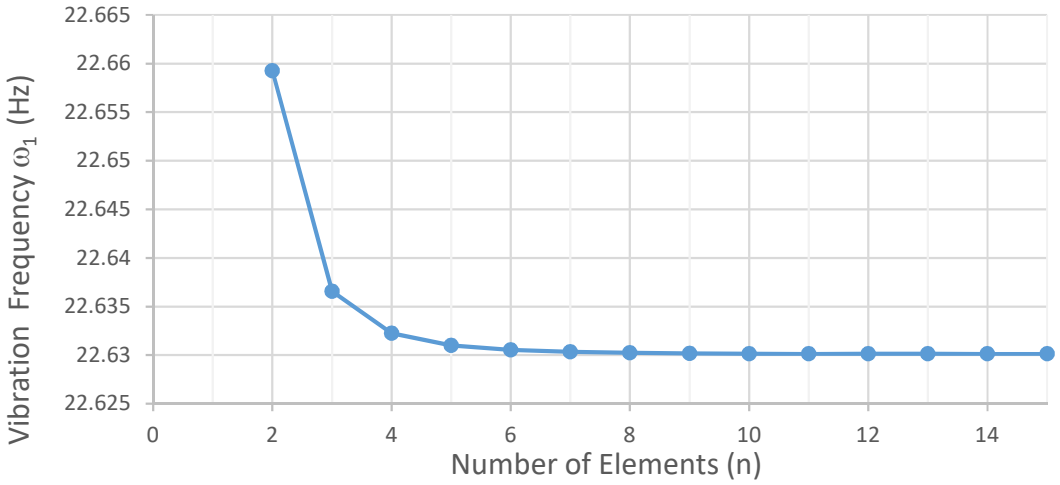

Fig. 3: Variation of first vibration frequency of a simply supported composite I-section ($[\pm 45]_{4S}$) beam subjected to axial preloading beam vs. number of elements

The beam is analysed for six different values of θ and three different axial preload values, and the vibration frequencies predicted are presented in Table 1. Table 1 also shows predictions by Vo & Lee [36] for the same problem, and it is observed that there is a good correlation between the predictions of the present model and the results of [36]. However, the predictions of the present model are slightly lower than the results of [36], and this slight discrepancy is due to the contribution of shear deformations considered in the model presented herein.

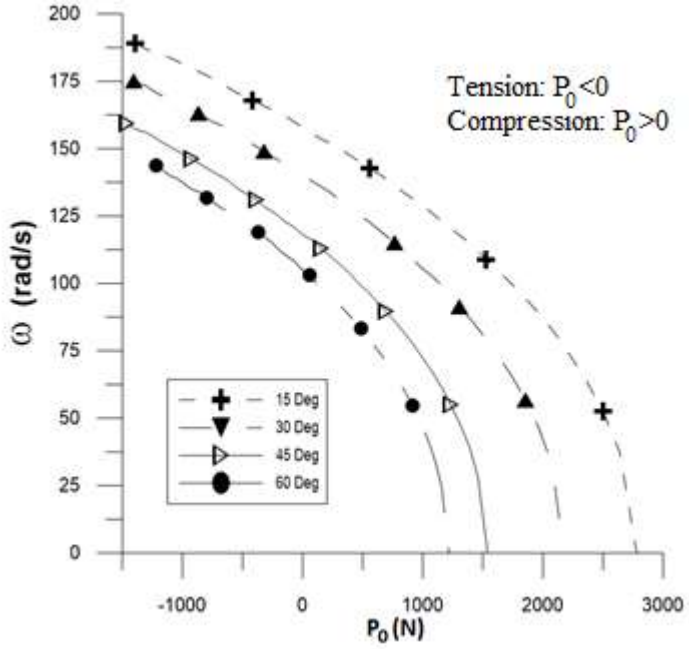

Fig. 4: Effect of axial preload (P_0) on the vibration frequency of a cantilever mono-symmetric composite I- beam

Table 1: Natural Frequencies (Hz) of the cantilever mono-symmetric composite I-beam with a symmetrical layup $[\pm\theta]_{4S}$ under different axial preloads

θ (deg.)	Axial Preload (N) #	Kim & Sin [37]*			Vo & Lee [36]*			Present +		
		f_1	f_2	f_3	f_1	f_2	f_3	f_1	f_2	f_3
0	1499.05	19.09	43.27	59.24	19.09	43.27	59.30	18.73	42.69	61.24
	0	26.30	46.47	61.99	26.30	46.47	62.05	25.93	45.91	63.83
	-1499.1	31.50	49.41	64.59	31.50	49.41	64.65	31.11	48.86	66.28
15	1406.9	18.51	44.52	56.21	18.46	44.39	56.27	18.14	43.71	58.18
	0	25.51	47.35	58.92	25.48	47.22	58.98	25.14	46.57	60.73
	-1406.9	30.57	49.97	61.48	30.54	49.85	61.55	30.18	49.22	63.16
30	1100.55	16.40	46.34	48.30	16.30	45.16	48.36	16.06	44.35	50.11
	0	22.64	48.33	50.77	22.56	47.21	50.83	22.30	46.42	52.43
	-1100.6	27.16	50.21	53.10	27.09	49.15	53.15	26.79	48.38	54.64
45	781.2	13.84	40.14	45.88	13.71	40.18	42.79	13.54	41.68	41.96
	0	19.13	42.24	47.27	19.02	42.29	44.29	18.82	43.47	43.67
	-781.2	22.97	44.22	48.59	22.89	44.27	45.72	22.63	44.91	45.55
60	620.75	12.34	35.69	42.65	12.22	35.73	39.16	12.07	37.08	38.38
	0	17.06	37.58	43.83	16.96	37.62	40.45	16.78	38.85	39.69
	-620.75	20.49	39.35	44.96	20.39	39.39	41.69	20.18	40.53	40.94
75	567.25	11.79	34.27	37.99	11.73	34.31	36.48	11.58	35.59	35.77
	0	16.29	36.07	39.21	16.24	36.10	37.76	16.07	37.06	37.28
	-567.25	19.56	37.75	40.37	19.51	37.79	38.97	19.31	38.29	38.88

* Without shear deformation + With shear deformation # Tension has negative sign

To study the effect of axial preload (P_0), the composite beam is analysed by varying the magnitude of P_0 over a wide range for θ = 15º, 30º, 45º and 60º, and the results are shown Fig. 4. It is clearly seen from Fig. 4 that axial preloading exerts a stiffening effects on the natural frequency of the beam for axial tension loading, and the opposite, i.e. a softening effect on the on the natural frequency for axial compression loading.

3.1.2. Vibration of a simply supported box section beam preloaded with axial force and end moment loading

The effects of different preloads on the vibration frequencies of a composite box section beam of width 100 mm, depth d = 200 mm and length l = 8 m is studied for different laminate lay-ups of the webs. All walls are assume to be made of two layers, each having a thickness of 2.5 mm (total thickness: t = 5mm), with assumed material properties of E_1/E_2=25, G_{12}/E_2=0.6, $G_{13}=G_{23}=G_{12}$, ν_{12}=0.25. The top and bottom flanges are assumed to have unidirectional laminate lay-ups $[0]_2$, while the webs have $[\pm\theta]$ lay-ups.

Initially, the box analysed assuming that it is only subjected to pure axial compressive loading (no end moment) to determine the critical value P_{cr}, and secondly analyses are conducted assuming pure end moment loading (no axial force) to evaluate M_{cr}. Following this, the first three non-dimensional vibrational frequencies [$\bar{\omega}=(l^2\omega/d)\sqrt{\rho/E_2}$] are calculated for three different combinations of axial and end moment preloads for four different fibre angles θ, and the results are displayed in Table 2 along with predictions of Vo et al. [13]. From Table 2 it is seen that the predictions of the model posted here correlate well with the predictions of [13]. However, the present model predicts slightly lower frequencies than reported by Vo et al. [13], which is due to the effect of the shear deformations that are included in the proposed model. Also, Table 2 shows that a change of axial preload from compression to tension results is a rapid increase of the vibrational frequencies due to the stabilizing effects of the axial tension, as can be intuitively be expected.

Table 2: Non-dimensional natural frequencies of a simply supported composite box-beam preloaded with axial and end moments (flanges: $[0]_2$ and webs: $[\pm\theta]$)

θ (deg.)	Pre Load #	Non-dimensional Natural frequencies					
		Present +			Vo et al. [13]*		
		ω_1	ω_2	ω_3	ω_1	ω_2	ω_3
0		6.504	16.350	37.892	6.656	16.704	39.937
30	$0.5\overline{P}_{cr}$	4.022	14.673	23.755	4.088	14.750	24.511
60	$0.5\overline{M}_{cr}$	2.827	13.964	16.775	2.868	14.097	17.209
90		2.764	13.894	16.404	2.804	14.068	16.823
0		9.342	18.047	40.841	9.401	18.392	42.041
30	$0.5\overline{M}_{cr}$	5.763	15.410	25.551	5.780	15.487	25.835
60		4.050	14.350	18.031	4.055	14.481	18.137
90		3.959	14.265	17.631	3.964	14.436	17.730
0		11.494	19.597	43.563	11.499	19.937	44.034
30	$-0.5\overline{P}_{cr}$	7.087	16.112	27.229	7.078	16.191	27.093
60	$0.5\overline{M}_{cr}$	4.980	14.726	19.205	4.966	14.855	19.019
90		4.869	14.627	18.779	4.854	14.795	18.591

* Without shear deformation + With shear deformation # Tension has negative sign

The same box beam is now reanalysed changing the laminate lay-ups of the top flange and left web to $[\theta]_2$, while specifying $[0]_2$ lay-up for the other walls to activate more coupling effects. Similarly, the effect of preloading (axial and end moment loads) on the non-dimensional natural frequencies are investigated for different lamination angles θ. The results obtained by the proposed model are presented in Table 3 along with results published in [13]. Similar trends are seen as for the previous comparative studies (Tables 1 and 2).

Table 3: Non-dimensional natural frequencies of a simply supported composite box-beam preloaded with different axial and moments (top flange and left web: $[\theta]_2$; other walls: $[0]_2$)

θ (deg.)	Pre Load	Non-dimensional Natural frequencies					
		Present +			Vo & Lee [13] – FEM *		
		ω_1	ω_2	ω_3	ω_1	ω_2	ω_3
0	$0.5\overline{P}_{cr}$	6.464	16.337	38.914	6.656	16.704	39.937
30		4.564	12.790	23.102	4.656	13.113	23.652
60	$0.5\,\overline{\mathrm{M}}_{\mathrm{cr}}$	3.047	11.622	18.168	3.135	11.918	18.624
90		2.936	11.533	17.739	3.020	11.867	18.095
0		9.163	17.944	40.988	9.401	18.392	42.041
30	$0.5\,\overline{\mathrm{M}}_{\mathrm{cr}}$	6.387	13.751	24.832	6.555	14.139	25.438
60		4.311	12.167	19.146	4.429	12.458	19.650
90		4.157	12.017	18.637	4.269	12.375	19.074
0	$-0.5\overline{P}_{cr}$	11.172	19.507	42.933	11.499	19.937	44.034
30		7.813	14.730	26.348	8.038	15.093	27.118
60	$0.5\,\overline{\mathrm{M}}_{\mathrm{cr}}$	5.308	12.610	20.106	5.427	12.973	20.629
90		5.116	12.554	19.494	5.230	12.859	20.007

* Without shear deformation + With shear deformation

Further, the vibration behaviour of a box beam subjected to axial preloading (P_0) is now investigated by varying the preload over a wide range from tension to compression (from $P_0 / P_{cr} = -1$ to $P_0 / P_{cr} = 1$) for a number different values of the fibre angle θ. Fig. 5 shows the predicted variation of the non-dimensional frequency. As expected, Fig. 5 displays a monotonic decrease of the vibration frequency with increasing axial load going from tension to compression for all fibre angles. Fig. 5 also confirms the reduction of the vibrational frequency of the box beam as the axial stiffness reduces with increasing fibre angle θ, albeit it is noted that this reduction diminishes (and almost vanishes) for fibre orientation angles θ above 45^0.

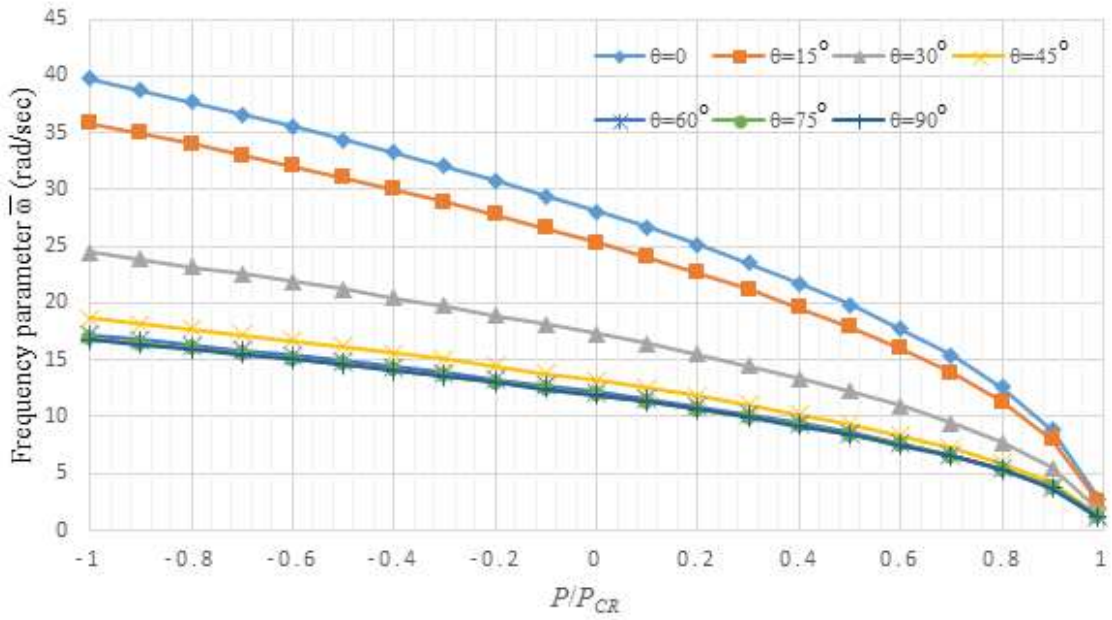

Fig. 5: Effect of axial preload on the first vibration frequency of a simply supported composite box-beam

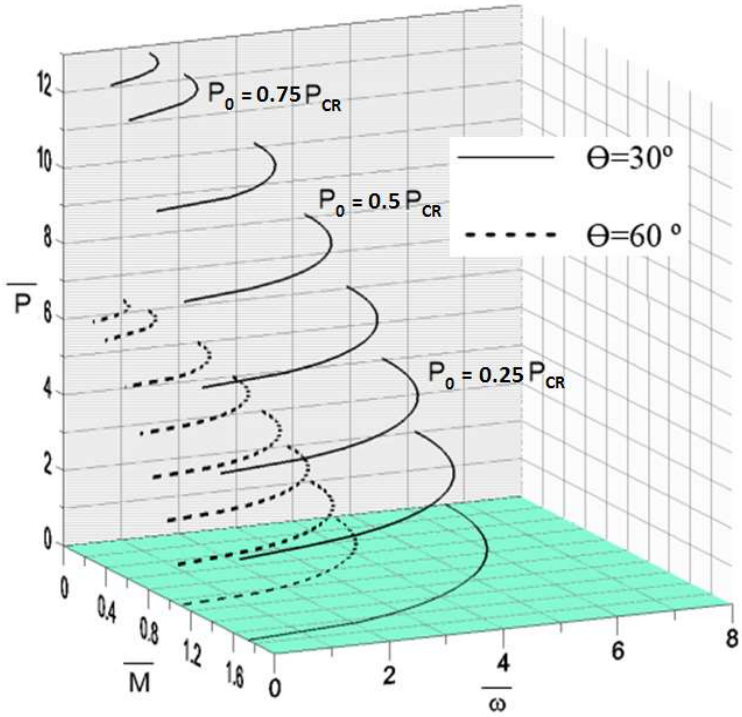

Fig. 6: Interaction curves for vibration frequencies of simply supported composite box section beam with respect to axial force and end moment loads

Finally, the influence of both axial and end moment loads (combined preloading) on the vibration characteristics of composite box beam is investigated for two specific fibre angles;

$\theta = 30^0$ and 60^0. By varying the axial load (from $P_0 / P_{cr} = 0$ to $P_0 / P_{cr} = 0.875$ in increments of 0.125) and end moments ($M_0 < M_{cr}$), the composite box beam is analysed, and the predicted frequencies ($\bar{\omega}$) are plotted in Fig. 6 as interaction curves with respect to the non-dimensional axial force ($\bar{P} = P_0 l^2 / (d^3 t E_2)$) and end moments ($\bar{M} = M_0 l / (d^3 t E_2)$). Fig. 6 shows that the amplitude of the moment-frequency interaction curves reduces as the axial load increases. Similarly, the amplitude of the 3D interaction surface that correlates the critical axial load, critical end moment and frequency reduces with increasing fibre angle (θ). Interestingly, as the axial preload increases, a monotonic reduction of the vibration frequency is observed. Moreover, as the axial preload approaches $\bar{P}_{cr}$, the interaction curves vanish to a single point, representing the degenerated case of natural vibration with zero frequency and zero end moment (preload). Similar behaviour is also observed when end the moment approach $\bar{M}_{cr}$.

3.2. Dynamic Instability

3.2.1. Dynamic stability of a simply supported box section beam preloaded with axial force

The dynamic stability of a composite box section beam of width 100 mm, depth d = 200 mm and length l = 8 m is studied for three different laminate lay-ups of the webs. All walls are assumed to be made of four layers, each having a thickness of 2.5 mm (total thickness: t = 10mm), with material properties of E_1/E_2=25, G_{12}/E_2=0.6, $G_{13}=G_{23}=G_{12}$, ν_{12}=0.25. The top and bottom flanges are assumed to have unidirectional laminate lay-ups $[0]_4$, while the webs have $[\pm\theta]_2$ lay-ups. The non-dimensional natural vibration frequency ($\bar{\Omega}=(l^2\Omega/d)\sqrt{\rho/E_2}$) and the critical axial buckling loads are estimated by using the proposed model, and the results are presented in Table 4. For the validation of the predictions of the model proposed, the box beam structure is analysed using the commercial finite element code Abaqus. The results obtained from this detailed finite element model based on assemblage of laminated shell elements are included in Table 4. Moreover, the dynamic instability ranges predicted by the proposed model as well as the detailed finite element model (Abaqus) are presented in Fig. 7, where the static component is taken as $\alpha = P_{ST} / P_{cr} = 0.2$ while the dynamic component $\beta = P_{Dyn} / P_{cr}$ is varied over a wide range for three different values of the fibre angle (θ). Although the present model utilizes a formulation with a significantly reduced

number of degrees of freedom for finite element analyses, Table 4 and Fig. 7 show that the proposed model performs very well. However, minor deviations between the results obtained from the two modelling techniques is observed. This is due to the difference in the modelling of the beam ends in imposing the axial load as well as the support conditions. The stiffness of the beam is increased with lower values of θ (all fibres oriented along the beam axis when θ = 0) which is clearly reflected in the increase of frequencies.

Table 4: Normalized Natural frequencies and critical axial buckling load of a simply supported composite box-beam (top flange and left web: $[0]_4$; other walls: $[\pm\theta]_2$)

θ	$\bar{\omega}$		$\bar{P}_{cr}$	
	Abaqus	Present	Abaqus	Present
0^0	10.434	10.818	33.118	35.585
30^0	6.313	6.663	12.115	13.500
90^0	4.082	4.574	5.068	6.362

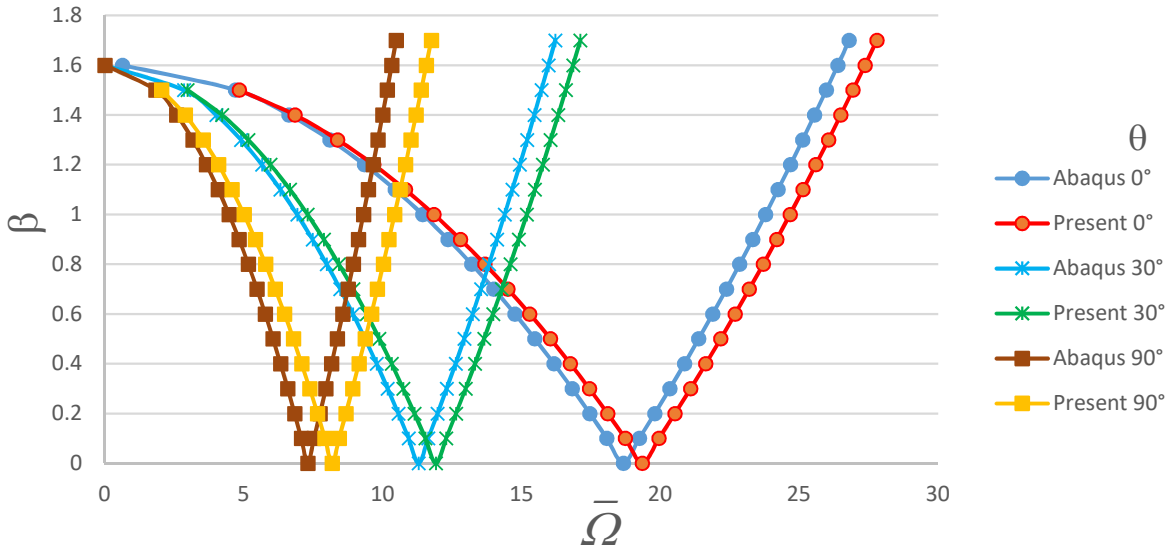

Fig. 7: Non-dimensional dynamic instability regions for simply supported composite box section beam subjected to a static axial load factor ($\alpha = 0.2$) (flanges: $[0]_4$; webs: $[\pm\theta]_2$)

The performance and efficiency characteristics of the proposed 1D beam finite element model and the detailed FE shell element model (Abaqus) used for analysing the box beam structure (both models with adequately converged solutions) are presented in Table 5. The table clearly shows that proposed model requires considerably less number of degrees of freedom (DOF), more than 90 times lower than the shell FE model, to achieve a similar degree of accuracy. This difference in efficiency becomes even more pronounced when considering the number of

floating point operations (FLOPS) needed to complete the analysed. For an example, the number of FLOPS required to calculate the inverse of the stiffness matrix having a size of $n \times n$ will be in the order of n^3, which indicates that the computational effort to conduct this operation using the detailed finite element model (Abaqus) is approximately 760,000 times higher than the proposed model for a simple static analysis. This difference in performance and efficiency will be further magnified further when solving an Eigenvalue problem, as is necessary for vibration and buckling problems, due to the iterative nature of such a solution. This clearly shows that the proposed model predicts an accurate behaviour of thin walled composite beams with great computational efficiency.

Table 5: Comparison of model performance and efficiency for simply supported beam between the proposed model and shell FE model developed using Abaqus

Model	Element Type	Number of Elements	Number of Nodes	Degrees of Freedom	FLOPS Matrix Inversion
Present	Beam 3 Noded	10	21	127	2.05E+06
Abaqus	Shell 4 Noded	1920	1932	11592	1.56E+12
Ratio	Abaqus/ Present	192	92	91	7.60E+05

3.2.2. Dynamic stability of a simply supported box section beam preloaded with axial force and end moments

The composite box section beam discussed in section 3.1.2 is now investigated with respect to its behaviour in terms of dynamic instability region within two limiting frequency plots. Initially, an axial preload $P_0 = P_{ST} + P_{Dyn}$ is assumed, where the static component is taken to be $\alpha = P_{ST} / P_{cr} = 0.5$, whilst the dynamic component is varied over a wide range and $\beta = P_{Dyn} / P_{cr}$. The dynamic instability range predicted by the proposed model is shown in Fig. 8 for four different values of the fibre angle θ. The dynamic instability region is found to move towards the lower frequency region with increasing values of θ (i.e., reduction of axial stiffness) as expected. Moreover, the range of the instability region is narrowed with increasing θ values. Now the value of the load parameter α is varied over a range for a specific value of the fibre angle ($\theta = 45^0$), and the predicted dynamic stability regions are shown in Fig. 9. It is observed that the dynamic component of the preload can be larger than the critical buckling load P_{cr} obtained for the static case, i.e. $\beta > 1$, when the static

component of the preload is less than 50% of P_{cr} (i.e. α< 0.5). For example, the value of P_{Dyn} is found to be $1.6P_{cr}$ (i.e. $\beta = 1.6$) for $P_{ST} = 0.2P_{cr}$ (i.e. $\alpha = 0.2$).

Now the beam is analysed with imposed end moments instead of axial preloading, and the non-dimensional results ($\bar{Y} = (l^2 Y / d)\sqrt{\rho / E_2}$) predicted by the proposed model are presented in Figs. 10 and 11. In Fig. 10a, the dynamic instability region is plotted for five different values of θ (Fig. 10a) taking $\eta = 0.5$ (static component of the end moment is 50% of the critical moment for static loading conditions). Fig. 11 shows the instability regions for different values of η corresponding to a specific value of the fibre angle ($\theta = 30^0$). Similar to Fig. 8, Fig. 10a shows a shift of the dynamic instability regions towards the lower frequency domain with increasing values of θ. Also, it is seen that the range of the instability region is narrowed with increasing values of θ, and this pattern of behaviour is similarly to the trend observed in Fig. 9. Moreover, a similar trend of movement of the instability regions towards the lower frequency domain with increasing θ is observed in Fig. 10b.

In Fig. 11, the shift of the instability regions with increasing η values appears to display what resembles an arbitrary or erratic fluctuation. However, a closer examination of the mode shapes of the beam (not shown here) indicates that the cause of this behaviour is that the deformation of the beam changes from lateral instability to coupled lateral-torsional instability. Moreover, this sudden change of type/mode of instability also affects the gradual smooth variation of the bounding curve as observed for the lower bounding curves of $\eta = 0.2$ and 0.4.

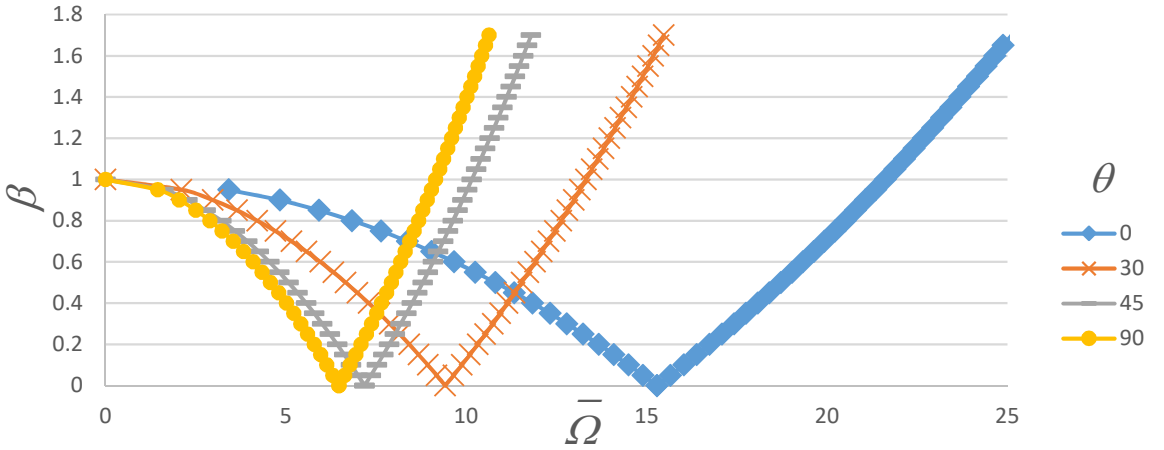

Fig. 8: Dynamic instability region for simply supported composite box section beam subjected to a specific static axial load ($\alpha = 0.5$) (flanges: $[0]_2$; webs: $[\pm\theta]$) for different θ values

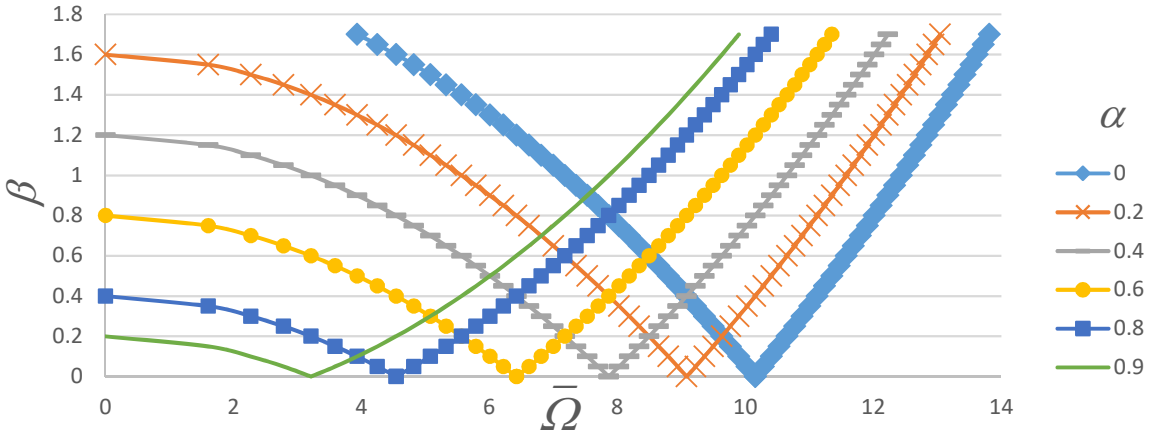

Fig. 9: Dynamic instability region for simply supported composite box section beam subjected to varying static axial loads α = 0 to 0.9 (flanges: $[0]_2$; webs: $[\pm 45^0]$)

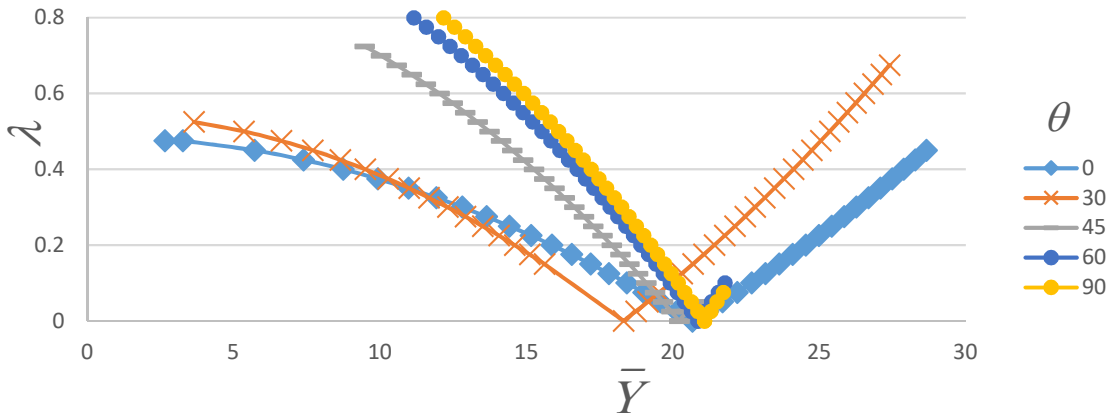

Fig. 10a: Dynamic instability region for simply supported composite box section beam subjected to specific static end moment loads ($\eta = 0.5$) (flanges: $[0]_2$; webs: $[\pm\theta]$) for different θ values

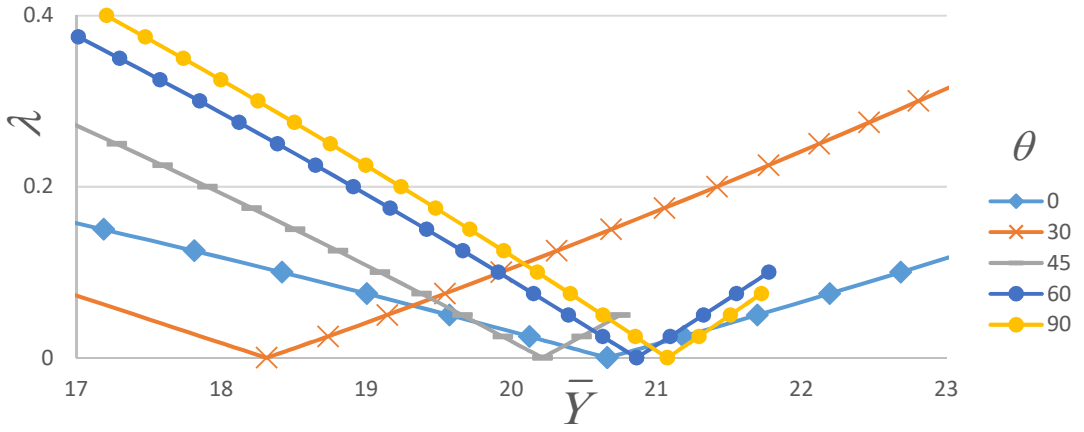

Fig. 10b: Magnified view a critical region of Fig. 10a around $\bar{Y}$=20

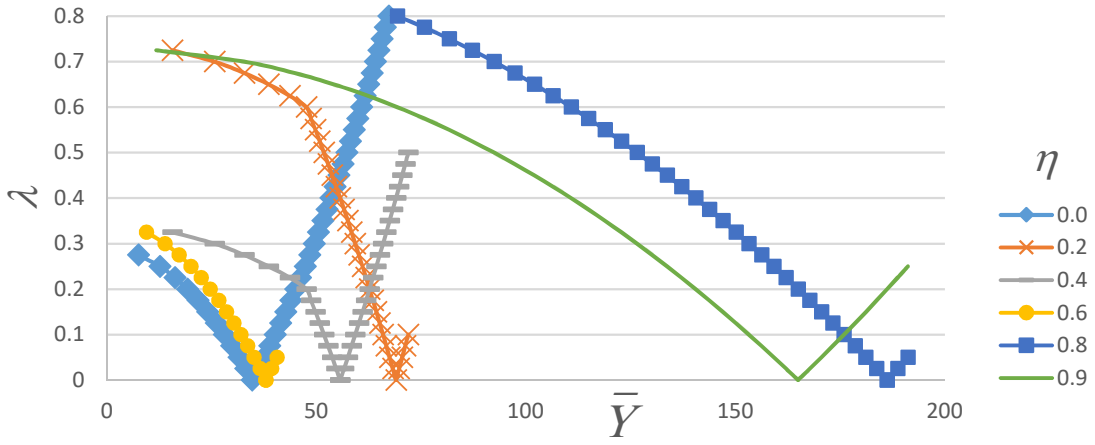

Fig. 11: Dynamic instability region for simply supported composite box section beam subjected to varying static end moment loads $\eta = 0$ to 0.9 (flanges: $[0]_2$; webs: $[\pm 30^0]$)

3.2.3. Dynamic stability of a simply supported I section beam preloaded with axial force and end moments

A composite I section beam having a span of l = 8 m is investigated to study its dynamic instability behaviour when subjected to different combinations of preloads. It is assumed that both flanges are 100 mm wide, while the section is 200 mm high. All section walls are assumed to be made of two plies, each 2.5 mm thick (total thickness: t = 5 mm), with unidirectional $[0]_2$ lay-up for the web, whilst the both top and bottom flanges have $[\pm\theta]$ lay-up. The material used for all the layers is assumed to have the following properties: E_1/E_2=25, G_{12}/E_2=0.6, G_{13}=G_{23} =G_{12}, ν_{12}=0.25. The dynamic stability regions when the beam is subjected to pure axial loading are first determined for different fibre angles θ, assuming a specific value of the static axial load, $\alpha = 0.5$. The predicted results are presented in Fig. 12. Similarly, the effects of static axial loading on the dynamic instability regions of the I section beam for a specific fibre angle, $\theta = 45^0$, are shown in Fig. 13, where the value of α is varied gradually from 0 to 0.9. Following the same procedure, the dynamic stability behaviour of the I section beam subjected to end moments is studied for η = 0.5, and the results predicted by the model are plotted in Fig. 14. Also, the effects of static end moments on the dynamic instability regions of the I section beam with the fibre orientation angle prescribed to $\theta = 30^0$ are presented in Fig. 15.

As demonstrated before, increasing values of the fibre angle θ reduces the cross sectional stiffness, which in turn leads to a softening of the beam with corresponding reduced

frequencies. This is demonstrated in the form of a shift of the bounding instability region towards the lower frequency range in Figs. 12 and 14. A similar behaviour is observed in Figs. 13 and 15, where the softening of the beam, in the form of reduction of its effective stiffness, is caused by an increase of the static preload. In Figs. 15, the maximum value of the upper bounding frequency curves is found to be stabilised at a fixed value (e.g. 5.13 Hz for all the cases of η), which corresponds to the static buckling load.

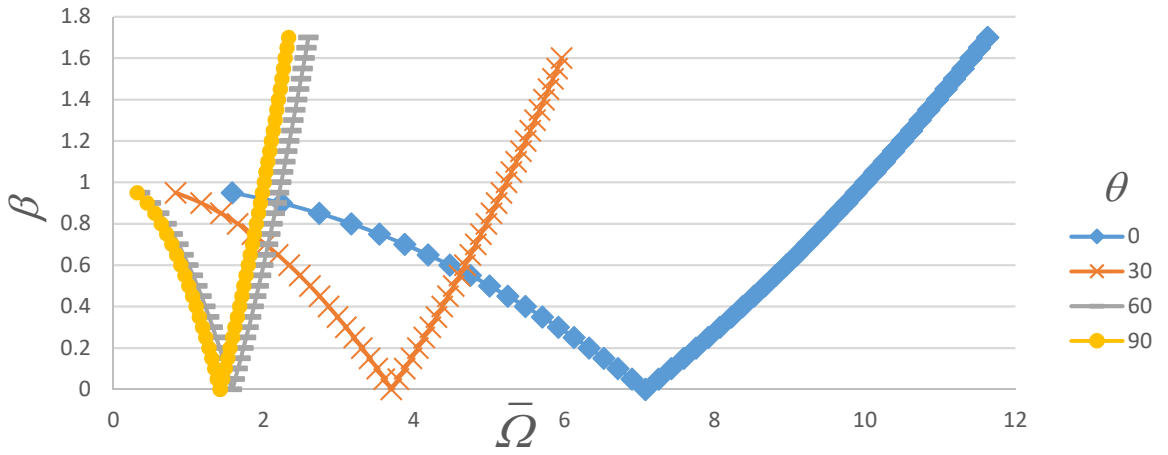

Fig. 12: Dynamic instability region for simply supported composite I-section beam subjected to a specific static axial load ($\alpha = 0.5$) (flanges: $[\pm\theta]$, web: $[0]_2$)

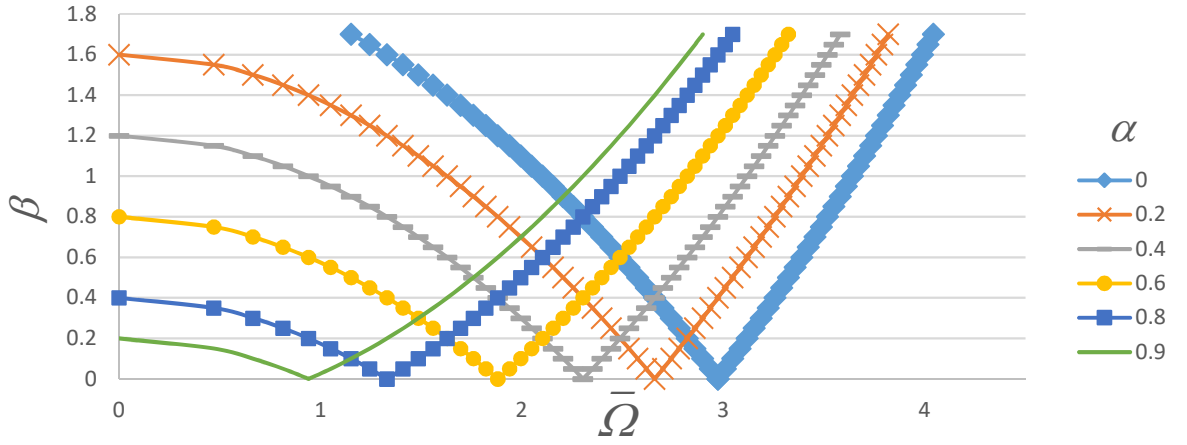

Fig. 13: Dynamic instability region for simply supported composite I section beam subjected to varying axial preloading α = 0 to 0.9 (flanges: $[\pm 45^0]$, web: $[0]_2$)

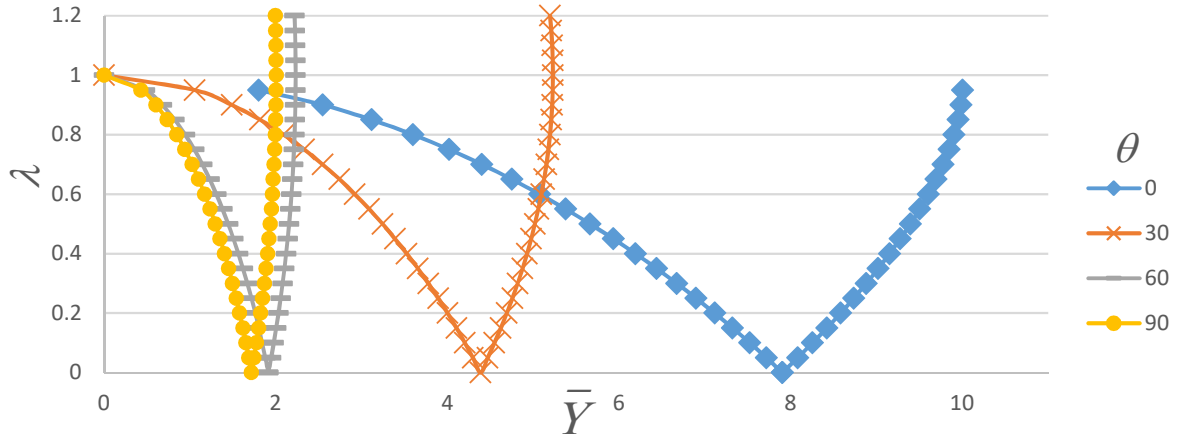

Fig. 14: Dynamic instability region for simply supported composite box section beam subjected to specific static end moment loads ($\eta = 0.5$) (flanges: $[\pm\theta]$, web: $[0]_2$)

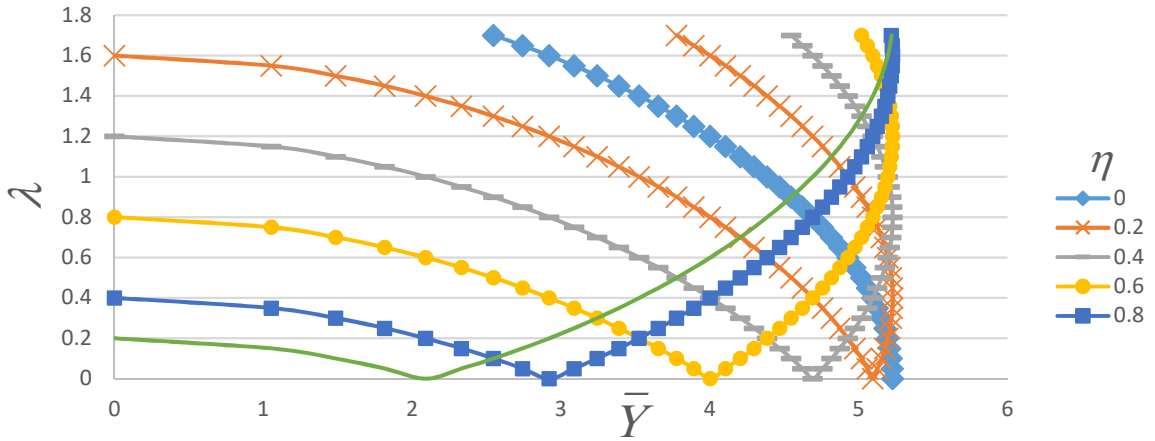

Fig. 15: Dynamic instability region for simply supported composite box-section beam subjected to varying static end moment loads $\eta = 0$ to 0.9 (flanges: $[\pm 30^0]$, web: $[0]_2$)

4. CONCLUSIONS

The paper has presented a new model for the static and dynamic analysis of slender composite beams structures. The new model is based on an efficient one-dimensional beam finite element formulation for dynamic stability and includes the effects of axial and end moment preloads. The formulation is applicable for the analysis of both open and closed beam cross sections, and encompasses the effects of axial, torsion, bi-axial bending and transverse shear deformations, as well as out of plane cross-sectional warping. The cross-sectional stiffness matrices of the composite section are derived analytically and include all possible couplings between the abovementioned modes of deformation. The effect of shear deformation of the beam section walls is included in the formulation, which typically demands a C^0 continuous

finite element formulation for the bending deformations coupled with transverse shear deformations. Such a formulation is susceptible to shear locking problem, which may be avoided by using the reduced integration technique to supress the problematic terms related to shear energy. However, this affects the solution accuracy and leads to stress oscillations and other related issues due to inadequate integration of the energy terms of the structural system. The issue is circumvented in this paper by adopting a C^1 continuous formulation that enables full integration for accurate evaluation of the various energy terms. This is achieved by adopting a novel formulation for coupled bending and shear deformation. The proposed model is used to analyse a series of challenging example problems involving thin-walled laminated composite beams having open (I) and closed (box) sections, accounting for different boundary conditions, section wall stacking sequences, as well as different loading conditions. For most of the presented example cases, the predicted results for the vibration of preloaded thin-walled composite beams are compared against analytical and/or numerical results available in literature, and a very good match is found. However, due to a lack of similar studies in open literature for dynamic instability, the commercial and generally recognised finite element code Abaqus is used to verify the dynamic instability predictions generated by the proposed model. Collectively, the comparative results demonstrate that the proposed model performs very well. Finally, an extensive parametric study is conducted to demonstrate the effect of various important design parameters on the dynamic stability characteristics of slender open and closed section composite beam structures. This also includes complex load interactions that occur by the simultaneous application of axial and/or end moment loadings. This has produced new results, which are anticipated to be useful as benchmarks for future research in this area.

REFERENCES

[1] N.R. Bauld, L.S. Tzeng, A Vlasov theory for fiber-reinforced beams with thin-walled open cross section, Int. J. of Solid and Struc. 20(3) (1984) 277–97.

[2] R. Chandra, A.D. Stemple, I. Chopra, Thin-walled composite beams under bending, torsion, and extensional load, AIAA Journal 27(7) (1990) 619-626.

[3] C.E.S Cesnik, D.H. Hodges, VABS: A new concept for composite rotor blade cross section modelling, J. of the American Helicopter Society 42(1) (1997) 27–38.

[4] L.P. Kollar, Springer GS. Mechanics of Composite Structures, Cambridge University Press, 2003.

[5] H.A. Salim, J.F. Devalos, Torsion of open and closed thin-walled laminated composite sections, J. of Compos. Mat. 39(6) (2005) 497-524.

[6] J. Lee, Flexural analysis of thin-walled composite beams using shear-deformable beam theory, Compos. Struc. 70(2) (2005) 212-222.

[7] L. Librescu, O. Song, Thin-walled Composite Beams, Springer, 2006.

[8] H.X. Nguyen, J. Lee, T.P. Vo, D. Lanc, Vibration and lateral buckling optimisation of thin-walled laminated composite channel-section beams, Comp. Struc. 143(2016) 84–92.

[9] L. SHANG, P. XIA, D.H. HODGES, Geometrically exact nonlinear analysis of pre-twisted composite rotor blades, Chinese J. of Aeronautics 31(2) (2018) 300–309.

[10] M. Gupta, D.H. Hodges, Modeling Thin-Walled Beams using VAM, Structural Dynamics, and Materials Conference, AIAA SciTech Forum, (2017) (AIAA 2017-1832), https://doi.org/10.2514/6.2017-1832.

[11] D. Harursampath, A.B.Harish, D. H. Hodges, Model reduction in thin-walled open-section composite beams using variational asymptotic method. Part I: Theory,Thin-Walled Struc. 117 (2017) 356-366.

[12] K. Kashefi, A.H. Sheikh, MS.M. Ali, MC. Griffith, An efficient modelling approach based on a rigorous cross-sectional analysis for analysing box girder bridge superstructures, Adv. in Struc. Eng. 19(3) (2016) 513–528.

[13] T.P. VO, J. Lee, Interaction curves for vibration and buckling of thin-walled composite box beams under axial loads and end moments, App. Math. Model. 34(2010) 3412-3157.

[14] T.P. VO, J. Lee, K. Lee N. Ahn, Vibration analysis of thin walled composite beams with I-shaped cross-sections, Composite Structures 93 (2011) 812-820.

[15] T.P. VO, J. Lee, Vibration and Buckling of thin-walled composite I-Beams with Arbitrary Lay-ups under axial Loads and End Moments, Mech. of Adv. Mat. and Struc. 20(8) (2013) 652-665.

[16] T.P. VO, J. Lee, On Sixfold coupled buckling of thin-walled composite beams, Compos. Struc. 90 (2009) 295-303.

[17] T.P. VO, and J. LEE, Flexural-torsional coupled vibration and buckling of thin-walled open section composite beams using shear-deformable beam theory, Journal of Mechanical Sciences 51(9-10) (2009) 631-641 (doi:10.1016/j.ijmecsci.2009.05.001).

[18] N-I. KIM, D. K. SHIN, and M-Y KIM, Flexural-Torsional buckling loads for spatially coupled stability analysis of thin-walled composite columns, Adv. in Eng. Softw. 39 (2008) 949-961.

[19] N-I. KIM, D. K. SHIN, and Y-S. PARK, Coupled stability analysis of thin-walled composite beams with closed cross section, Thin-walled Struc. 48 (2010) 581-596.

[20] N-I. KIM, C.K. Jeon, Coupled Static and Dynamic Analyses of Shear Deformable Composite Beams with Channel-Sections, Mech. Based Design of Struc. and Mach., (2013), https://doi.org/10.1080/15397734.2013.797332.

[21] N-I. Kim, D-H. Choi, Super convergent shear deformable finite elements for stability analysis of composite beams, Composites: Part B 44 (2013) 100-111.

[22] N-I. Kim, Dynamic stability behavior of damped laminated beam subject to uniformly distributed sub tangential forces, Composite structures 92(11) (2010) 2768-2780.

[23] SP. Machado, VH. Cortinez, Non-linear model for stability of thin-walled composite beams with shear deformation, Thin-Walled Struct. 43(10) (2005) 1615–45.

[24] S.P. Machado, Interaction of combined loads on the lateral stability of thin-walled composite beams, Engineering Structures 32(11) (2010) 3516-3527.

[25] SP. Machado, VH. Cortinez, Free vibration of thin-walled composite beams with static initial stresses and deformations, Engineering Structures 29 (2007) 372-382.

[26] SP. Machado, Geometrically non-linear approximations on stability and free vibration of composite beams, Engineering Structures 29 (2007) 3567-3578.

[27] S.P. Machado, C.P. Filipich, V.H. Cortinez, Parametric vibration of thin-walled composite beams with shear deformation, J. of Sound and Vib. 305 (2007) 563-581.

[28] SP. Machado, VH. Cortinez, Dynamic stability of thin-walled composite beams under periodic transverse excitation, Journal of Sound and Vibration 321 (2009) 220-241.

[29] S.P. Machado, C.M. Saravia, Shear-deformable thin-walled composite Beams in internal and external resonance, Composite Structures 97 (2013) 30-39.

[30] S.P. Machado, C.M. Saravia, F.E. Dotti, Non-linear oscillations of a thin-walled composite beam with shear deformation, App. Math. Modelling 38 (2014) 1523-1533.

[31] C.M. Saravia, S.P. Machado, V.H. Cortinez, Free vibration and dynamic stability of rotating thin-walled composite beams, European J. of Mech. A/Solids 30 (2011) 432-441.

[32] A.H. Sheikh, New Concept to include shear deformation in a curved beam element, J. of Struc. Eng. 128(3) (2002) 406-410.

[33] A.H. Sheikh, O.T. Thomsen, An efficient beam element for the analysis of laminated composite beams, Compos. Sci. and Tech. 68(2008) 2273–2281.

[34] A.H. Sheikh, A. Asadi, O.T. Thomsen, Vibration of thin-walled laminated composite beams having open and closed sections, Compos. Struc. 134(2015) 209–215.

[35] V.V. Bolotin, The dynamic stability of elastic systems, USAF, 1962.

[36] T.P. VO, J. Lee, K. Lee, On triply coupled vibration of axially loaded thin-walled composite beams, Comp. and Struc. 88(2010) 144-153.

[37] N-I. Kim, D.K. Shin, Dynamic stiffness matrix for flexural-torsional, lateral buckling and free vibration analysis of mono-symmetric thin-walled composite beams, Int. J. of Struc. Stab. and Dyn. 9(3) (2009) 411-436.

APPENDIX A

The non-zero elements appearing in the upper triangle of the symmetric matrices $[C_g]$ (Eq. (24)) are presented in their explicit form as follows (applicable for I and box sections):

$$C_{11}^{gP} = C_{22}^{gP} = A,\ C_{13}^{gP} = -B\cos\alpha - A(q\sin\alpha + r\cos\alpha)$$

$$C_{23}^{gP} = -B\sin\alpha + A(q\cos\alpha - r\sin\alpha),\ C_{33}^{gP} = C + 2rB + A(q^2 + r^2)$$

where $(A, B, D, F) = \int_t (1, n, n^2, n^3)dn$

APPENDIX B

The non-zero elements appearing in the upper triangles of the symmetric matrices $\left[F_g^P\right]$ and $\left[F_g^M\right]$ (Eq. (24)) are presented in their explicit form as follows (applicable for I section, Fig. 16(a)):

$$F_{11}^{gP} = F_{22}^{g} = b_1A_1 + b_2A_2 + dA_3,\ F_{13}^{gP} = -b_1(A_1d/2 + B_1) + b_2(A_2d/2 + B_2),\ F_{23}^{gP} = -B_3d$$

$$F_{33}^{gP} = b_1^3A_1/12 + b_1(0.25A_1d^2 + B_1d + D_1) + b_2^3A_2/12 + b_2(0.25A_2d^2 + B_2d + D_2) + A_3d^3/12 + D_3d$$

and

$$F_{11}^{gM} = F_{22}^{gM} = b_1(0.5A_1d + B_1) - b_2(0.5A_2d + B_2),$$

$$F_{13}^{gM} = -b_1(0.25A_1d^2 + B_1d + D_1) - b_2(0.25A_2d^2 + B_2d + D_2) - A_3d^3/12,$$

$$F_{33}^{gM} = b_1(b_1^2dA_1 + 2b_1^2B_1 + 3d^3A_1 + 18d^2B_1 + 36dD_1/2 + 24F_1)/24$$
$$-b_2(b_2^2dA_2 + 2b_2^2B_2 + 3d^3A_2 + 18d^2B_2 + 36dD_2/2 + 24F_2)/24$$

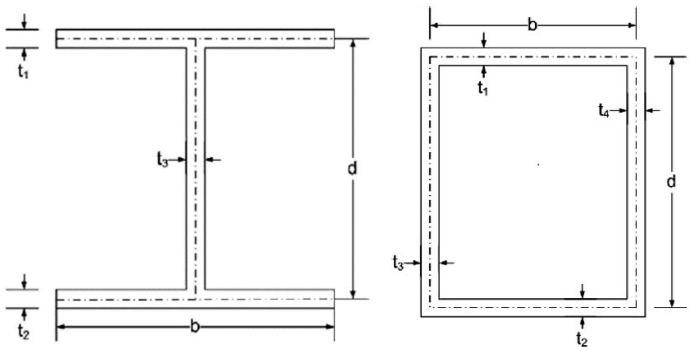

(a) (b)

Fig. 16: Thin-walled beam having open and closed section

The non-zero elements appearing in the upper triangle of the symmetric matriec $\left[F_g^P\right]$ and $\left[F_g^M\right]$ (Eq. (24)) are presented in their explicit form as follows (applicable for box section, Fig. 16(b)):

$$F_{11}^{gP}=F_{22}^{gP}=b(A_1+A_2)+d(A_3+A_4),\ F_{13}^{gP}=bd(A_2-A_1)/2-b(B_2-B_1),$$

$$F_{23}^{gP}=bd(A_4-A_3)/2+d(B_4-B_3),$$

$$F_{33}^{gP}=b^3(A_1+A_2)/12+bd^2(A_1+A_2)/4+b^2d(A_3+A_4)/4+bd(B_1+B_2+B_3+B_4)$$
$$+b(C_1+C_2)+d^3(A_3+A_4)/12+d(C_3+C_4)$$

and

$$F_{11}^{gM}=F_{22}^{gM}=bd(A_1-A_2)/2+b(B_1-B_2),$$

$$F_{13}^{gM}=-bd^2(A_1+A_2)/4-bd(B_1+B_2)-b(D_1+D_2)+d^3(A_3+A_4)/12,$$

$$F_{33}^{gM}=b^3d(A_1-A_2)/24+b^3(B_1-B_2)/12+bd^3(A_1-A_2)/8+3bd^2(B_1-B_2)/4$$
$$+3bd(D_1-D_2)/2+b(F_1-F_2)$$

6. Chapter 4a - Buckling of Thin-Walled Laminated Composite Beams Having Open and Closed Sections Subjected to Axial Load and End Moment

Seminar Paper 3 –Presented

ACAM9 - 9th Australian Congress on Applied Mechanics
Event: Conference
Duration: 27 - 29 November 2017
City: Sydney
Country: Australia
Degree of recognition: National event

Buckling of Thin-Walled Laminated Composite Beams having Open and Closed Sections subjected to Axial Load and End Moment

A. Asadi[1] and A.H. Sheikh[1]
[1]School of Civil, Environmental and Mining Engineering
University of Adelaide
Adelaide, SA 5005
AUSTRALIA
E-mail: abdul.sheikh@adelaide.edu.au

Abstract: *An efficient modelling technique based on one dimensional beam finite element analysis is proposed for buckling of thin-walled laminated composite beams having open/closed sections. The proposed formulation is quite generic that can accommodate any stacking sequence of individual walls and consider all possible couplings between axial, shear, bending and torsional modes of deformation. The effect of transverse shear deformation of walls and out of plane warping of the beam section is incorporated where the warping can be restrained or it can be free. The incorporation of shear deformation in the finite element formulation of the beam has imposed difficulties, which are successfully addressed by using a concept proposed by one of the authors. Numerical examples of open I section and closed box section beams are solved by the proposed approach and the effect of axial load and end moments is studied. The results are compared with those available in literature which show a very good performance of the proposed model.*

Keywords: *Thin-walled composite beams, Buckling, Shear deformation, Warping, FE model.*

1. Introduction

The application of thin-walled laminated composite beams is found in various engineering constructions such a wind turbine blades, helicopter rotor blades and the many other beam like long structures. The behaviour of this type of structures is complex due to thin-walled cross-sectional geometry and multi-layered laminated composite walls with arbitrary ply orientations. A detailed finite element modelling of these structures using 3D or shell elements can provide a good solution of this problem, but such modelling scheme is highly demanding computationally and may not always be affordable in practice. In order to address this problem, a group of researchers tried to develop techniques for modelling these structures using 1D beam elements with enhanced cross-sectional features so as to achieve a computational efficient solution of the problem [1-8]. However, the formulation of these techniques involves new challenges in capturing all effects of thin-walled composite beam sections and their coupling.

The existing research in this direction can be divided into two broad group based on the approaches used to determine the constitutive matrix of the beam element. The first approach is based on 'analytical techniques' while the second approach utilises a 2D cross-sectional analysis utilising a 2D finite element model for calculating cross-sectional matrixes. Hodges and co-workers [3] may be regarded as the major contributors toward the development of the second approach which seems to have merit but this approach needs a 2D cross-sectional finite element analysis to evaluate the cross-sectional stiffness coefficients. On the other hand, the first approach (analytical approach) adopted in this study does not need this 2D finite element analysis in addition to complex mathematical treatments involved with the second approach.

The study of Vo and Lee [8] is one of the representative examples belonging to the first approach where the cross-sectional matrices are derived analytically. The focus of this specific study [8] is on the buckling of thin-walled composite beams having open sections where the effect of shear deformations and lamination schemes on axial buckling behaviour has been investigated. The formulation proposed by Vo and Lee [8] considered the effect of coupling between flexure, torsion and shear deformations following the first-order shear deformable beam theory. They used a quadratic isoparametric element having three nodes where each node contains seven unknowns (three displacements, torsional rotation, two bending rotations and warping rotation). Though the isoparametric formulation helped to simplify

the derivation of the element metrics, the treatment of the torsional deformation made the formulation unappealing as it involved non-physical parameters. Vo and Lee [9] have also studied the effect of lamination schemes, axial loads and end moments on vibration and buckling behaviour of thin-walled composite box beams using a different model where this model did not include the effect of shear deformation which helped to get a reduced number (four) of field variables (three displacement and torsional rotation). The axial displacement is expressed using linear Lagrangian interpolation functions while cubic Hermitian polynomial functions are adopted for the remaining displacement fields. This helped to develop a two node heterogeneous beam element having seven degrees of freedom per node (three displacements, torsional rotation, derivatives of two bending displacements and derivative of the torsional rotational angle). Subsequently, Vo and Lee have extended their model [9] to vibrational and buckling analysis under axial loads and end moments [10].

Kim et al. [11] have investigated the effects of ply orientations of laminated walls, boundary conditions and axial loads on the flexural-torsional stability of thin-walled composite beams having open cross sections. Their model [11] utilised four filed variables (three displacements and torsional rotation) where the axial displacement is approximated using linear Lagrangian interpolation functions and cubic Hermitian functions are used for the other field variables in a manner similar to that of Vo and Lee [9]. They studied the behaviour of symmetrically laminated doubly and mono symmetric I-beams and arbitrary laminated mono-symmetric I-beams. Later, Kim et al. [12] have extended their formulation for modelling beams having non-symmetrical laminations. Kim et al. [13] have extended their model further for analysing thin-walled composite beams having closed cross section and studied the effects of different boundary conditions, lamination schemes, and axial loads on the stability of symmetrically laminated box beams.

In this paper, a comprehensive formulation for modelling buckling of thin-walled laminated composite beams having both open and closed sections under axial loads and end moments is presented. The different modes of deformations and their coupling considered in the development of the proposed closed-form analytical model are axial, torsional rotation, bi-axial bending, bi-axial shear as well as warping for the torsional deformation. The cross-sectional matrixes are derived explicitly specifically for the open I section and the closed box section. The propose formulation has the provision of considering plane stress condition as well as plain strain condition of a lamina.

The 1D beam problem is solved using finite element approximations in an innovative manner so as to avoid any involvement of non-physical parameters as found in the formulation of Vo and Lee [8]. This is achieved by using mixed approach where a C^1 continuous finite element formulation using cubic Hermitian polynomials is applied for the torsion while other deformations are modelled using C^0 continuous formulations. The treatment of shear deformations within a C^0 formulation needs reduced integrations for avoiding shear locking problems but the implementation of the reduced integration technique within the present formulation is a challenge due to mixing C^1 and C^0 formulations. This problem is addressed satisfactorily utilising the concept proposed by Sheikh [14], which does not require the reduced integration technique. For the 1D beam finite element analysis, a three node beam element as shown in Figure1 has been developed where each end node contains 7 degrees of freedom (three displacements, three rotations and the derivative of the torsional rotation) and the middle node contains 5 degrees of freedom (three displacements, two bending rotations).

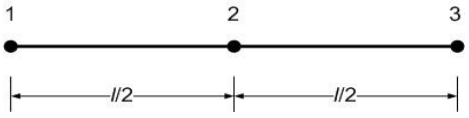

Figure 1 – A Typical Beam Element

A computer code is written in Matlab to implement the present formulation. Numerical examples of thin-walled composite beams having different cross sections and other conditions are analysed by the proposed model and the results obtained in the form of critical axial loads and end moments for buckling and mode-shapes are validated with the available results in literature. These results demonstrate a very good performance of proposed finite element model.

2. Formulation

Figure 2 shows a representative segment of a shell wall of a thin-walled composite beam along with two orthogonal axes system and displacement components. In this figure, *x-y-z* is taken as the global axis system where *x* is directed along the beam axis and passing through the centroid of the beam section, while *x-s-n* is the local axis system where *x-n* plane passes through the tangential plane of the beam wall mid plane (local *x*-axis is parallel to the global *x*-axis) and *n* is directed along the wall thickness. The displacement components at the mid-plane of the shell wall in the local coordinate system (*x-s-n*) can be expressed in term of the global displacement components of the beam [1] as

$$\begin{aligned} \bar{u} &= U + y\theta_y + z\theta_z + \varphi\theta_x', \\ \bar{v} &= V\cos\alpha + W\sin\alpha - r\theta_x, \\ \bar{w} &= -V\sin\alpha + W\cos\alpha + q\theta_x, \end{aligned} \tag{1}$$

where φ is the warping function, θ_x is the torsional rotation and θ_y, θ_z are bending rotations of the cross-section of the beam along *x* and *y*, respectively. These bending rotations can again be expressed as $\theta_y = -V' + \Psi_y$ and $\theta_z = -W' + \Psi_z$, where Ψ_y and Ψ_z are shear rotations of the beam section about *z* and *y*, respectively, and V', W' and θ_x' are respectively the derivatives of *V*, *W* and θ_x with respect to *x*.

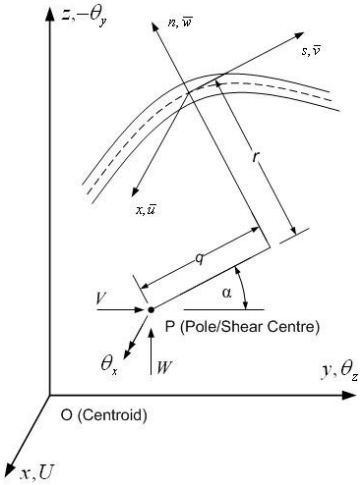

Figure 2 – Cross-section of a portion of a beam shell wall along with local and global axes system and displacement components

Although the effect of warping displacements in beams having closed sections is not as significant as that of beams with open sections [14], warping displacements are considered for both type of cross sections. The displacement at any point of the shell wall at a distance n from the mid-plane may be expressed using bending and shear deformation of the beam as

$$\begin{aligned} u &= \bar{u} + n\left(-\frac{\partial \bar{w}}{\partial x} + \psi_{xn}\right), \\ v &= \bar{v} + n\left(-\frac{\partial \bar{w}}{\partial s} + \psi_{sn}\right), \\ w &= \bar{w}, \end{aligned} \tag{2}$$

where ψ_{xn} and ψ_{sn} are shear rotations of the shell wall section about *s* and *x*, respectively. It is assumed that $\psi_{sn} = 0$ whereas ψ_{xn} can be expresses in terms of the corresponding global components (Ψ_y and Ψ_z) as $\psi_{xn} = -\Psi_y \sin\alpha + \Psi_z \cos\alpha$.

Substituting the above relationship along with Eq. (1) in the above equation (2), the displacements at any point within the shell wall along its local axis system (*x-s-n*) can be expressed in terms of the global displacement components of the 1D beam as

$$\begin{aligned} u &= U + (y - n\sin\alpha)\,\theta_y + (z + n\cos\alpha)\,\theta_z + (\varphi - nq)\theta_x', \\ v &= V\cos\alpha + W\sin\alpha - (r + n)\,\theta_x, \\ w &= -V\sin\alpha + W\cos\alpha + q\theta_x. \end{aligned} \tag{3}$$

With the deformation kinematics of the beam presented in Eq. (3), the governing equation for the buckling of the beam can be derived using energy principle. The total energy of a structure consists of strain energy (*U*) and energy or work done by the externally applied axial loads or end moments (U_g), which can be used to derive the stiffness matrix $[K]$ and the geometric stiffness matrix $[K_g]$, respectively. As the derivation of the stiffness matrix has already been shown elsewhere [15], this is not repeated in this paper. For the derivation of the geometric stiffness matrix, the combined effect of axial load (*P*) and uniaxial end moment (M_y) can be taken in the form of longitudinal stress $\bar{\sigma}_x = \frac{P}{A} + \frac{M_y}{I_y} z$ where *A* is the cross-sectional area of the beam section and I_y is the corresponding second moment of area. The energy due to this longitudinal stress can be expressed as

$$\mathrm{U_g} = \frac{1}{2}\int_{\mathrm{V}} \bar{\sigma}_{\mathrm{x}}(\mathrm{v'^2} + \mathrm{w'^2})\,\mathrm{dv} = \frac{1}{2}\int_{\mathrm{V}} \{\mathrm{v'} \quad \mathrm{w'}\}\,\bar{\sigma}_{\mathrm{x}} \begin{Bmatrix} \mathrm{v'} \\ \mathrm{w'} \end{Bmatrix} \mathrm{dv} = \frac{1}{2}\int_{\mathrm{V}} \{\varepsilon_{\mathrm{g}}\}^{\mathrm{T}}\,\bar{\sigma}_{\mathrm{x}}\,\{\varepsilon_{\mathrm{g}}\}\,\mathrm{dv} \tag{4}$$

Using Eq. (3), the geometric strain vector appeared in the above equation can be written as

$$\{\varepsilon_{\mathrm{g}}\} = \begin{Bmatrix} \mathrm{v'} \\ \mathrm{w'} \end{Bmatrix} = \begin{bmatrix} \cos\alpha & \sin\alpha & -(\mathrm{r}+\mathrm{n}) \\ -\sin\alpha & \cos\alpha & \mathrm{q} \end{bmatrix} \begin{Bmatrix} \mathrm{V'} \\ \mathrm{W'} \\ \theta_{\mathrm{x}}^{'} \end{Bmatrix} = [\mathrm{H_g}]\{\bar{\varepsilon}_{\mathrm{g}}\} \tag{5}$$

Using the relationship of the longitudinal stress in terms of axial load (*P*) and end moment (M_y) and substituted of the above equation in Eq. (4), it leads to

$$\begin{aligned} \mathrm{U_g} &= \frac{\mathrm{P}}{2\mathrm{A}}\int_{\mathrm{V}} \{\varepsilon_{\mathrm{g}}\}^{\mathrm{T}}\{\varepsilon_{\mathrm{g}}\}\,\mathrm{dv} + \frac{\mathrm{M_y}}{2\mathrm{I_y}}\int_{\mathrm{L}} \{\varepsilon_{\mathrm{g}}\}^{\mathrm{T}}\,\mathrm{z}\{\varepsilon_{\mathrm{g}}\}\,\mathrm{dx}, \\ \mathrm{U_g} &= \frac{\mathrm{P}}{2\mathrm{A}}\int_{\mathrm{L}} \{\bar{\varepsilon}_{\mathrm{g}}\}^{\mathrm{T}}\left[\mathrm{F_g^P}\right]\{\bar{\varepsilon}_{\mathrm{g}}\}\,\mathrm{dx} + \frac{\mathrm{M_y}}{2\mathrm{I_y}}\int_{\mathrm{L}} \{\bar{\varepsilon}_{\mathrm{g}}\}^{\mathrm{T}}\left[\mathrm{F_g^M}\right]\{\bar{\varepsilon}_{\mathrm{g}}\}\,\mathrm{dx}. \end{aligned} \tag{6}$$

where

$$\begin{aligned} \left[\mathrm{F_g^P}\right] &= \int_{\mathrm{A}} \left[\mathrm{H_g}\right]^{\mathrm{T}}\left[\mathrm{H_g}\right]\mathrm{dsdn} = \int\left(\int \left[\mathrm{H_g}\right]^{\mathrm{T}}\left[\mathrm{H_g}\right]\mathrm{dn}\right)\mathrm{ds} = \int\left[\mathrm{C_g^P}\right]\mathrm{ds}, \\ \left[\mathrm{F_g^M}\right] &= \int_{\mathrm{A}} \left[\mathrm{H_g}\right]^{\mathrm{T}}\mathrm{z}\left[\mathrm{H_g}\right]\mathrm{dsdn} = \int_{\mathrm{A}}\left[\mathrm{C_g^M}\right]\mathrm{dsdn}. \end{aligned} \tag{7}$$

The above equations can be used to derive the geometric stiffness matrix using finite element approximation of the geometric strain vector $\{\bar{\varepsilon}_g\}$. The individual elements of the matrices $\left[\mathrm{C_g^P}\right]$ and $\left[\mathrm{C_g^M}\right]$ are derived explicitly. Also, the individual elements of the matrices $\left[\mathrm{F_g^P}\right]$ and $\left[\mathrm{F_g^M}\right]$ are derived explicitly for I and box sections.

For the finite element implementation of the beam, quadratic Lagrangian interpolation functions are used for the axial deformation while cubic Hermetian interpolation functions are used for the torsional deformation which ensured the desired C^1 continuity of torsional rotation (θ) as the displacement field (Eq. 3) contains derivative of θ. As mentioned earlier, the bending deformations along with the shear

deformations are treated in a different manner following the concept of Sheikh[14] where the shear rotations Ψ_y and Ψ_z are adopted as field variables instead of θ_y and θ_z in addition to the bending displacements *V* and *W*. Taking a linear approximation for Ψ_y and Ψ_z, and a cubic approximation for *V* and *W*, the field variables can be written as

$$\begin{gathered} U = a_1 + a_2 x + a_3 x^2 ,\ V = a_4 + a_5 x + a_6 x^2 + a_7 x^3 ,\ W = a_8 + a_9 x + a_{10} x^2 + a_{11} x^3 , \\ \Psi_y = a_{12} + a_{13} x ,\ \Psi_z = a_{14} + a_{15} x ,\ \theta_x = a_{16} + a_{17} x + a_{18} x^2 + a_{19} x^3 \end{gathered} \tag{8}$$

Though Ψ_y and Ψ_z are taken as field variables, they are not used as nodal degrees of freedom. Interestingly, the corresponding nodal degrees of freedom are θ_y and θ_z which are introduced with the help of bending deformations and can be expressed using the above equations as

$$\begin{aligned} \theta_y &= \Psi_y - V' = a_{12} + a_{13} x - a_5 - 2a_6 x - 3a_7 x^2 , \\ \theta_z &= \Psi_z - W' = a_{14} + a_{15} x - a_9 - 2a_{10} x - 3a_{11} x^2 . \end{aligned} \tag{9}$$

The unknown constants (a_1, a_2, a_3 ..... a_{19}) found in Eq. (8) can be replaced in terms of nodal displacements by substitution of *U*, *V*, *W*, (Eq.8) θ_y and θ_z (Eq. 9) at the three nodes of the element (Figure 1), and θ_x (Eq. 8) and its derivative θ_x' at the two end nodes as

$$\{\delta\} = [R]\{a\} \quad \text{or} \quad \{a\} = [R]^{-1}\{\delta\} \tag{10}$$

where $\{a\}^T = [a_1 \ \ a_2 \ \ a_3 \ \cdots \ a_{19}]$, [*R*] consists of coordinates (*x* values) of the 3 nodes and $\{\delta\}^T = [U_1 \ V_1 \ W_1 \ \theta_{x1} \ \theta_{y1} \ \theta_{z1} \ \theta'_{x1} \ U_2 \ V_2 \ W_2 \ \theta_{y2} \ \theta_{z2} \ U_3 \ V_3 \ W_3 \ \theta_{x3} \ \theta_{y3} \ \theta_{z3} \ \theta'_{x3}]$ is the nodal displacement vector.

With the help of Equations (8) and (10), the geometric strain vector $\{\bar{\varepsilon}_g\}$ as defined in Eq. (5) can be expressed in terms of nodal displacement vector $\{\delta\}$ as

$$\left\{\bar{\varepsilon}_g\right\} = \left[V' \quad W' \quad \theta_x'\right]^T = [S_g]\{a\} = [S_g][R]^{-1}\{\delta\} = [B_g]\{\delta\} \tag{11}$$

The above equation is substituted in Eq. (6) and it is rewritten as

$$\begin{aligned} U_g &= \frac{P}{2A}\int_L \{\delta\}^T \left[B_g\right]^T \left[F_g^P\right]\left[B_g\right]\{\delta\}\,dx + \frac{M_y}{2I_y}\int_L \{\delta\}^T \left[B_g\right]^T \left[F_g^M\right]\left[B_g\right]\{\delta\}\,dx \\ &= \frac{P}{2}\{\delta\}^T \left[K_g^P\right]\{\delta\} + \frac{M_y}{2}\{\delta\}^T \left[K_g^M\right]\{\delta\} \end{aligned} \tag{12}$$

Where $\left[K_g^P\right] = \frac{1}{A}\int_L \left[B_g\right]^T \left[F_g^P\right]\left[B_g\right] dx$ and $\left[K_g^M\right] = \frac{1}{I_y}\int_L \left[B_g\right]^T \left[F_g^M\right]\left[B_g\right] dx$ are the components of geometric stiffness matrix of the beam element corresponding to axial load and end moment, respectively. With these matrices and the stiffness matrix [*K*], the governing equation of an element can be written as

$$\left([K] - P[K_g^P] - M_y[K_g^M]\right)\{\delta\} = 0 \tag{13}$$

The above equation (Eigen-value problem) is similarly applicable for a beam which can be solved to get the buckling of the beam subjected to axial load (*P*) and end moment (M_y) where the critical value of one of these loads (P^{cr} or M_y^{cr}) can be determined when the other load is kept constant as preload (

$M_y^0 < M_y^{cr}$ or $P^0 < P^{cr}$) or critical value of both loads (P^{cr} and M_y^{cr}) when they are increased together maintaining a constant ratio between them.

3. Results and Discussions

A number of examples of thin-walled composite beams are studied using the proposed model but some sample cases are only presented in this section due to page restriction.

Example 1: The proposed model is used to predict the buckling characteristic of a 12m long thin-walled box section composite beam simply supported at its two ends under the action of an axial load. The box section is 300mm wide and 600mm deep where all walls consist of four plies each 7.5mm thick. Three different cases of stacking sequence (0/0/0/0, 45/-45/-45/45 and 0/90/90/0) are studied where all walls are having same stacking sequence in each case. The material used for each ply is graphite-epoxy (AS4/3501) which is having the following properties: E_1 = 144GPa, E_2 = 9.65GPa, G_{12} = G_{13} = 4.14GPa, G_{23} = 3.45GPa, ν_{12} = 0.3. The critical loads of buckling predicted by the proposed model are presented along with those reported by Cortinez and Piovan [16] and Kim et al. [13] in Table 2 which shows a very good agreement between the results obtained from different sources.

Table 1 Critical buckling load (MN) of a simply supported box section thin-walled composite beam

Staking Sequence	**References**		
	Cortinez and Piovan [16]*	Kim et al. [13]**	Present**
0/0/0/0	9.33	9.35	9.00
45/-45/-45/45	0.97	0.97	0.97
0/90/90/0	4.97	5.02	4.94

*Without deformation, **With shear deformation

Example 2: The buckling of a simply supported 8m long (l) thin-walled open section composite beam subjected to different combination of axial load and end moment is studied using the proposed model. The beam has a double symmetric I section where the flange is 100mm wide and the web is 200mm deep (d). All flange and web walls are made of two plies each 2.5mm thick (total wall thickness t: 5mm) where flanges are having a staking sequence of [θ/-θ] and this is $[0]_2$ for the webs. The material properties used for all plies are: E_1/E_2 = 25, G_{12}/E_2 = 0.6, G_{13} = G_{23} = G_{12}, ν_{12} = 0.25. For different values of θ (fiber orientation of flange plies), the critical values of the axial load or the end moment causing bucking of the beam as predicted by the proposed model are presented in Table 2 in non-dimensional form ($\bar{P}^{cr} = P^{cr}l^2/(d^3tE_2)$ and $\bar{M}_y^{cr} = M_y^{cr}l/(d^3tE_2)$) along with those reported by Vo and Lee [10]. The results shows a good performance of the proposed element.

Table 2 Critical buckling load/moment of a simply supported I section thin-walled composite beam

Loading Condition	**Reference**	**Fibre orientation (θ)**			
		0	30	60	90
$\bar{P} = \bar{P}^{cr}$, $\bar{M}_y = 0.0$	Vo and Lee [10]*	5.153	1.404	0.225	0.206
	Present**	5.139	1.403	0.225	0.206
$\bar{P} = 0.5\bar{P}^{cr}$, $\bar{M}_y = \bar{M}_y^{cr}$	Vo and Lee [10]	4.451	2.358	0.701	0.528
	Present	4.455	2.086	0.686	0.523
$\bar{P} = 0.0$, $\bar{M}_y = \bar{M}_y^{cr}$	Vo and Lee [10]	7.370	3.496	1.009	0.763
	Present	7.372	3.130	0.989	0.755
$\bar{P} = -0.5\bar{P}^{cr}$, $\bar{M}_y = \bar{M}_y^{cr}$	Vo and Lee [10]	10.175	4.472	1.258	0.953
	Present	10.175	4.041	1.233	0.943

*Without deformation, **With shear deformation

Example 3: The interaction of axial loads and end moments causing buckling of a 5m long simply supported thin-walled composite beam having a double symmetric I section is studied in this section. For this section, the flange is 50mm wide and the web is 50mm deep (*h*) where both flange and web are having 16 plies each 0.13mm thick with a stacking sequence of $[\theta/\text{-}\theta]_{4s}$. The material properties of glass-epoxy used for all plies are: E_1 = 53.78GPa, E_2 = 17.93GPa, G_{12} = G_{13} = 8.96GPa, G_{23} = 3.45GPa, ν_{12} = 0.25. The analysis is carried out taking three different values of the eccentricity (*e*) of the axial load (*e* = 0, *h*/2, *h*) and three different values of the fiber orientations (θ = 0, 30 and 60 degrees) where different combinations of critical axial loads and end moments causing buckling of the beam are determined. These and used to produce the interactional curves which are plotted in Figure 3 where these curves followed an expected trend.

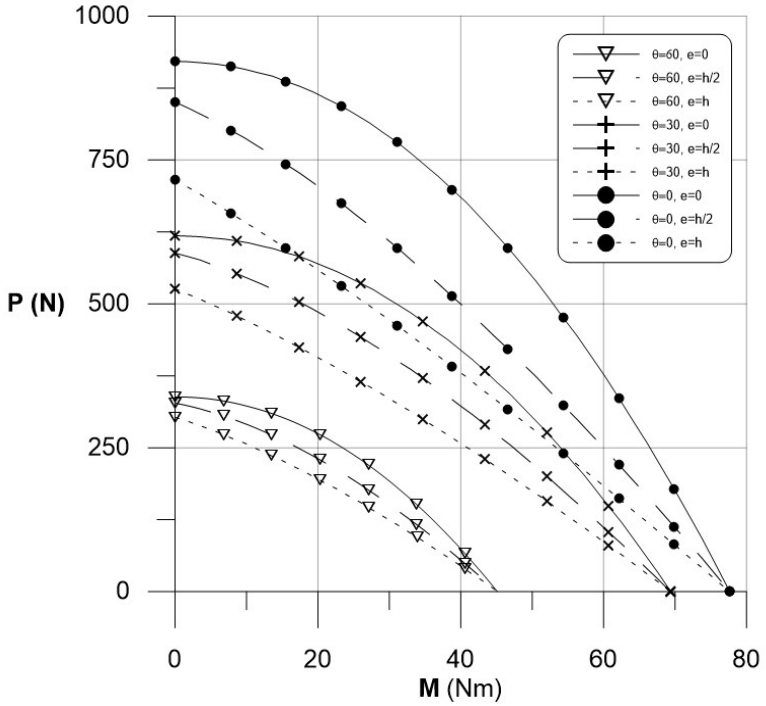

Figure 3 – Interaction curves for axial eccentric loads and end moments causing buckling of thin-walled open section (I section) composite beams

4. Summary and Conclusions

An efficient 1D beam element is developed for buckling of thin-walled composite beams having open and closed sections subjected to axial loads and end moments. The formulation of the element followed a comprehensive treatment considering the effects of axial displacement, torsion, bi-axial bending and transverse shear deformations as well as out of plane sectional warping. The cross-sectional matrices required for the formulation of geometric stiffness matrix of the beam are derived analytically where all possible couplings between the abovementioned modes of deformation are considered. The effect of shear deformation of the beam walls is included which usually requires a C^0 continuous finite element formulation of the bending deformation coupled with the shear deformation. On the other hand, the torsional deformation requires a C^1 continuous FE formulation due to the incorporation of warping deformation. The difficulty associated with the implementation of both these formulations in the present coupled problem is successfully overcome by using a novel concept proposed by of one of the authors. The proposed analysis technique is used to solve numerical examples of thin-walled laminated composite beams having open I and closed box sections taking different stacking sequences of the beam walls. In many cases, the results predicted by the proposed technique are validated with the analytical and/or numerical results available in literature. The agreement between the results is found to be very good in most of cases which ensures the reliability and range of applicability of the proposed element.

5. REFERENCES

1. N.R. Bauld and L.S. Tzeng, A Vlasov theory for fiber-reinforced beams with thin-walled open cross section, International Journal of Solid and Structures. 1984; 20(3): 277–97.

2. Chandra R, Stemple AD, and Chopra I. Thin-walled composite beams under bending, torsion, and extensional load. AIAA Journal. 1990; 27(7): 619-626.

3. Cesnik CES, Hodges DH, VABS: A new concept for composite rotor blade cross section modelling. Journal of the American Helicopter Society. 1997; 42(1): 27–38.

4. Kollar LP, Springer GS. Mechanics of Composite Structures. Cambridge University Press; 2003.

5. Salim HA, Devalos JF. Torsion of open and closed thin-walled laminated composite sections. Journal of composite materials. 2005; 39(6): 497-524.

6. Lee J. Flexural analysis of thin-walled composite beams using shear-deformable beam theory. Composite Structures. 2005; 70(2): 212-222.

7. Librescu L, and Song O. Thin-walled Composite Beams. Springer; 2006.

8. Vo TP, Lee J. On sixfold coupled buckling of thin-walled composite beams. Composite Structures. 2009; 90: 295-303.

9. Vo TP, Lee J, Interaction curves for vibration and buckling of thin-walled composite box beams under axial loads and end moments, Applied Mathematical Modelling, 2010, 34, pp.3412-3157

10. Vo TP, Lee J. Vibration and buckling of thin-walled composite I beams with arbitrary lay-ups under axial loads and end moments. Mechanics of Advanced Materials and Structures. 2013; 20: 652-665.

11. Kim N-I, Shin DK, Kim M-Y. Improved flextural-torsional stability analysis of thin-walled composite beam and exact stiffness matrix, International Journal of Mechanical Science, 49, 2007, pp. 950-969.

12. Kim N-I, Shin DK, Park Y-S. Flextural-Torsional buckling loads for spatially coupled stability analysis of thin-walled composite columns, Advances in Engineering Software, 39, 2008, pp. 949-961.

13. Kim N-I, Shin DK, Park Y-S. Coupled stability analysis of thin-walled composite beams with closed cross-section. Thin-Walled Structures. 2010; 48: 581–596.

14. Sheikh AH. New concept to include shear deformation in a curved beam element. *Journal of structural engineering*. 2002; 128(3): 406-410.

15. Sheikh AH, Thomsen OT. An efficient beam element for the analysis of laminated composite beams. *Composites Science and Technology*. 2008; 68: 2273–2281.

16. Cortinez VH, Piovan MT. Vibration and buckling of composite thin-walled beams with shear deformability. *Journal of Sound and Vibration*. 2002; 258(4): 701-723.

7. Chapter 5 – Conclusion and Recommendations for future study

A new efficient technique is developed for an accurate prediction of the behaviours of thin-walled laminated composite beams having open and closed sections in this thesis under different scenarios. This includes free vibration; buckling under axial load, end moments and their interactions; vibration with preloading (axial load, end moments and their combinations); and dynamic instability with/without preloads of these composite beams. The new model is based on an efficient one-dimensional beam element formulation that is capable of simulating the behaviour of thin-walled open and closed section beams accurately by capturing the complex deformation modes and their interactions of these structures. The formulation is sufficiently general, which included axial deformation, torsion, bi-axial bending, transverse shear deformation, out of plane cross-sectional warping and their coupling. In order to achieve the above model having all these capabilities, the use of a rigorous cross-sectional analysis became necessary for deriving different sectional matrices which are utilised by the beam finite element model. These cross-sectional matrices are derived analytically for beams having I and box section. The effect of shear deformation of beam walls included in the formulation usually demands C^0 continuity in its finite element implementation for modelling the bending deformations of the beam element coupled with transverse shear deformations. However, the incorporation of cross-sectional warping demands a C^1 continuous formulation for the torsional deformation due to the appearance of second order derivatives of the torsional rotation (twist) in the strain vector. A C^0 continuous formulation for shear deformable beam is typically susceptible to shear locking problems, which is generally circumvented by using the reduced integration technique by supressing the problematic terms in the shear energy. However, this affects the solution accuracy, including stress oscillations and other related issues due to inadequate integration of other terms in the strain energy of the structural system. Moreover, it is challenging to apply reduced integration only for the shear coupled bending deformation whereas full integration for the other deformation modes (to retain accuracy of these terms) in the present problem having coupling between bending/shear deformation with other deformations. In order to solve this problem, there is an attempt by a previous researcher who tried to forcefully model the torsional deformation with a

C^0 continuous formulation but it requires inclusion of fictitious nodal parameters that cannot be attributed with any physical meaning. In order to have a satisfactory solution of this problem, an attempt has been made to model the shear coupled bending deformation in a different way and this innovative approach has helped use a full integration for this deformation mode which in turn allowed a C^1 continuous formulation for the torsional deformation with full integration. Thus the proposed model has overcome the crucial obstacles encountered by the researchers in this area for long time. The new modelling technique is used to solve a large number of numerical examples of thin-walled laminated composite beams having open (I) and closed (box) sections taking different boundary conditions, laminated wall stacking sequences, and loading conditions. The results produced by the model are thoroughly validated against analytical and numerical results available in literature, which demonstrates that the proposed model performs very well in terms of both accuracy and computational efficiency. Moreover, a detailed 3D finite element model of few composite beams are modelled using commercially available code Ansys and Abaqus for the validation of the proposed model in some cases where there is no available results. Finally, the new finite element model is used to conduct extensive parametric studies to demonstrate the effect of varying different parameters on the behaviour of thin-walled laminated composite beams subjected to different loading scenarios including their interactions (axial load and end moments). It is anticipated that these new results can prove to be useful as benchmarks for future research in this area.

Some recommendations for the future research are as follows:

1- Extend the model to incorporate the effect of geometric non-linearity in the analysis of thin-walled laminated composite beams having open and closed cross sections.

2- Extend the model for thin-walled composite beams having multi-cell closed cross sections connected with/without open sections.

3- Extend the model for accurately simulating the behaviour (specifically torsion) of stiffening members of stiffened panels.

4- Extend the model to undertake dynamic response of these thin-walled laminated composite structures.